THE EFFECT OF THERMOCHEMICAL TREATMENT ON THE FATIGUE PROPERTIES OF ALLOY STEELS

Ph.D. THESIS

by

MUNIR ABDULWAHID MAJID

Department of Metallurgy and Materials Engineering
University of Aston in Birmingham

December 1980

THE EFFECT OF THERMOCHEMICAL TREATMENT ON THE FATIGUE PROPERTIES OF ALLOY STEELS

MUNIR ABDULWAHID MAJID

Thesis submitted for
the award of the degree
of Doctor of Philosophy

SUMMARY

The effect of thermochemical treatment namely carburising on the fatigue behaviour of one carbon and two alloy steels has been studied in rotating and unidirectional bending. The effect of carbon profile on the unidirectional bending fatigue strength of 635A14 was assessed, and it was found that single stage carburising with a surface carbon content of 0.8% has resulted in a higher fatigue strength than other types of carbon profiles. Residual stresses and other metallurgical variables arising from different carbon profiles, were also considered. The highest compressive stresses have resulted from boost-diffuse-carburising. On the other hand surface decarburisation was associated with tensile residual stresses and a reduced fatigue strength. Retained austenite was found to be detrimental in unidirectional bending fatigue; however its presence in carburised 835A15 did not seem to influence the rotating bending fatigue strength. Carbide particles in globular and/or intergranular form were detrimental to compressive residual stresses; the unidirectional bending fatigue strength is markedly lowered. The highest fatigue strength was accomplished by vacuum carburising. The absence of internal oxidation was the key factor in the increased fatigue strength; the presence of uniformly distributed fine carbide particles did not upset the superior fatigue strength of vacuum carburised pieces.

The effect of mean stress on the fatigue strength of carburised 635A14 was studied. Increasing the mean stress as would be expected resulted in a decreased fatigue strength. Carburisation showed its advantages at low mean stress, but at high mean stress it offers little advantage over the uncarburised hardened conditions.

Notch effect was also studied in unidirectional bending of carburised 080M15. The general trend showed that the fatigue strength decreases with increasing the stress concentration factor. But different carburising conditions have different effect on notch sensitivity.

KEY WORDS: Carburising (Gas, Vacuum), Carbon Profile, Bending Fatigue strength, Notch Sensitivity, Mean Stress

CONTENTS

LIST OF TABLES

LIST OF FIGURES

1. OBJECTIVE

The present project is a study of the bending fatigue strength of carburised and hardened as well as through hardened, carburising steels, under rotating and unidirectional bending.

In particular the project investigates the effect of the following, on the bending fatigue strength based on initiation and failure.

1. Carbon Profile

   Different carbon profiles, i.e. conventional single stage, over-carburised, boost/diffuse with and without decarburisation were produced by conventional gas carburising.

   Moreover, boost/diffuse and over-carburised profiles were produced by partial pressure carburising.

2. Mean Stress

   The bending fatigue strength was studied at different levels of mean stress.

3. Stress Concentration

   The effect of a range of stress concentration factors on the bending fatigue strength was determined in unidirectional bending.

2. INTRODUCTION

This work was planned to investigate the effect of thermo-chemical treatment, namely carburising, on the fatigue behaviour of carburised steel.

In order to improve fatigue properties as well as abrasion and wear resistance, a steel component may be given a carburising treatment.

Gas carburising is the most popular method of case hardening, its objective is to increase the surface carbon content of a steel component at its immediate surface, in order to develop optimum hardness and/or fatigue resistance on subsequent quenching. The degree of atmosphere control in conventional gas carburising favours it over other carburising processes.

However "vacuum" or partial pressure carburising is carried out in cold wall vacuum furnaces, and the potential of this process is based on the clean atmosphere, short process time on one hand, and the improved mechanical and fatigue properties on the other hand.

Carburising and hardening produce a microstructural variation within the component, depending upon the type of carbon profile and the hardenability of the steel in question. Microstructural variations are possible as the carbon content varies across the section, and consequently residual stresses are generated within a carburised and hardened component. Metallurgical effects arising from

carburising are:

1. Internal oxidation
2. Decarburisation
3. Carbides
4. Residual stresses
5. Retained austenite

These may all influence the fatigue performance of a carburised component.

Different types of carbon profile may produce different transformation sequences, resulting in different residual stress distribution, and it is well documented that compressive residual stresses are beneficial while tensile residual stresses are detrimental.

"Fatigue durability of Carburised Steel" A.S.M. 1957 [1] is probably the most comprehensive investigation in this field. However this investigation is out of date and has several deficiencies. For example the subsequent development of the sealed quenched furnace, as well as the progress in utilising partial pressure carburising make earlier work out-of-date.

Tempering treatment is a common practice after carburising, in order to reduce the brittleness of the case. However tempering is known to relieve residual stresses.

The fatigue behaviour of carburised and hardened steel is generally expressed as the failure stress on the S-N curve. However the significance of crack initiation in a

component life; and the initiation stress compared to that of failure was not given concern.

Most of the fatigue data of carburised and hardened components are derived from rotating bending, where alignment and axiality are difficult to ensure. Moreover a mean stress of zero in rotating bending bears little relevance to many engineering components in practice, which may undergo a mean stress value other than zero.

Engineering components in practice may have a stress concentration feature, for instance, a gear component encounter a stress concentration feature at the tooth root.

Information about the effect of stress concentration on the fatigue strength of carburised component is limited. Data in that respect are derived from rotating bending again, and are confined to high values of stress concentration factor; while in practice lower values may be encountered in unidirectional bending.

3.0 LITERATURE SURVEY

3.1 Factors Affecting the Performance of a Carburised Component

As far as carburised components are concerned, a variety of properties are required like resistance against wear, abrasion, scuffing, bending fatigue and impact loading. For instance when a gear is transmitting a torque, its teeth are subjected to a bending and contact load and under repeated loading will fail by tooth breakage, pitting and spalling as documented by ASM(2).

The production of the necessary properties on a carburised component is related to the base steel composition, as well as to the hardening treatment. To fulfil the property requirements of a carburised component, the necessary surface hardness and an overall toughness are essential.

The performance of a carburised and quenched component may be influenced by the properties of the base steel, carburising factors, hardening and post-hardening treatments.

3.1.1 Hardenability and Core Carbon

Carburising steel covers a wide range of composition, with varying amounts of alloying elements necessary to enhance one property or another, particularly hardenability.

Hardenability is an essential feature of carburised steel. In this context molybdenum would provide case and core hardenability, however moderate additions of chromium and manganese will improve the core hardenability. Nickel on the other hand contributes primarily to the toughness of both case and core, whereas the necessary core strength is adjusted by the carbon content. Too much core carbon could adversely influence the residual stresses and consequently the fatigue properties [3]. However Sagaradze [4] showed that the strength of carburised steel depends upon the yield strength of the core and the residual compressive stresses in the case. He also showed that increasing the carbon content will result in increased yield strength of the core and decrease the compressive stresses in the case. Therefore only sufficient core strength to resist local yielding at the design load is desirable.

3.1.2 Surface Carbon

The combination of the high hardness case and the relatively softer more ductile core provide the characteristic requirement for fatigue resistance and impact loading [5].

Fatigue strength is related to the surface carbon content and surface hardness. Increasing the surface carbon from the base content of about 0.15%C to about 0.5%C would generally produce the maximum strength increase. However, steel components are commonly carburised to a

higher surface carbon content - around 0.8% C - in order to attain the required hardness, wear resistance, surface fatigue strength and ultimately the carbon profile suitable to produce a favourable residual stress distribution in the surface layer.

The microstructure encountered in a carburised steel component will be related to the carbon content, cooling rate and the steel composition. Typically the microstructure within the case of a carburised and quenched component is martensitic with some retained austenite in the high carbon layer, or even carbides. On the other hand the core material might contain ferrite, bainite and/or martensite.

The high hardness of the martensitic case is accompanied by high brittleness. However, the austenite will lower the hardness of the resulting microstructure.

3.1.3 Carbon Profile

When a steel component is carburised for a fixed length of time in an atmosphere at a fixed carbon potential, the surface carbon content of the steel is increased and at the same time a carbon gradient is produced within the steel by diffusion of carbon through the austenite lattice. The typical shape of a carbon profile produced in this way is shown in Fig. 1A. If carburising was continued for increasing lengths of time the carbon concentration at the surface of the steel approaches the carbon potential in the atmosphere, while the carbon

gradient produced within the steel becomes less steep, as can be seen in Fig. 1B.

The resulting carbon profile may depend upon the carburising process, as well as on the technique employed in the carburising process.

In conventional carburising, the single stage technique produces a carbon profile with a surface carbon content around 0.8% C, the resulting profile is gradually formed by absorbing carbon as well as duffising it within the steel. The profile is steep and the maximum carbon content is at the surface.

In the boost/diffuse technique for gas carburising the surface is over-carburised and then diffused inwards and decarburised outwards to obtain the required carbon level. So the surface carbon is approached from higher carbon content, unlike the single stage where the required surface carbon is approached from lower surface carbon level. The carbon profile resulting from a boost/diffuse technique, could take different shapes depending upon the diffusion treatment potential and time. It could be very similar to the one produced by a single stage but with deeper case, or a carbon profile with a plateau near the surface, or incorrect control of carburising parameters could result in a carbon profile with the maximum carbon below the surface by some distance (0.2 - 0.3 mm) and the resulting profile will appear as decarburised.

Figure 2 shows optimisation of boost/diffuse ratio for an En354 carburised in endothermic gas/propane at 925°C [6].

However in vacuum carburising process, again the boost/diffuse is the technique employed, as in the boost period the steel surface is saturated with carbon and on diffusion the surface carbon is brought down to the required level, as well as the required case depth is developed. In this case no "decarburisation" occurs due to the use of a high vacuum during the diffusion stage. Figure 3 [7] compares carbon profiles obtained on SAE 8620 by the following treatments:

Vacuum carburised, boost at 1.9% C for ½ hour at 1038°C
diffuse at 1.0% C for ½ hour at 1038°C

Vacuum carburised, single stage at a reduced pressure for 5.5 hours at 0.92% C at 927°C.

Conventional gas carburised, boost at 1.2% C for 4.5 hrs at 927°C
diffuse at 1.0% C for 1 hr. at 927°C

The type of carbon profile produced on a carburised component may have a bearing on its performance in practice. This may depend upon residual stresses produced and other metallurgical variables associated with it as will be discussed in following sections.

3.1.4 Decarburisation

Decarburisation is the phenomenon referred to whenever the carbon content of the outermost surface layer is less than that at any location underneath.

Surface decarburisation takes place whenever the carbon potential of the furnace falls below that adjusted to sustain the surface carbon content, whilst the temperature is above 700°C.

As far as conventional gas carburising is concerned, this phenomena can occur during cooling or reheating for hardening, when the temperature continuously changes, and as a result equilibrium conditions at the gas/metal interface cannot be attained. Consequently atmosphere control to prevent decarburisation is difficult.

The excess concentration of the decarburising gases (CO_2, H_2O) upon reacting with carbon atoms at the gas/metal interface will eventually extract carbon from the steel. As a result carbon oxidation at the surface of the component will occur, and a gradient of carbon is created. The surface carbon decrease and the depth of decarburisation increase with time [8].

3.1.4.1 Effect of Decarburisation on Microstructure and Material Properties

Surface carbon and the cooling rate both will have a role on the resulting microstructure. For instance, a carbon profile of the type A shown in Figure 4 will produce the

required surface microstructure, namely martensitic. On the other hand a carbon profile type B will produce a microstructure consisting of high carbon martensite some distance beneath the surface and low carbon martensite at the immediate surface will appear. However ferrite may also appear at the immediate surface depending upon the severity of decarburisation.

The surface hardness, as a property requirement of a carburised component, would be influenced and adversely affected, in the event of decarburisation, according to the resulting microstructure and surface carbon content. The surface hardness may drop significantly if the surface is decarburised severely. However, a slight decrease in macrohardness will occur, when low carbon martensite is produced [8].

The M_s temperature increases with the decrease of carbon and this will be accompanied by incorrect transformation sequence [9]. The surface layer of a decarburised component will be softer (lower strength) than a properly carburised one. As far as fatigue strength is concerned, and in particular fatigue crack initiation, it is generally a surface phenomena. So it is to be expected that decarburisation will lower the resistance to crack initiation. However such decarburised layer may deform under contact fatigue and consequently accommodate the applied load,

this perhaps will modify the residual stresses favourably at the contacting surfaces. On the other hand soft decarburised surfaces are expected to wear and scuff readily [8].

Surface decarburisation as a phenomena takes place as the carbon diffuses both inward in the steel and outward to the gas phase at the metal surface during gas carburising.

In vacuum carburising diffusion is possible only inwards, and therefore, whatever the carbon potential is, the surface will always have the maximum carbon content.

3.1.5 Retained Austenite

On quenching a carburised steel component, the resulting microstructure will be martensitic and it is possible for some austenite to remain in the final microstructure.

Depending upon the M_f temperature, if it lies below the quenchant temperature, austenite will be retained.

Alloying elements lower the M_s temperature but the carbon plays the major part [9].

In a carburised component there will be a carbon gradient through the case, and that will be associated with a gradient in the M_s temperature. Therefore upon carburising, the surface with the high carbon content will have its M_s and M_f temperatures lowered, and the M_f may lie below the

quenchant temperature and therefore austenite retention occurs [9].

The co-existance of the soft austenite with the hard martensite will reduce the overall hardness of the microstructure. As the hardness is controlled by the carbon content up to about 0.5% C, then it will be the retained austenite and its amount which will influence the hardness [10].

The failure of austenite to transform during quenching means that the volume expansion which accompanies the austenite to martensite reaction will not have fully taken place [11].

Koistinen[12] stated that both the distribution and magnitude of residual stress were determined by the extent and the sequential martensitic transformation as will be discussed in detail under the residual stress heading.

Fatigue properties of a case hardened component is expected to depend upon increasing the inherent strength of the material and the development of compressive residual stresses in the surface layer; however, the presence of retained austenite reduces both, and therefore the resistance to fatigue failure is expected to be lowered [13].

Diesburg [14] showed that a microstructure containing >40% retained austenite is less resistant to crack initiation than microstructure having larger amounts of martensite. Retained austenite between 15% and 25% is claimed to offer some resistance to crack initiation, however once the crack is formed austenite will offer little resistance to its propagation depending upon the toughness of the martensite and the residual stresses ahead of the crack tip.

Retained austenite on the other hand is favoured to increase the contact fatigue properties. Balter et al [15] and Diamant et al [16] agreed that high austenite containing surfaces were superior to those containing only small amounts. The property of austenite which is most responsible for the favourable effect reported, must be its ability to plastically deform and work harden. Austenite can either work harden or transform to martensite under loading, as stated by Richman et al [17], this transformation is associated with enhanced ductility as the resulting martensite is more ductile than thermally formed martensite [17].

3.1.5.1 Effect of Sub-Zero Treatment on Retained Austenite

The retention of austenite and its effect on the mechanical behaviour of the resulting microstructure, suggests sometimes the necessity for a sub-zero quenching treatment.

As has been mentioned, the quenching temperature should go below room temperature so that complete decomposition of austenite is possible.

R. G. Dawes [18] showed that sub-zero treatment is detrimental to fatigue resistance, and attributed that to the increase in hardness upon austenite transformation being associated with a reduction in the resistance to brittle fracture. Roberts et al [19] showed that refrigeration to produce a more complete austenite to martensite transformation has a slightly adverse effect on fatigue properties.

3.1.6 Carbides

During carburising if the carbon concentration is higher than the saturation level of austenite at the carburising temperature, carbide will be formed.

3.1.6.1 Globular Carbides

Globular carbides form during heating the component slowly between the Ac_1 and Ac_m up to the carburising temperature in a carburising atmosphere at high carbon potential.

With endothermic gas carburising the carbon potential is extremely high at the Ac_1 temperature, decreasing as the temperature increases, therefore during heating the atmosphere condition will favour the globular carbide formation.

The chemical composition of the steel will influence the tendency to form carbides [20].

Kozloviskii et al[21], Fig. 5 showed how the amount of carbide phases increase towards the surface, while the proportion of chromium and manganese in the solid solution decreases.

3.1.6.2 Network Carbide

Slow cooling of super-saturated austenite from the carburising temperature will be associated with precipitation of carbide at the austenite grain boundaries, however if cooled quickly much, if not all, of the excess carbon would be retained by the resulting martensite austenite structure.

Austenite will reject some carbon as carbides Fe_3C from the solution. As the grain boundaries are high energy tracks and the mobility of carbon atoms as an interstitial is higher than within the grain, which eventually will result in carbide network.

Carbide formation and its subsequent growth will be at the expense of the matrix elements and consequently the solid solution will be impoverished in the elements involved.

As a result there is a local lowering of hardenability in the vicinity of the carbides and the possibility of forming low alloy martensite or even non-martensitic microstructure upon quenching [21].

3.1.6.3 Carbides and Material Properties

Surface hardness of a carburised component is an important requirement, which could be influenced by many factors. Carbide microhardness is high, but any non-martensitic structural features would tend to upset any hardness increase due to carbide.

Transformation upon quenching will result in residual stresses; (discussed in section 3.8). However, as carbide does not undergo the martensitic expansion along with any non-martensitic transformation products, the overall resulting expansion will be reduced. Moreover, the occurrence of a high temperature non-martensitic transformation near the surface before that of the underlying martensite will be accompanied by a non-ideal transformation sequence. Consequently the magnitude of the surface residual compressive stress will be less than if no carbide had formed and the structure had been martensitic [20].

Due to Parrish [20] it would be expected that with the reduced compressive or even with tensile stresses, the bending fatigue strength of the carburised component will be adversely affected.

3.1.7 Internal Oxidation

Carburising steel at temperature 900-950°C, is generally associated with internal oxidation of some alloying elements in the steel. The degree of which depends upon the elements affinity for oxygen.

Parrish reported that in gas carburising the atmosphere is decidedly reducing to the base metal iron. However, for alloying elements with greater affinity for oxygen than iron, the atmosphere is potentially oxidising and the ratio of the partial pressures of the oxidising and reducing constituents in the atmosphere $\frac{P_{H_2O}}{P_{H_2}}$ and $\frac{P_{CO_2}}{P_{CO}}$; will determine the oxidation potential of the elements involved [3].

Parrish [3] reported such oxidation potential at 930°C as Fig. 6 illustrates, and Fig. 7 shows that elements which favour internal oxidation are generally necessary to the steel.

Oxygen is absorbed on the metallic surface of the steel component, then it diffuses and penetrates along the austenite grains and sub-grain boundaries. Generally penetration depth is less than 25 μm. However, oxide can be found within the grains when the extent of oxidation is severe and the steel composition is encouraging [20].

Mitchell et al [22] illustrated the increase of internal oxidation with manganese content and suggested that the severity of attack is governed by the time of the gas metal reaction.

Arkhipove [23] however, reported a less extensive oxidation of chromium in 0.8% Cr than in a1.65% Cr steel. On the other hand he and others [24] showed that oxides observed in the surface up to 8 μm contained manganese chromium and silicon, and only silicon oxides persisted at greater depths.

Work by Arkhipove [23] again showed that, whereas chromium migrated to the surface, the nickel migrated into the body and as a result nickel content exceeded 5% in some zones.

Robinson [25] confirmed that the diffusion of elements reduce the composition gradient, however it is understood that much of the elements migrating to the surface is

utilised in forming oxide leaving the matrix material below average alloy content [26].

So it is to be expected that the formation of oxides would produce a local compositional gradient.

3.1.7.1 Effect of Internal Oxidation on Material Properties

The elements involved in the oxidation process will leave the austenite matrix adjacent to the oxide particles. However, the carbon level may also be reduced [3]. The removal of elements from solid solution at high temperature will be accompanied by reduced hardenability in the affected zone, and it is possible that a moderately agitated oil quench would fail to induce martensitic transformation.

The chemical and microstructural effects which have been discussed will influence the properties of the carburised component.

A martensitic microstructure is essential to provide the necessary hardness (800 Hv) and the required strength in a carburised steel surface. However due to internal oxidation a non-martensitic microstructure may be formed and consequently, low microhardness values are obtained in the affected zone. Moreover the inherent strength of the material in the affected zone will be lowered due to the migration of the alloying elements to form oxides [24].

The problem of internal oxidation and its detrimental effect on the material properties recommend the prevention of such surface oxidation.

Vacuum or partial pressure carburising may be favoured to conventional gas carburising due to the freedom from internal oxidation.

3.2 Residual Stresses and Carburising Factors

Carburising factors that are likely to influence the fatigue behaviour of a carburised and quenched component have already been discussed. However residual stresses as an outcome of carburising are expected to influence fatigue properties directly and through those factors previously discussed.

In this section residual stress origin and development in a carburised and quenched steel component will be discussed. Moreover the effect of other carburising factors on the residual stress distribution and magnitude will be considered.

The transformation of austenite to ferrite, pearlite, bainite, and/or martensite is accompanied by volume changes of the steel, Fig. 8, because of the compositional gradient, namely that of carbon within the case and the core. On quenching, different parts of the component will undergo the transformation at different temperatures, and therefore at different times[27]. The time lag of transformation within the carburised component gives rise to internal compatability stresses, which will consequently be accompanied by the generation of residual stresses [28] (see Fig. 9).

3.2.1 Residual Stresses Generated by Phase Transformation in Case Carburised Steel

The generation of the residual stress can be followed by using the continuous cooling transformation curve, shown in Fig. 10, that of low carbon steel with carbon gradient through the case.

It can be seen that the core with its low carbon content will transform before the beginning of transformation in the high carbon case. Therefore the core will expand in the radial and circumferential as well as in the axial direction. While the case has no tendency to change its volume at that time, the austenite which comprises the case is sufficiently plastic at that temperature, that it will undergo sizeable plastic deformation to maintain compatability with the (now larger) core. It will, however, afford some resistance to the forces causing deformation, so that axial tension will be created in the case, with the corresponding compressive stresses being generated in the core. The resulting stress distribution is shown in panel b of Fig. 10.

On further cooling, the austenitic surface undergoes its plastic deformation and would tend to exhibit the attendant increase in volume on transformation. However the presence of the (now) cool rigid core prevents the surface, or case, from undergoing its full free-body expansion. Consequently the case actually has smaller dimensions than it could otherwise have, and thus it will be under a state of compressive stresses, and the final stress distribution in the axial direction is shown again in Figure 10, panel c.

Austenite transformation in a case of carburised component may generate a variety of residual stress distribution. They may be tensile or compressive on the surface and vice versa in the core; moreover the peak of the stress distributions may also vary [28].

Uncarburised quenched components would have a different residual stress distribution, as Fig. 11 illustrates.

3.2.2 Factors Influencing Residual Stresses

In the following sections the effect of different carburising factors on residual stresses will be reviewed.

3.2.2.1 Retained Austenite

In a carburised and hardened component the development of residual stresses in the case will be in some way related to the amount of untransformed austenite. Koistinen [12] showed that both the distribution and magnitude of residual stress were determined by the extent and sequence of the martensite transformation.

Maximum compression occurs at some distance from the surface, where the martensite transformation was essentially total, but lower values of residual compression were observed at the surface where the amount of untransformed austenite was relatively large. High values of compressive residual stresses were favoured to negate applied tensile stresses; Fig. 12 shows the residual stress distribution as related to the amount of retained austenite. On the other hand, Diesburg [14] showed that high retained austenite causes the highest level of compressive residual stresses. He also showed that there is no direct relationship between retained austenite and residual stresses in a given area, except that the amount of retained austenite appeared to limit the maximum compressive stress attainable in the martensite. He

showed that the specimens having the highest amount of retained austenite, exhibited the highest level of compressive residual stress.

Refrigeration, i.e. sub-zero treatment, transformats the retained austenite, in doing so one would expect modification of the residual stresses. Coleman et al [29] showed that sub-zero treatment does not result in a significant change in the residual stress. Table 1 summarises results by Balter et al [30] where it can be seen that sub-zero treatment reduces the bending and impact strength, while Fig. 13 shows the residual stress distribution before and after sub-zero treatment at -120°C, however a repeated sub-zero treatment is claimed to produce a more significant effect on the residual stress [29], as Fig. 14 illustrates.

3.2.2.2 Decarburisation

The reduction of carbon content due to decarburisation at the surface will be accompanied by an increase in the austenite decomposition temperature. Therefore upon quenching a decarburised component, transformation will take place prematurely at the surface, besides progressing outward and inward from the case core interface, as shown in Fig. 15, and tensile residual stresses will be produced in the surface when the underlaying austenite eventually transforms to martensite [8].

The influence of decarburisation on residual stresses has been investigated by V.S. Sagaradze et al [31] and results are shown in Fig. 16, where it can be seen that with no

decarburisation the residual surface compression of 20 Kh2N4A steel was about 400 N/mm^2, but with decarburisation to a depth of 0.3 mm the surface compressive stress was virtually zero. Where severe decarburisation had taken place to a depth of about 0.5 mm then the surface was in a state of tension to a value of 200 N/mm^2.

3.2.2.3 Carbides

Carbide formation process, as has been discussed, is associated with extracting alloying elements from the matrix material and eventually result in the impoverishment of the zone adjacent to the carbide.

Carbide itself does not undergo the martensitic expansion, along with any non-martensitic transformation products adjacent to it, and that in effect will reduce the overall transformation expansion of that part of the case containing it. Added to this, is the fact that in the event of a non-martensitic transformation taking place near the surface, the transformation temperature will be above that of the underlaying martensite, and hence correct transformation sequence will not occur. Consequently the magnitude of surface or near-surface residual stresses will be lower than if the structure had been martensitic. The loss of surface compressive residual stresses due to the presence of carbides was documented by Kuo [32], other factors may have contributed, a greater part was probably due to the presence of free alloy-containing carbides [20] (Fig. 17).

The extent of reduction in the compressive residual stresses will somehow be related to the size and the amount of carbides formed.

Koistinen [12] showed the effect of a film of carbide and suggested the development of a high residual tensile stress in the outer 0.025 mm of the surface, see Fig. 12.

3.2.2.4 Internal Oxidation

As has been shown that internal oxidation in depths greater than 13 μm influence the surface microhardness and bending fatigue strength. Consequently, it is to be expected that residual stresses at the surface of the case are adversely affected[3]. In this respect work by Arkhipov et al [24] showed the effect of internal oxidation (the existence of non-martensitic product as a result of internal oxidation); such results are summarised in table 2.

3.2.2.5 Tempering

Following carburising and hardening, components are usually heated to some temperatures within the range 140-250°C and soaked at that temperature for 2 to 10 hours. The microstructure of a carburised component is unlikely to be greatly modified by tempering below 200°C [33].

However residual stress magnitude and distribution are influenced by tempering. Work by Kirk[34] and others is presented in Fig. 18 where it can be seen that tempering at 60°C has a little effect. While tempering at 100°C produce a positive

reduction, being maximum between 100 and 160°C. It can also be seen that at above 160°C there is a tendency for the curves to level off.

Parrish [33] concludes that tempering appears to shift the peak compressive stress towards the core, Fig. 19, and that the magnitude of the compressive stresses is reduced. This must necessarily reduce the magnitude of the balancing tensile stresses.

Coleman and Simpson [29] illustrated the expected relief in residual stress with tempering. However it was noted that the effect of tempering is maximum in the high carbon positions of the case. They indicated as well that the maximum compressive stress increases somewhat with sections size, and the maximum compressive stress shift away from the surface.

Sagaradze et al [35] showed that maximum compressive residual stress of 1225 N/mm^2 at 0.05 mm depth drop to 540 N/mm^2 on tempering at 140°C for 1 hour.

3.2.2.6 Case Depth

Case depth is the depth to which the carbon penetrates. However, a more used term is the depth to 500 HV hardness generally effective case depth.

Deep case produced by prolonged carburising can modify the surface microstructure and hence the residual stress distribution in the quenched case. Increasing the case

depth is more likely to favour the formation of products, such as internal oxidation, excessive retained austenite and free carbides, all of which adversely affect the residual stress distribution, as have already been discussed. However Coleman and Simpson [29], in Fig. 20, showed how for two surface carbon contents, increasing the case depth causes a general shift of the peak compressive residual stress away from the surface. Meanwhile in the present work a fixed case depth has been aimed for the testing programme.

3.3 Fatigue Strength and Carburising Factors

The performance of a carburised component under repeated stresses may be influenced by the metallurgical features arising due to carburising.

In the past a lot of work has been carried out to investigate the effect of the carburising factors on the fatigue performance. However they have been considered separately. Perhaps the comprehensive investigation 'Fatigue Durability of Carburised Steels' was unique in its scope. Some published papers investigated the effect of carburising without considering the ratio of case depth to section size. In other instances there is no indication of the micro-structures involved. Deductions made by investigating the effect of decarburisation on a medium carbon spring steel are misleading as its carbon profile bears little similarity to that of a carburised piece subjected to decarburisation.

In this section we will review the carburising factors as they affect the fatigue strength.

3.3.1 Decarburisation

In practice carburised parts may exhibit slight surface decarburisation, as has been discussed. It is generally believed that such surface decarburisation lowers the fatigue durability.

Bidwell, J.B., [1] summarised instances in the literature where decarburisation has been reported to produce poor durability, benificial, or no effect.

However Chaney, J.M. [36] in his investigation showed 40% reduction in bending fatigue resistance upon 0.22 mm decarburisation of carburised 3% Ni-Cr steel; similarly Sagaradze, V.S. [4] showed a reduction in bending fatigue limit in excess of 50% by decarburising KhGT steel to a surface hardness of 410 HV when the depth of decarburisation was about 0.5 mm. He and Malygina [31] using 20 Kh 2N4A steel showed 50% reduction in bending fatigue when surface carbon content is reduced from 0.8% to 0.35%, as they quoted. They also showed that decarburisation does not necessarily reduce the static bending strength.

As example of the effect of decarburisation on the fatigue limit is shown in Fig. 21.

Jackson et al [37] reported a marked decrease in the fatigue limit of SAE 4140 steel when a reduction of the order of 50% was produced. Sachs [38] however stated the effect of a shallow decarburised layer to be comparatively harmless provided it is thinner than the case.

Robinson's[39] results indicate that at low testing stresses (690 N mm^{-2}) homogeneous (non decarburised) martensitic steel has considerably better life than decarburised steel, however at high testing stresses (1034 N mm^{-2}) the reverse is true.

3.3.2 Retained Austenite

Many studies have been carried out to investigate the influence of retained austenite on the fatigue behaviour of a carburised and hardened steel component.

Parrish[8] in his review of the literature suggested that the effect of retained austenite is complicated for the fact of austenite ability to transform and/or work harden by applied stresses.

In this context Kozyrev and Toporove [40], using a 12% Cr alloy steel, showed that the impact fatigue resistance increase with the austenite content at high level of applied stress and vise versa at low level of applied stress, however at intermediate stress level retained austenite seems not to influence the impact fatigue resistance as Fig. 22 illustrates. Richman et al [17] however, using SAE 4027 steel showed that the stress induced transformation produced a more ductile martensite than thermally generated martensite.

Meanwhile Razim [41] using 14 NiCr 14 steel showed 13 and 26% reduction in rotating bending fatigue strength in a tempered and untempered condition when the retained austenite was 80% compared to a martensitic structure with less than 2% retained austenite. Accordingly he quoted a fatigue limit of 598 N/mm^2 in rotating bending specimens carburised to a case depth of 1.0 mm, surface carbon 0.75% and 800 HV surface hardness. He went on and showed that shot peening improved the fatigue behaviour of gears if the structure contains amount of retained austenite. Parrish[33] referring to work by Wiegand et al [42] suggested that 15%-25% retained austenite results in a noticeable reduction in the fatigue limit, as shown in Fig. 23.

On the other hand Kern [43] has quoted this range not to cause any problem in gear performance provided the hardness is at least 570 HV.

George, Krauss et al [44] on the other hand using SAE 8620 steel specimens carburised for 6 hours at 927°C in a 1.0% carbon potential showed that the unidirectional bending fatigue strength is increased from 965 N/mm^2 to 1650 N/mm^2 when the retained austenite is decreased from 35% to 18% by re-hardening, as shown in Fig. 24. Although the fine microstructure with the finely spherodised carbides may also have contributed, the main cause would be the retained austenite. The carbide possible effect will be discussed later.

In assessing the effect of retained austenite, consideration must be given to the type of loading the component (containing it) will be subjected to.

For instance, in a gear component where direct contact loading is acting along with bending as well as other stressing conditions, deformation of the surfaces containing retained austenite is likely to improve the overall fatigue performance of the gear, as has been confirmed by Kern and Weigand [42,43]. However as the present work is dealing with only the bending fatigue strength therefore the effect of retained austenite will be confined to a pure bending condition.

3.3.3 Sub-Zero Treatment

It has been mentioned that sub-zero treatment reduces the amount of retained austenite, and consequently influences the fatigue strength.

For instance, Richman et al [17] showed that refrigeration of Fe-16Ni alloy steel has no effect on the axial fatigue strength, however 40126 steel containing about 43% retained austenite showed superior life in axial fatigue than being refrigerated to 23% retained austenite.

However work by Sargaradze et al [35] showed that the cold treatment has a negative influence on the fatigue limit of carburised 20 Kh 2N4A, as he quoted about 7% decrease in the bending fatigue upon cold treatment. He pointed out that such treatment produced the lowest fatigue strength.

Meanwhile, on the same issue, Roberts et al [45] showed that refrigeration results in reduction in the fatigue durability. He attributed the reduction to the transformation of austenite sub-surface, rather than at the surface, consequently it is only to be expected that tensile stresses are responsible for the reduced durability.

Refrigeration influences the fatigue behaviour through its effect on residual stresses and retained austenite, in particular the proportion of austenite within the case and at the surface.

Whatever the outcome of refrigeration is the literature underlines its detrimental effect on the fatigue properties. However such treatment has not been applied in the present work.

3.3.4 Carbides

It has been discussed how the carbide formation influence the microstructure and the resulting residual stresses. However, their effect upon fatigue properties may depend upon their shape and distribution [20].

For instance, Kozlovskii [46] showed that the presence of free carbides in a martensitic matrix structure have a detrimental influence, and as a result the bending fatigue strength has been quoted to be reduced by 25%-30%. Similarly Gyulikandanov et al [47] using 20 Kh NV4MF steel showed that continuous carbide network reduced the fatigue limit. Meanwhile Robinson [48] showed that partial or discontinuous carbide network has no detrimental influence on the reversed bending fatigue durability of SAE 6120 carburised to about 1.0 mm case depth. This can be seen in Fig. 25.

Referring to results by Krauss et al [44] it can be suggested that the bending fatigue strength of SAE 8620 increased from 965 N/mm^2 to about 1650 N/mm^2 upon the reduction of retained austenite as well as the formation of spheroidised carbides as was mentioned earlier, but Sagaradze [49] using 20 Kh 2N4A showed in a separate study that the formation of spheroids of carbides did not reduce the fatigue limit.

Geller et al [50] showed that free carbides are detrimental to contact fatigue properties. However when finely distributed their presence is claimed to be beneficial. Meanwhile carbide network was shown by Razim [51] to be beneficial under contact loading conditions.

3.3.5 Internal Oxidation

Internal oxidation in the surface layer of conventionally carburised components result in a localised reduction in microhardness and inherent strength of the material in the affected zone. As the fatigue behaviour of a carburised component is related to both, the formation of internal oxides will be associated with reduced fatigue strength.

For instance, Arkhipove et al [52] using a range of carburising and carbon-nitriding steels showed how increasing the microhardness is accompanied by increase in the bending fatigue strength, as shown in Fig. 26. Weigand and Tolsch [27] have reported that surface hardness must fall below 680 HV for a decrease in the fatigue to occur, as can be seen in Fig. 27.

Robinson [25], using SAE 8620, produced results where he indicated that the special atmosphere treated samples (oxide free surfaces) showed a better bending fatigue strength than the conventionally treated ones.

The severity and depth of internal oxidation may have the say in affecting the fatigue behaviour of a carburised component. Beumelburg [53] found that oxides to depth of

6-10 μm did not significantly influence the rotating bending fatigue strength as compared to a non-oxidised test piece, and difference was noted when the depth of oxidation exceeded 16 μm. A threshold depth of 13 μm has been suggested over which reduction in the fatigue limit was obtained.

An increase of depth of oxidation from 13 to 30 μm reduced the fatigue strength of 15 Cr steel by 45% [3]. However, Robinson [25] using SAE 8620 steel showed that 13 to 15 μm of internal oxidation caused the fatigue limit to be reduced by 20%.

On the other hand, Diesburg [54] suggested that the depth of surface oxidation did not appear to control the impact fracture stress.

In spite of the possible conflict to the depth where the internal oxidation effect is significant, it does influence the microstructure, microhardness and the residual stresses at the surface of the component, as has been discussed. Consequently the bending fatigue resistance is expected to be adversely affected.

Summarised results of work by Arkhipov et al [52] are presented in table 2.

As for contact fatigue properties, it was indicated by Sheenen et al [55] that the presence of internal oxidation is not detrimental to contact fatigue resistance. They suggested that deformation within the oxidised layer would

bring about a more favourable distribution of the contact load.

Internal oxidation is associated with the oxygen potential of the carburising atmosphere gases, therefore oxygen free atmospheres will avoid internal oxidation. In this respect "vacuum" carburising may be preferred to conventional gas carburising, as the products vacuum carburised are free from internal oxides. Consequently components vacuum carburised should have no compositional gradient, neither non-martensitic transformation products in the surface layer. Therefore the fatigue properties are expected to be superior to those conventionally gas carburised. In this context Casper [56] using SAE 4320 steel specimens tested in rotating bending, showed the superiority of vacuum carburising, as Fig. 28 illustrates.

3.3.6 Tempering

The effect of tempering on the fatigue properties is seen through its effect upon the residual stresses on one hand and the overall toughening effect of tempering. In other words, the fatigue limit will be influenced by two opposing factors. The reduced brittleness of the case, which favours an increase in the fatigue limit, and the reduction of the compressive stresses which reduces the fatigue limit. Roberts et al [45] using SAE 8620 steel showed that tempering is detrimental to the bending fatigue strength and attributed that to the lower residual compressive stress near the surface, and the slight reduction in the gross hardness gradient.

In view of the present work it was felt that the relief of residual stresses upon tempering may overshadow the effect of different carbon profiles. So tempering treatment was not practiced in the present work.

3.3.7 Case Depth and Section Size

A lot of work has been done on case depth and section size effect on the fatigue properties. For instance, Dawes and Cooksey [5] illustrated how for a 7.6 mm diameter test piece the maximum bending fatigue strength was obtained with a case depth of about 0.6 mm, i.e. a case depth to section thickness ratio of about 0.08, see Fig. 29 .
In another study, B. Pathi Raj [58] has reported that a case to section size ratio of about 0.122 resulted in a maximum bending fatigue strength. Moreover Kiyoshi Funatani [59] in his investigation showed that a case to section size ratio of 0.0611 occurred at maximum bending fatigue strength.

Revising many other sources it was apparent that a range of case to section size ratio of 0.014 to 0.21, and as quoted by Tauscher [60], covers most of the findings for maximum bending fatigue strength.

Considering a gear component for instance, Kern [43] has described how to determine the case depth to resist case crushing of gear surfaces. First of all choosing the steel which develops a core hardness of 300-460 Hv, then

$$C.D. = \frac{2.1 \times 10^{-6} \, Wt}{F \cos x}$$

C.D. = effective case depth (to 530 HV) - mm

Wt = tangential tooth load - N

F = Face width - mm

x = Pressure angle

As far as the residual stresses are concerned, the work by Coleman and Simpson showed that the maximum compressive stress increases somewhat with section size and that the maximum compressive stress occurs deeper. Furthermore, they showed that increasing the case depth increases the depth of the stressed area. Meanwhile Luther, R.G. et al[61] has reported a compressive residual stress near the surface of 416 N/mm^2 in a 19 mm dia. bar having a case depth of 1.5 mm.

3.3.8 Residual Stresses

It has already been discussed how the residual stresses are influenced by many metallurgical variables. Therefore the influence of the residual stress on the fatigue strength is evident through those variables.

It is known that compressive residual stresses increase the fatigue strength. In this context, Bernhard Syrev et al[62] showed that the fatigue strength of CK 45 steel in reverse bending decreases as the residual stress decreases and changes from compressive to tensile. He quoted a bending fatigue strength of 920 N/mm^2 at -200 N/mm^2 residual stress in the hardened condition. It was also observed by

Ya Umaniskii et al [63] using 30Kh GSA steel, that increasing the compressive residual stress improves the bending fatigue strength. However Thomson [64] summarised, stating that the residual stress pattern generally could not be directly correlated with fatigue durability.

3.4 Fatigue Strength and Stressing Mode

Different applications may require carburised components to be subjected to various stress system.

As far as fatigue testing is concerned, there are three common methods of applying a stress cycle varying from a maximum nominal tensile stress to a numerically equal nominal compressive stress, i.e. a zero mean stress loading cycle [65]:

1 - Reversed direct stress - Push-Pull

2 - Reversed plane bending

3 - Rotating bending

On the other hand, unidirectional stressing is an alternative method, with the absolute value of the minimum stress above zero.

As far as case-hardened specimens are concerned, fatigue data in reversed direct stress are limited, for the simple reason that axial loading in the presence of a tensile stress at the core provides the most deleterous fatigue condition, stated Luther et al [61]. In this context he has reported 2% increase and 5% decrease of fatigue strength respectively upon case hardening.

However most of the fatigue data has been in rotating bending, e.g. Luther [61] showed improvement in the bending fatigue strength of about 60% in reference to normalised samples. Similarly, Frost et al [65] quoted about 50% increase in fatigue limit of carburised and quenched as compared

to that in received condition. So did others, e.g. results by Gardiner [66] using S 82 (4% Ni) steel showed an increase of about 10% in bending fatigue strength of carburised and hardened in reference to a hardened piece. Pathi Raj [58] using IS 20 MnCr case hardened steel showed 30% increase in bending fatigue strength of carburised and hardened over that of through hardened.

Perhaps the alignment of a rotating bending specimen during the test is the most worrying feature. Distortion during quenching a carburised rotating bending sample and the difficulty to ensure complete alignment in practice makes it possible for sequential whirling to occur and consequently affecting the data produced this way.

Such alignment is not likely to influence results produced by plain bending, whether reversed or unidirectional. In this respect and as far as reversed bending is concerned, Eriksson et al [67] using C-Mn steel showed about 80% increase in bending fatigue strength of carburised compared to the non-treated. On the other hand, Lazaridis [68] using SAE 4027 showed 40% increase in bending fatigue strength at 10^5 cycles of carburised and quenched compared to quenched and tempered, despite the fact that the case depth was 2 mm on a section thickness of 6 mm, i.e. case to thickness ratio of 0.33, above the literature findings for maximum bending fatigue strength, see section 9.7.

Data about the bending fatigue strength unidirectional bending was introduced by Krauss et al [44], see Fig. 24, and others, e.g. Depaul [69], where he investigated the fatigue behaviour of a range of steel SAE 4118, 4626, 4620, 4817 and Ex.1, at different case depths. His results at a case depth of about 1.0 mm are shown in Fig. 30.

3.5 Fatigue Strength and Mean Stress

In practice components for automotive drivelines, e.g. gears, are generally subjected to unidirectional bending. Despite this, there is extremely limited amount of data compared to rotating bending. Moreover as some case hardened components may exist under a high mean stress in practice, data concerning this effect would be useful.

3.5.1 Stress Ratio - Mean Stress

Stress ratio is defined as the minimum to the maximum cyclic stress [73]

$$R = \frac{\sigma_{min}}{\sigma_{max}} \quad \ldots\ldots\ldots\ldots\ldots\ldots \quad (1)$$

Its value is -1 under reversed stressing condition.

Unidirectional bending represents the case where the stress ratio could be zero, if the minimum cyclic stress is or close to zero, or greater than zero depending upon the value of the minimum stress.

Referring to Fig. 31, the mean stress (σ_m) may be expressed as:

$$\sigma_m = \frac{\sigma_{max} - \sigma_{min}}{2} + \sigma_{min} \quad \ldots\ldots\ldots \quad (2)$$

Using equation (1) the mean stress can be expressed in terms of the stress ratio as:

$$\sigma_m = \sigma_{max}\left(\frac{1+R}{2}\right) \quad \ldots\ldots\ldots\ldots\ldots \quad (3)$$

The above equation shows how the mean stress is related to the stress ratio through the maximum cyclic stress.

The effect of mean stress on the fatigue strength of different metals is generally expressed by Goodman and Gerber [70], diagrams as shown in Fig. 32.a.

However as far as case hardened components are concerned, Karuss et al[44] has determined the bending fatigue strength of carburised SAE 8620 steel at a stress ratio of a value greater than zero, where he used an R value of 0.26.

Hayama et al[71] using S45C, SNC21 and SNC steels, studied the effect of mean stress on fatigue strength of carburised steel in the tempered condition. His results are shown in Fig. 32.b. as a reference, despite the fact that the case depth was about 1.8 mm on a section 4 mm thickness.

3.6 Stress Concentration

Engineering components in practice may contain some form of stress raiser, such as fillet, hole, etc. However, in laboratory testing, those different forms of stress concentration features are represented by a notch. The stress acting at the root of the notch depends upon its radius, or in other words on the stress concentration factor.

A lot of work has been done on different metal to show that stress concentration features reduces the fatigue limit. Published work is presented in the form of fatigue strength versus stress concentration factor. Fig. 33 is an example of such presentation on mild steel [65].

As for a case hardened component, not much interest has been shown to study the effect of stress concentration.

However, Toru Funukawa et al [72] in his investigation using SCM21 steel specimens tested in rotating bending, showed that the bending fatigue strength of carburised steel were very similar at a stress concentration factor of 3 and 6. He also reported that crack propagation rate increases with crack length at high root radius (0.5 mm), and stay almost constant at a root radius of 0.08 mm.

Meanwhile Pathi Raj [58] illustrated the decrease in bending fatigue strength of carburised IS-20 MnCr as the

stress concentration factor increases. He showed a decrease of about 100 N/mm^2 when the stress concentration factor is increased from 1.5 to 1.9, as can be seen in Fig. 34.

Apart from the above-mentioned two sources no data is available.

In a gear component the stress concentration is between 1.2 and 2 [73], but in other engineering components, higher values of stress concentration may occur. Existing data, e.g. that due to both Raj [58] and Funukawa [72] was derived from rotating bending. Therefore there is a need for further data to broaden our understanding of these effects.

3.7 Notch Sensitivity

The general term "notch sensitivity" is used to relate the actual effect of a notch on the fatigue strength of a member to the effect one might expect from elastic theory. It is generally accepted in the field of metal fatigue to define the notch sensitivity as:

$$Q = \frac{K_f - 1}{K_t - 1}$$

where Q = notch sensitivity

K_f = fatigue notch factor

K_t = stress concentration factor (elastic theory)

If materials conform to elastic theory and fatigue strength depends on the value of the maximum principle stress then K_f would be equal to K_t. In fact K_f is often less than K_t. This discrepancy, which is expressed in terms of notch sensitivity, is due to plastic deformation at the root of the notch during cyclic stressing, stress gradient, and in addition, the presence of biaxial or triaxial stresses. Also residual stresses may influence the notched fatigue strength.

Under reversed stressing the material must continue to deform plastically in every cycle if the range of stress at a notch is to remain reduced, the ability of materials to behave in this way is quite limited. Therefore notches exert large influences under such conditions.

Under cyclic bending plastic deformation may influence both the plain and notched fatigue strength depending upon the applied and yield stresses. In particular in unidirect-

ional bending if the test piece yields by the first loading cycle it will then cycle according to the developed compressive and externally applied stresses[74].

Notch sensitivity under rotating bending conditions at different specimen sizes and stress concentrations are given in table 3 for a number of carbon and alloy steels. It can be seen that notch sensitivity increases with carbon and alloying contents. The low notch sensitivity quoted for the 20 Cr 10 Ni steel in the annealed condition would suggest the possibility of work hardening and plastic deformation, consequently raising the notched fatigue strength.

Pathi Raj [58] in his investigation using carburised I.S. 20 $MnCr_1$ steel in the tempered condition produced notched fatigue strength results. Notch sensitivity of 0.43 was determined from his results. That is considerably lower than those listed in table 3. Weigand et al [75] showed that compressive residual stresses can reduce the notch sensitivity of brittle material. He also concluded that internal compressive stress would raise the alternating fatigue strength of specimens subjected to embrittlement whether due to material, i.e. hardening, or due to shape embrittlement from a notch effect. Therefore the notch sensitivity of a carburised component is likely to be influenced by residual stresses, mean stress and notch root radius.

3.8 Fatigue Crack Initiation

Fatigue failure is generally considered to be the consequence of crack initiation and its subsequent propagation. However the process can be initiation dominated, where most of the fatigue life is consumed in the formation of a microcrack. On the other hand, it can be propagation dominated process, where the crack initiates early and it takes it the rest of the fatigue life to propagate and cause final failure.

Fatigue data in the form of S-N curves generally represent failure with no indication to the stress to initiation.

This has been the case for the fatigue data about case hardened components except one or two investigations where the fatigue crack propagation was studied and the initiation life was estimated.

In particular and as far as a case hardened component is concerned, it has already been made clear that most of the fatigue data are produced by rotating bending, where it is difficult to detect crack initiation during testing.

Considering the case of a high strength material, crack initiation is slipless, i.e. not as a consequence of slip process. However the possible mechanism would be the coalescence of microcracks to form a macrocrack which when of critical size leads to propagation and eventually failure.

Morris et al[76] showed that the specimen lifetime is partly governed by the formation of such macrocracks. In the same context Lankford [77] showed that when fatigue life was 10^5 cycles for high strength steel, 10^3 cycles were required to initiate a matrix microcrack which may develop to a macrocrack stage. Moreover he suggested that most of the initiation period which is associated with the total fatigue life of martensitic steels consists of the intermitent growth of very small cracks impeded by prior austenite boundaries.

Kozyreve et al[78] has reported that the durability of the case hardened specimen containing a notch is mainly governed by the time of transmission of the fatigue crack into the core, and showed that about 94% of the total life was consumed in developing the crack.

On the other hand Magnusson et al [79], using low alloy case hardened steel, showed that the initiation of the fatigue crack tends to occur after about 90% of the fatigue life and pointed out that slag inclusions acted to initiate the crack.

3.9 Fatigue Fracture Mechanisms

Fatigue crack initiation in case hardened steel is believed to be associated with transgranular fracture, and then an intergranular propagation through the case.

For instance Krauss et al [44] showed that the case fracture surface away from the initiation zone is intergranular, and reported that not all the case fracture was intergranular. They stated that much of the fracture was transgranular through the martensite and retained austenite.

They also showed that fracture initiation was very smooth, flat and transgranular in the case.

Eriksson et al [67] confirmed that the fracture surface of the case is intergranular, and reported that the centre of the fish eyes on the fracture surface was 0.7 mm below the surface, and so he claimed a sub-surface origin of crack initiation.

Lazaridis [68] on the other hand made confirmation of the transgranularity of initiation and the intergranularity of crack propagation in the case, changing into a mixed mode, i.e. inter-transgranular, and finally to entirely ductile fracture with dimples.

It is apparent that the fracture surface gives an indication of the crack initiation site, microcracks and the intergranularity of propagation through the case.

3.10 Step Loading Technique

Fatigue test data are generally presented in S-N form; to produce part of the S-N curve, e.g. 10^5 - 10^6 cycles, at least 20 samples would be needed.

However fatigue testing may aim at a variety of purposes, depending upon which the number of samples tested and the procedure followed through the test will be selected.

In view of the wide aims of the present work and the need to restrict fatigue testing tomanaginable levels, it was decided to determine the bending fatigue strength at 10^6 cycles based on the ASTM "A Guide for fatigue testing and statistical analysis of fatigue data" [80].

It was felt that the increasing amplitude test - Step Method - would fit the present programme, although in this method it has been observed that under-stressing does not greatly affect the true fatigue limit of materials such as many of the alloy steels and a few nonferrous materials [81].

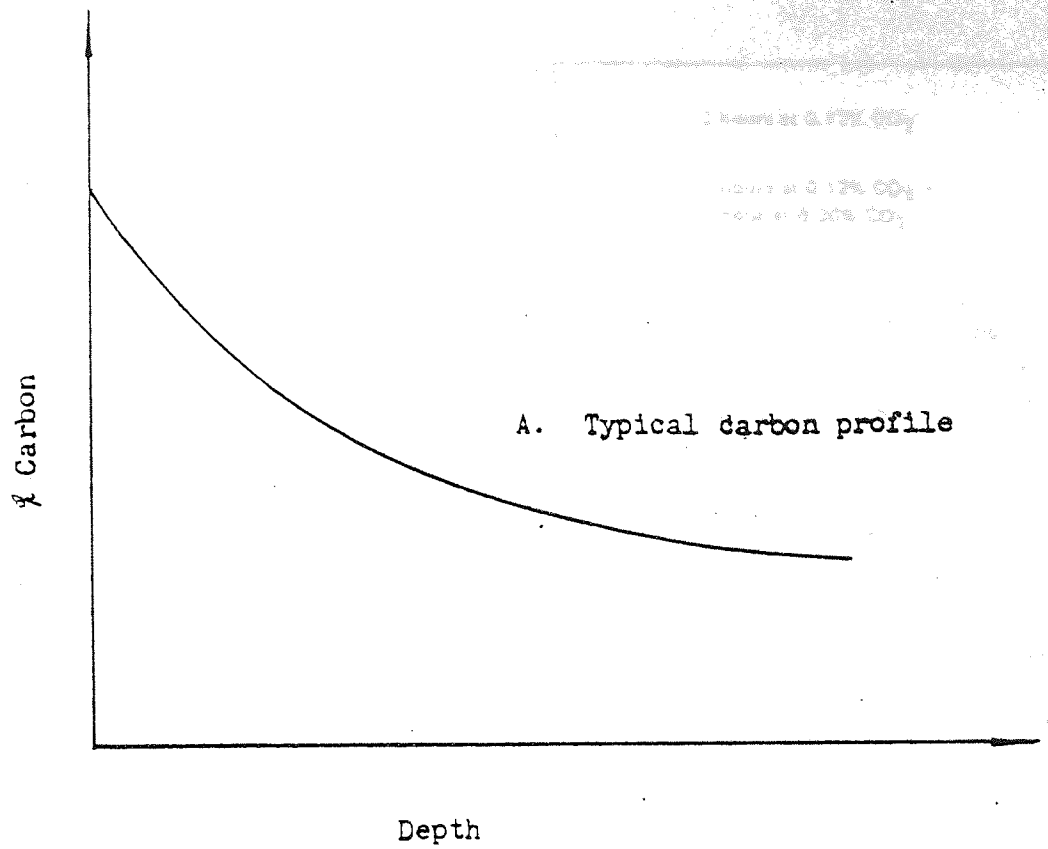

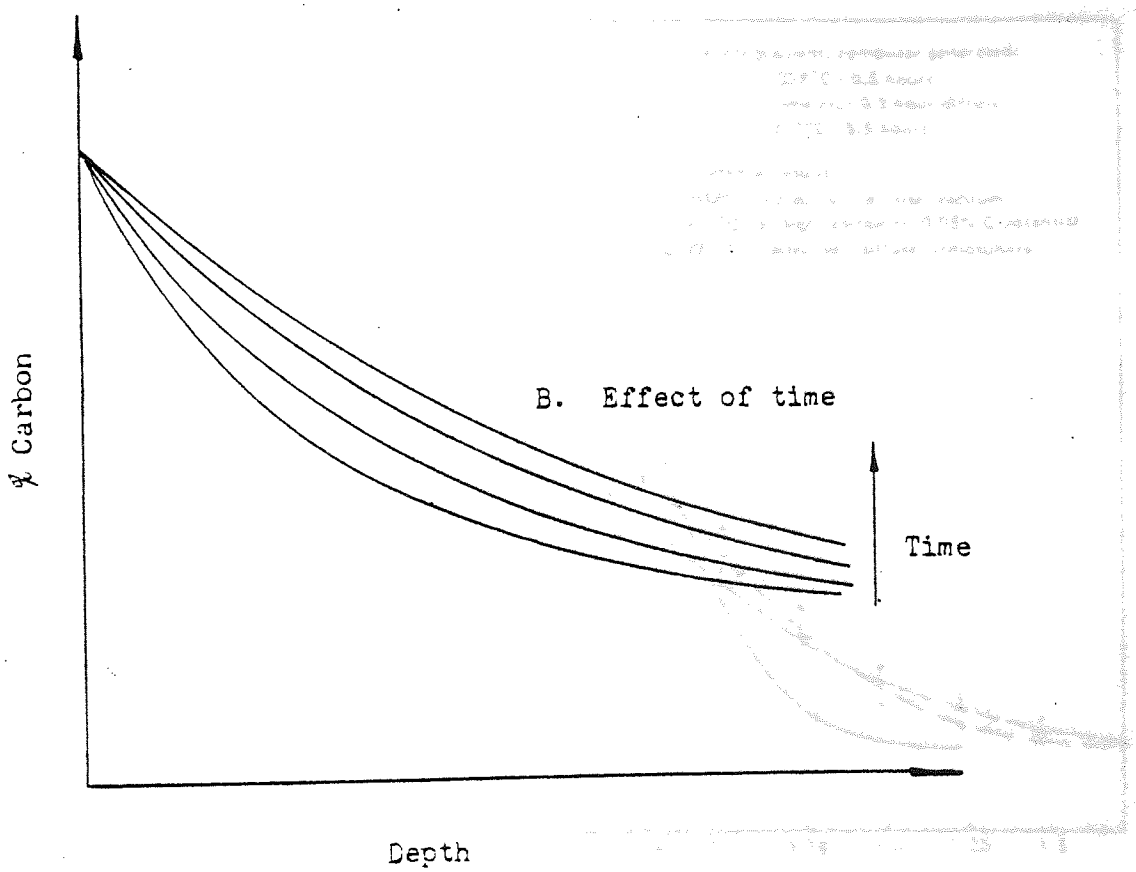

Fig. 1 Effect of diffusion on carbon profile.

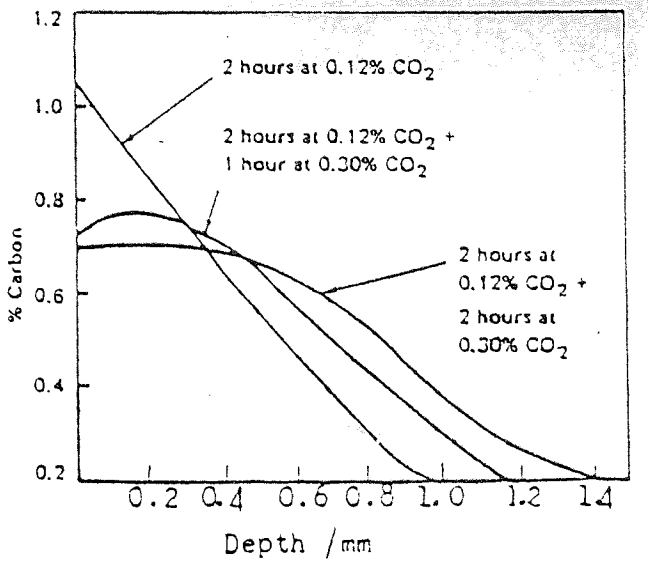

Fig.2 Optimisation of boost/diffuse ratio for En 354 carburised in endothermic gas/propan at 925°C.(6)

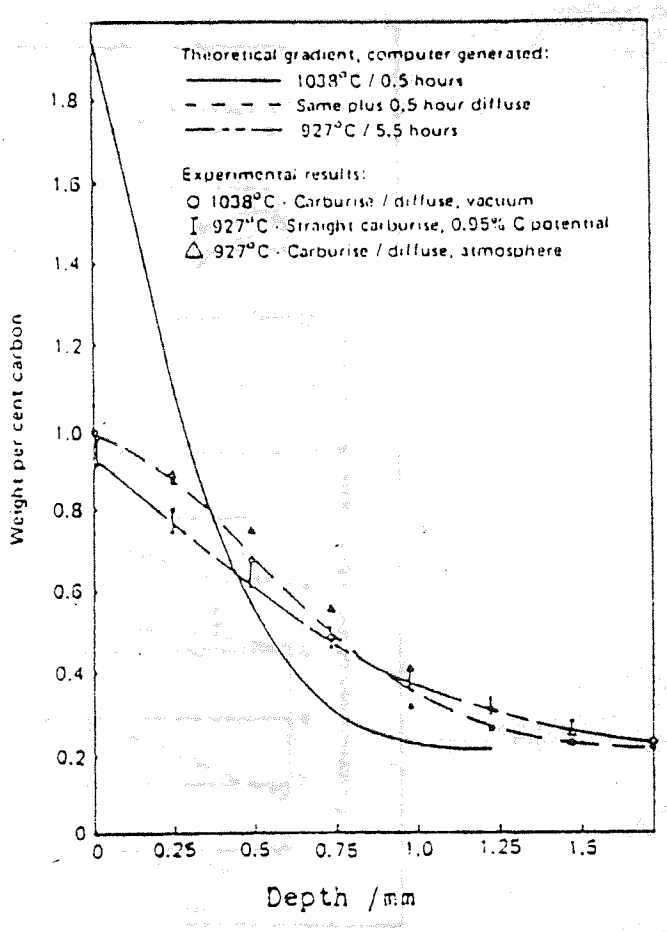

Fig.3 Carbon gradient of SAE 8620 steel.(7)

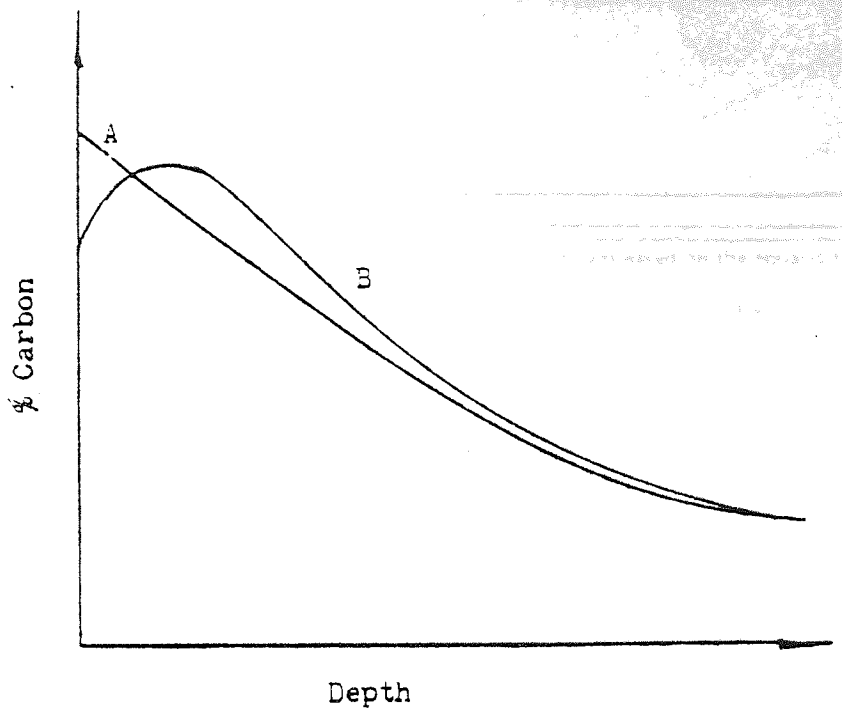

Fig.4 Carbon distribution in an as carburised surface (A), and in a carburised and diffused treatment (B).

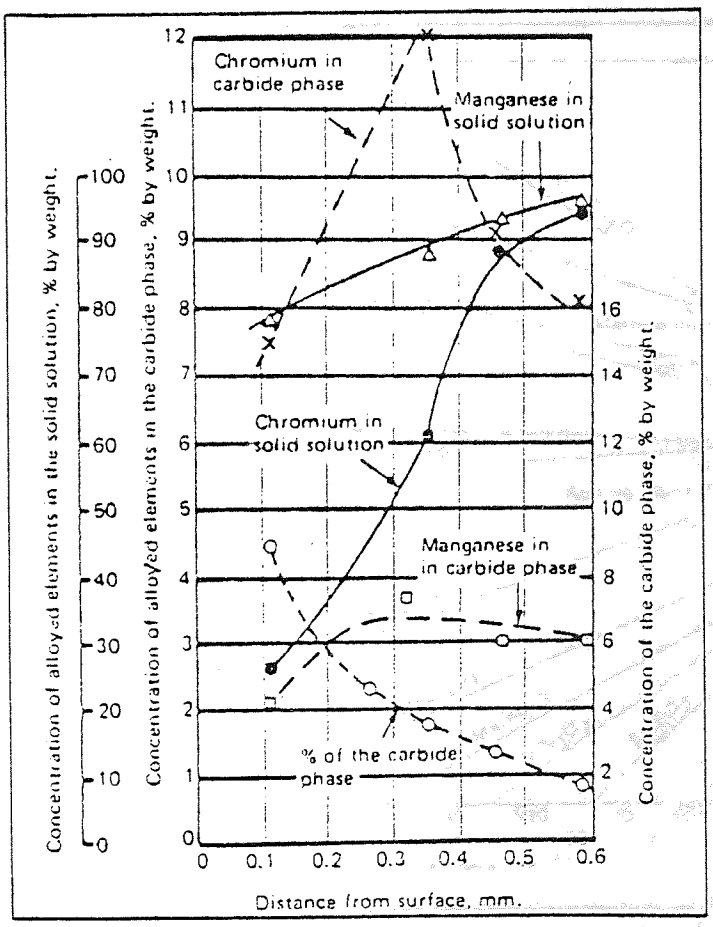

Fig. 5 The distribution of alloying elements between phases in the case-hardened layer of 25KhGT steel after quenching and tempering.(21)

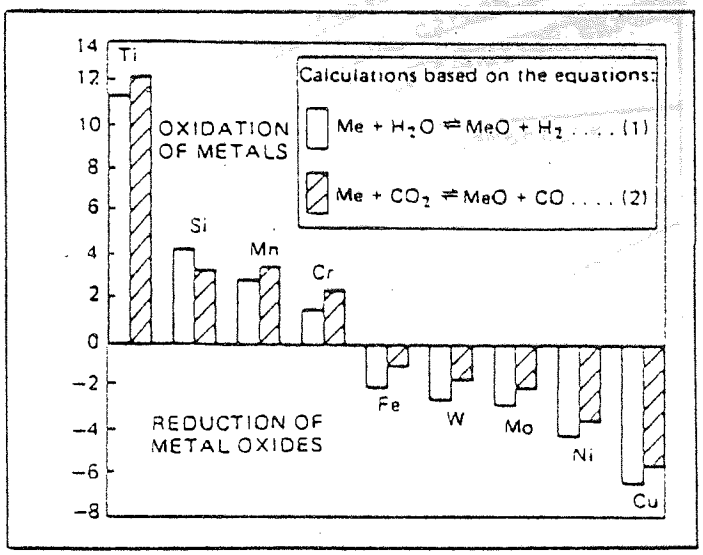

Fig,6 Oxidation potential of alloying elements and Iron in steel heated in endothermic gas with an average composition of 20%CO,1.5%CH_4,0.5%CO 0.28%H_2O (dew point -10C),37.72%N_2.[2] (3)

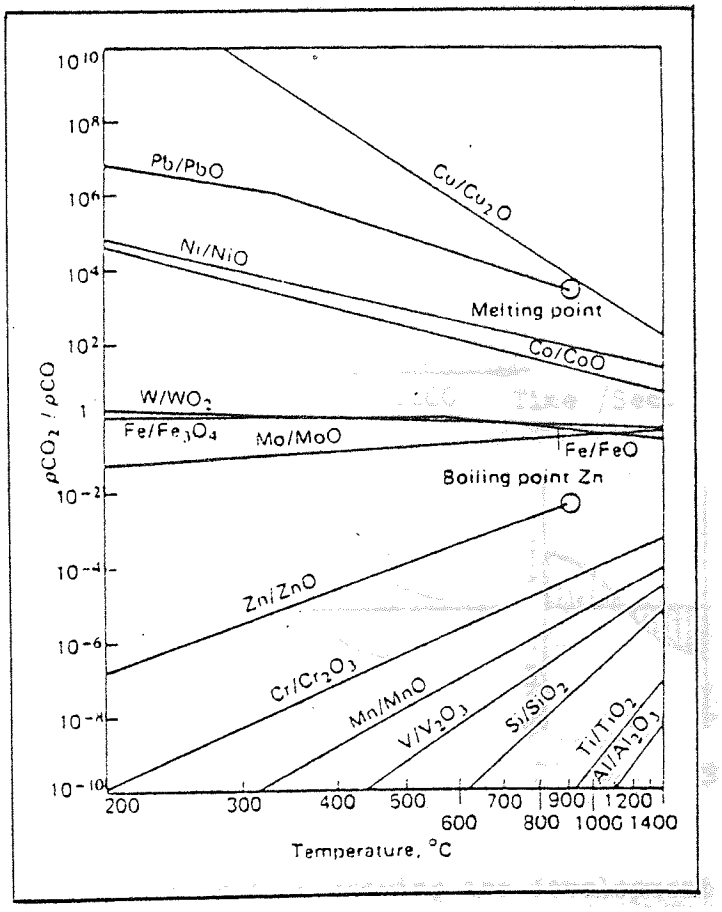

Fig.7 Effect of Carbon dioxide to Carbon monoxide potential at different temperatures on the oxidation of some metals.(3)

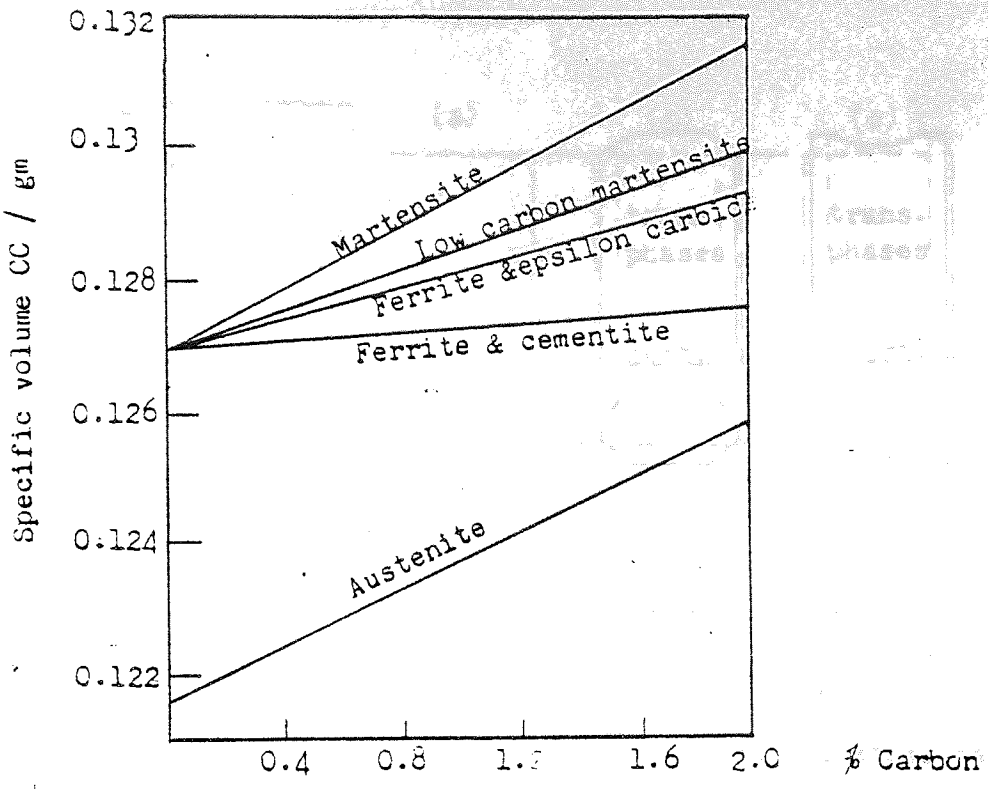

Fig. 8 Specific volume of steel phases versus carbon content.(88)

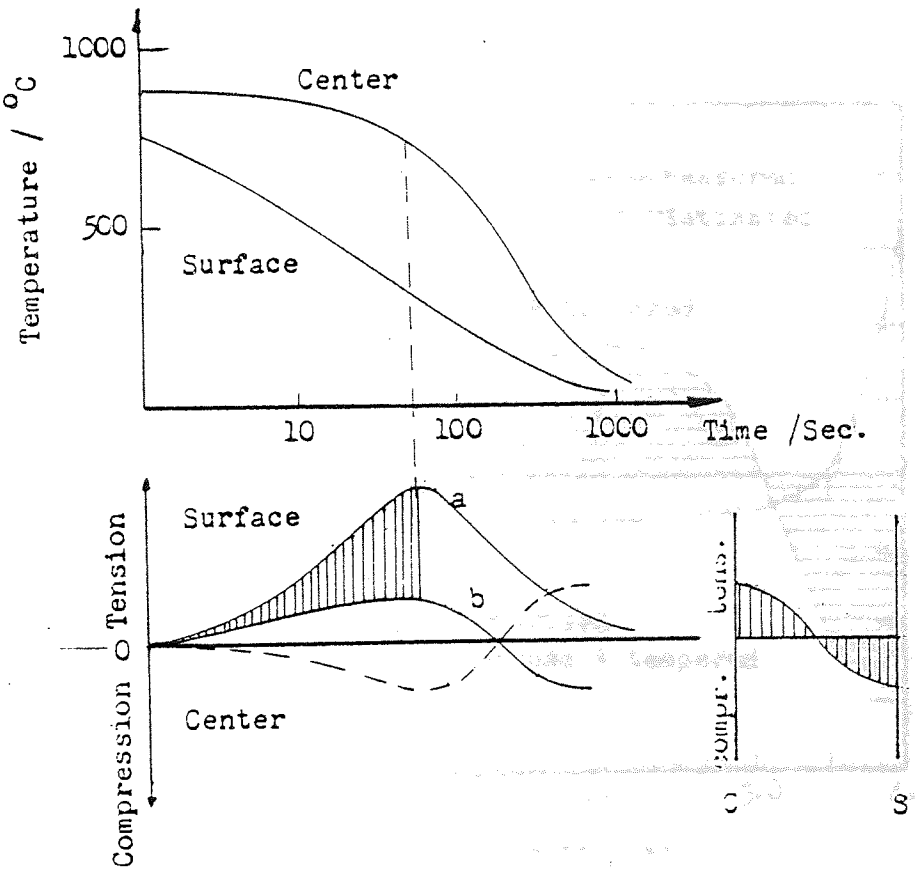

Fig.9 Schematic illustration showing the development of residual stresses on cool-down of metallic material.(27)

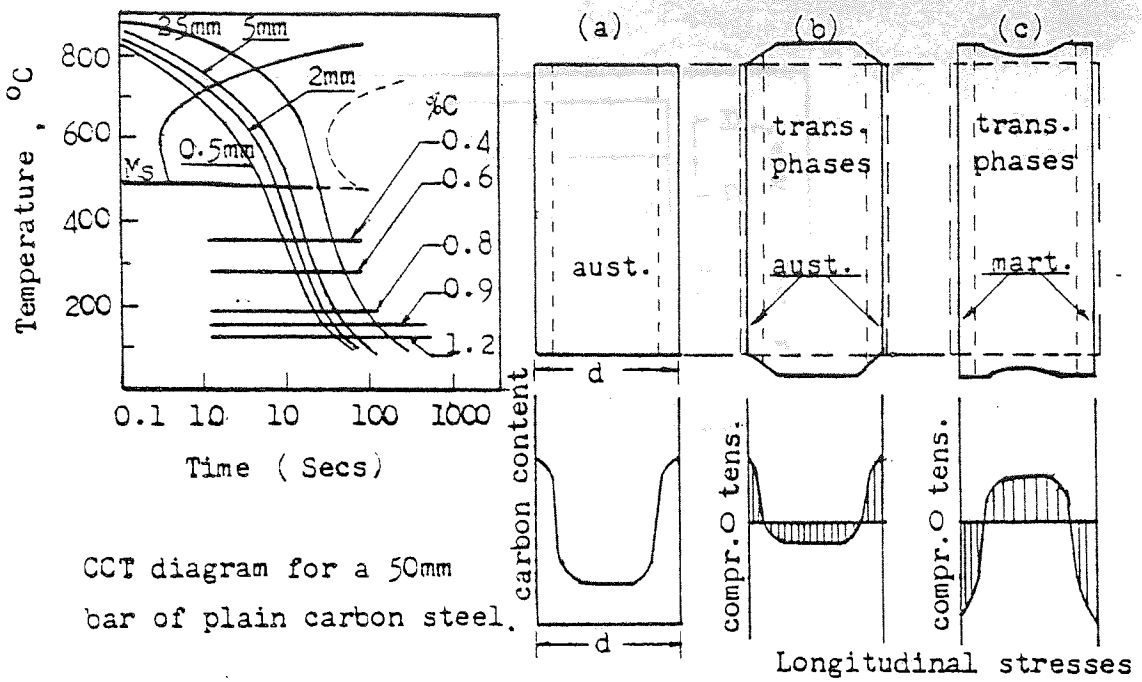

Fig.10 Schematic illustration of the development of residual stresses on quenching a case-carburised plain carbon steel (0.15%C) bar, 50mm dia. (28)

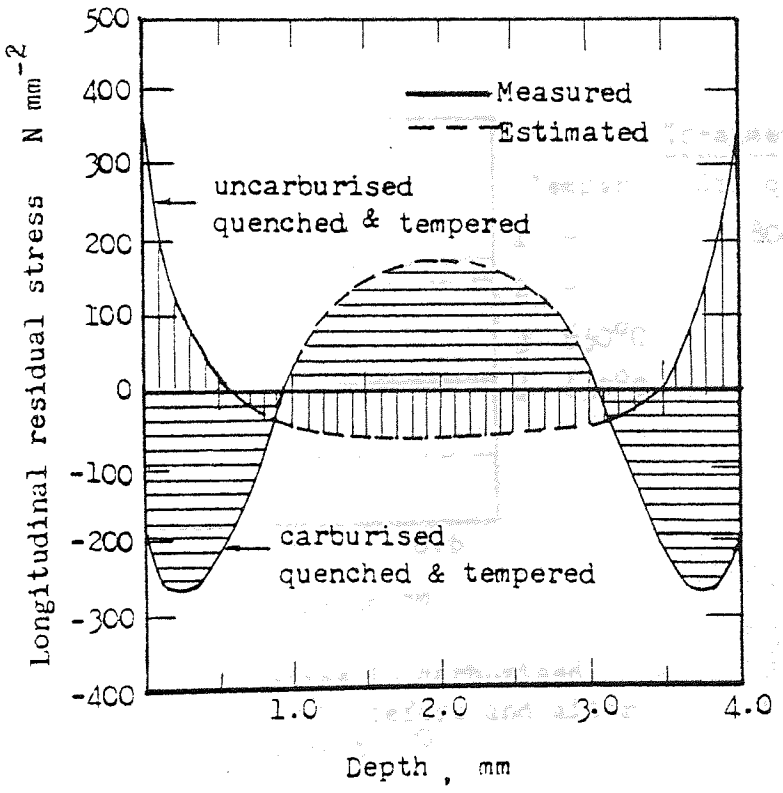

Fig. 11 Measured residual stress distributions (longitudinal only) in both carburised and uncarburised chrome-carbon steel. (28)

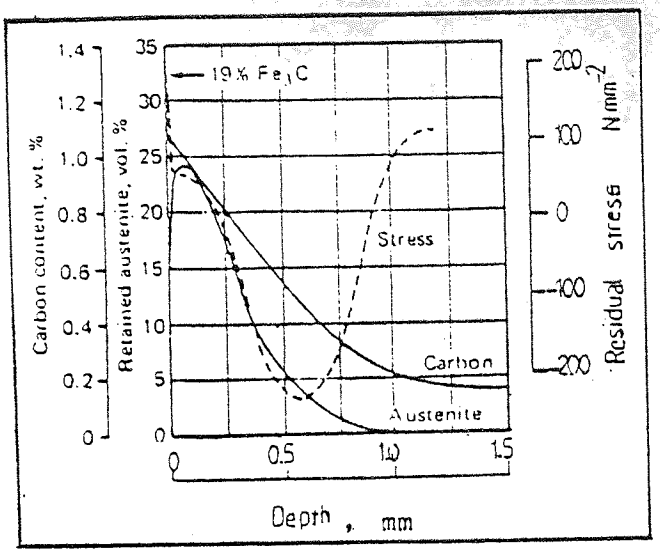

Fig.12 Surface tensile stresses in the outer layer of a carburised SAE1018 steel, caused by the presence of carbides (12).

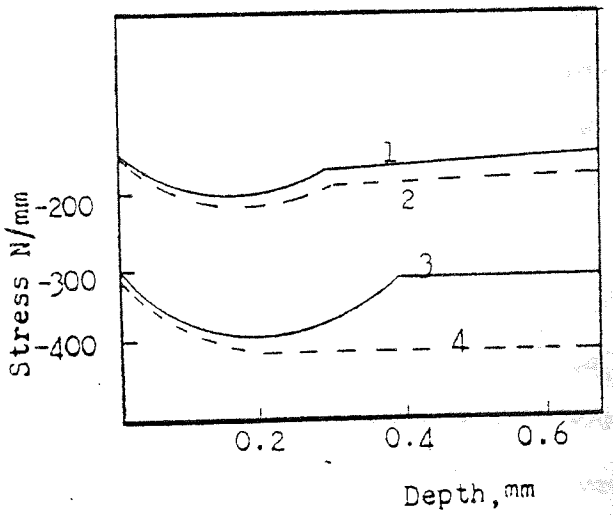

	Temper	Treatments: Oil quench	Sub-zero
1	-	800°C	-
2	-	"	-120°C
3	650°C	"	-
4	650°C	"	-120°C

Fig.13 Residual stresses in carburised case of 18Kh2N4VA before and after sub-zero treatment.(30)

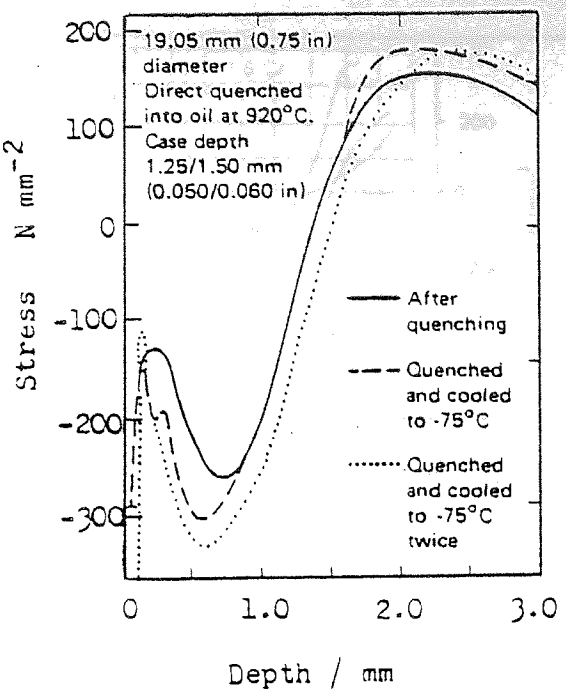

Fig. 14 Residual stress in carburised case of SAE 9310 before & after sub-zero treatment.(29)

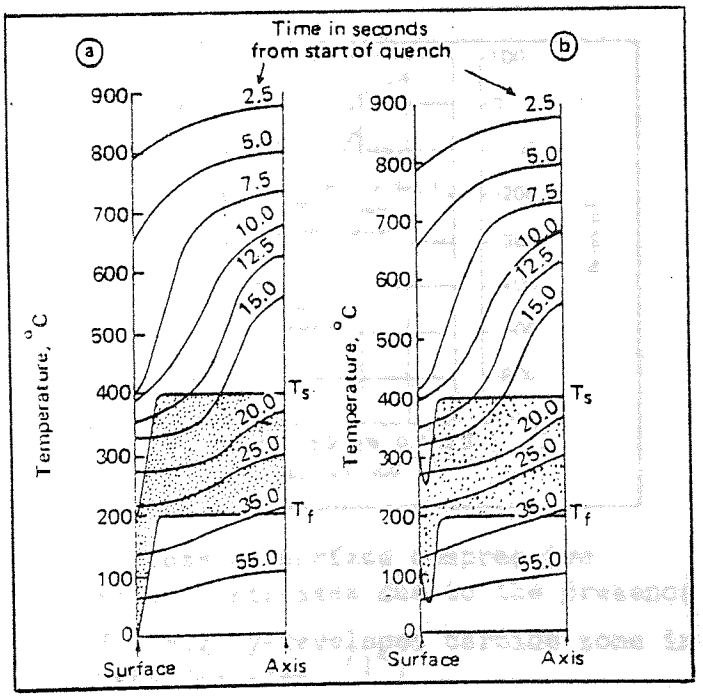

Fig. 15 The effect of decarburisation on the progress of transformation of a carburised surface(8):

a. Free from decarburisation.

b. Decarburised surface.

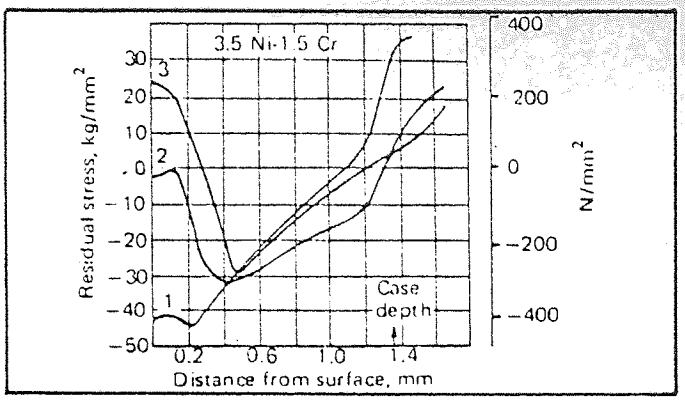

Fig 16 The effect of decarburisation on residual stresses developed in carburised and hardened plates. The carbon content at 0.002mm was estimated to be:-
Curve1, 1%; Curve2, 0.64%; Curve3, 0.35%(31)

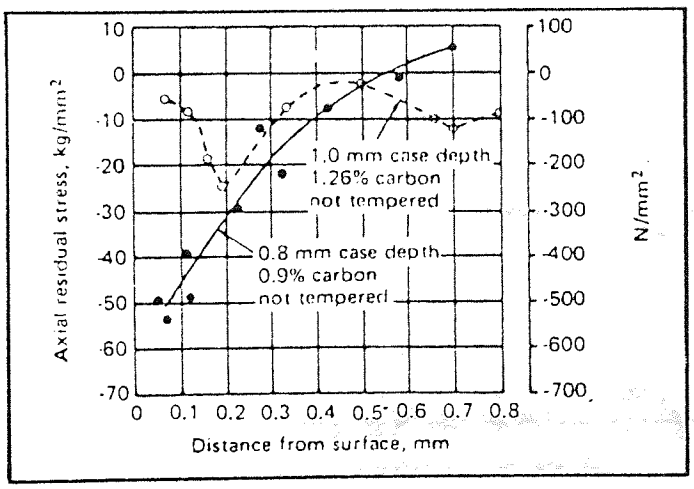

Fig.17 The loss of surface compressive residual stresses due to the presence of a highly-developed carbide zone in 20KhNV4MF steel.(47)

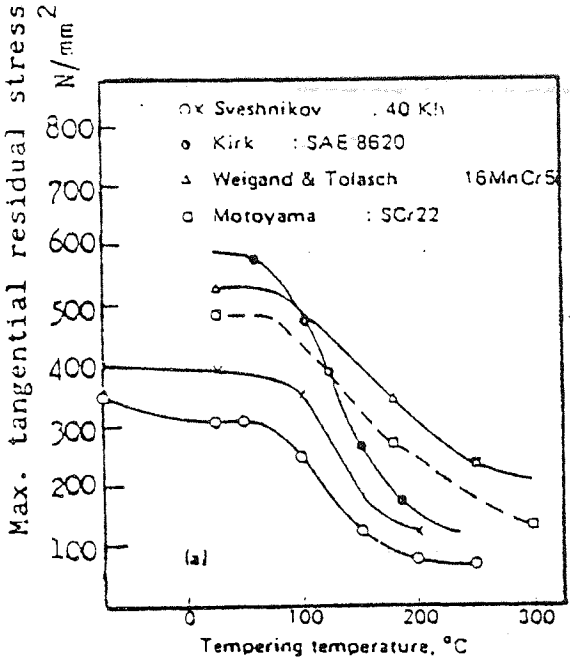

Fig.18 The change in peak compression due to tempering after carburising and oil quenching.(33)

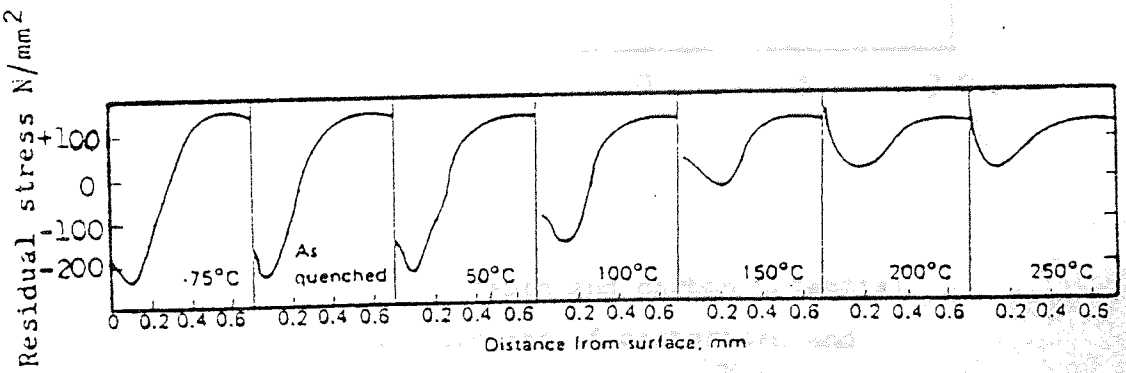

Fig.19 Residual stresses (tangential) in cyanide-hardened 40Kh rings before and after tempering.(33)

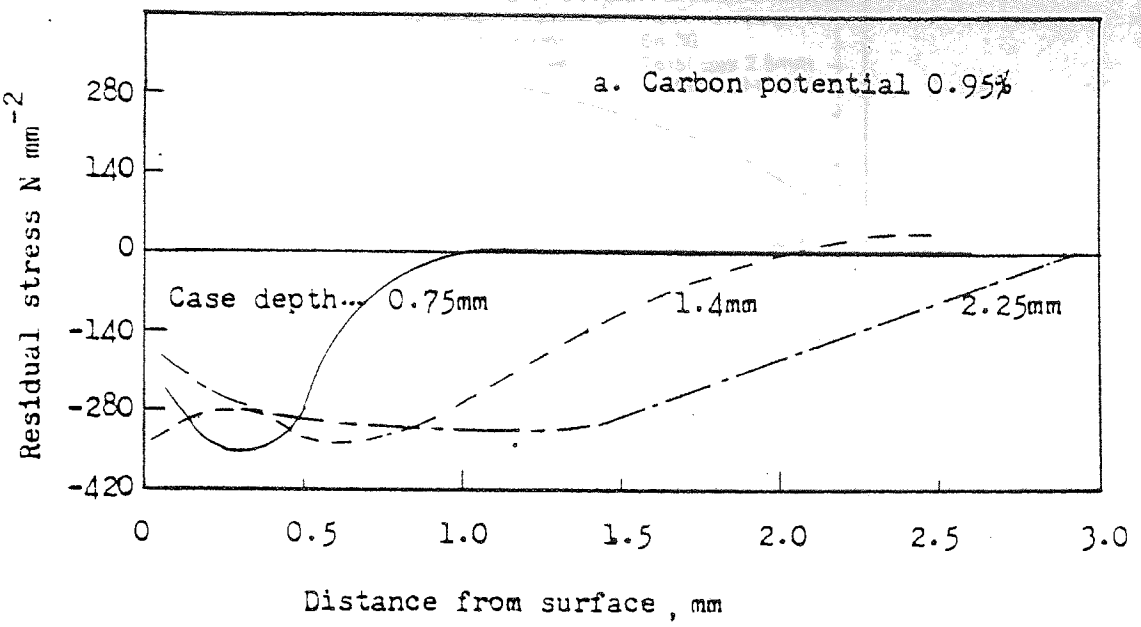

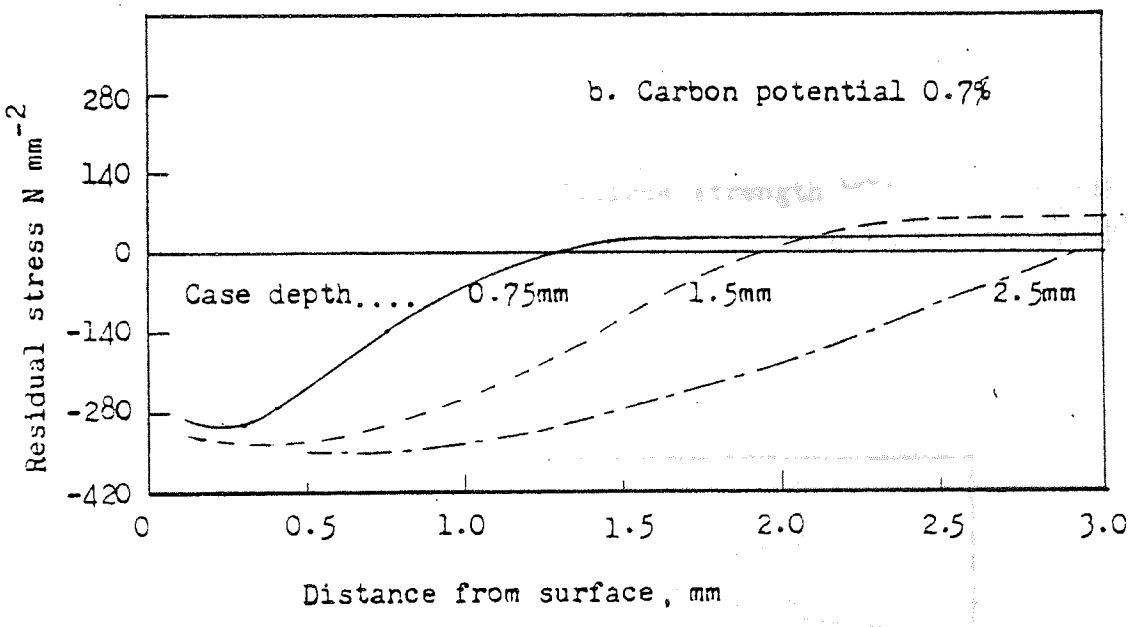

Fig. 20 The effect of case depth and carbon potential on the residual stresses of carburised and oil quenched, SAE 8617(19mm dia.).[29]

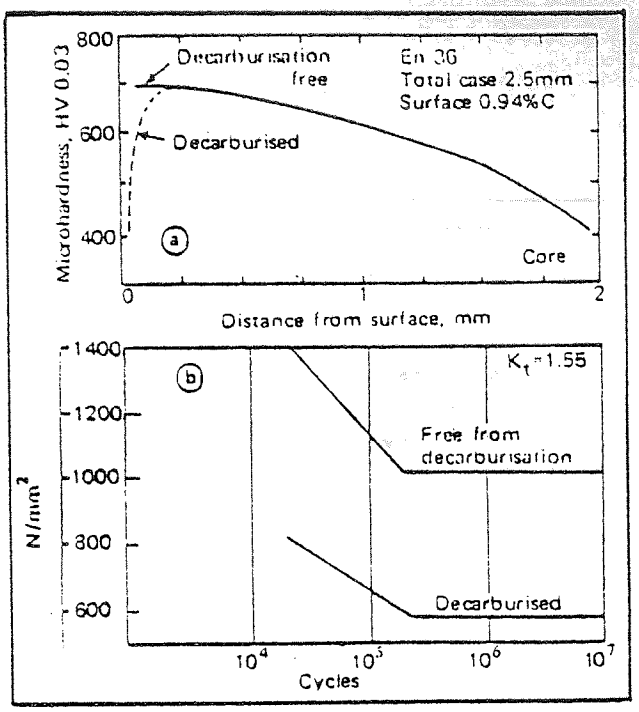

Fig.21 The effect of decarburisation in carburised En 36 steel, on a. Microhardness and b. Bending fatigue strength (36)

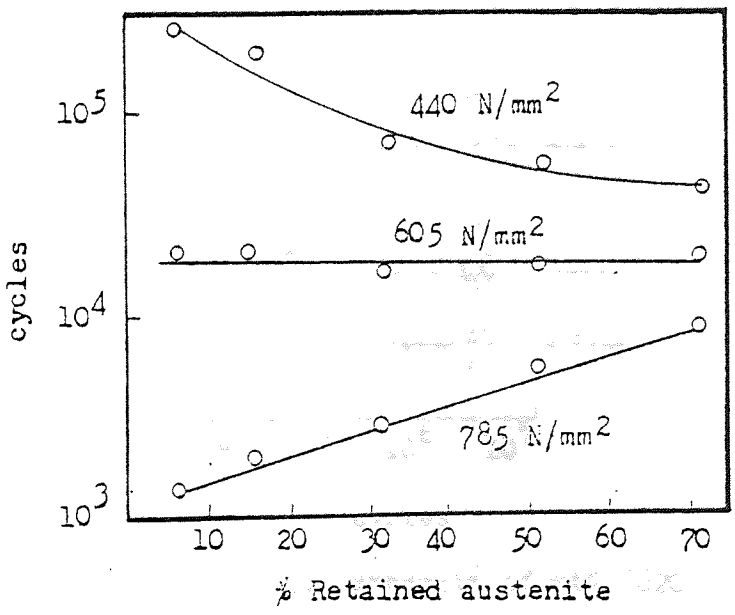

Fig. 22 Effect of retained austenite on the impact fatigue resistance of a 1.45%C / 11.5%Cr steel. (40)

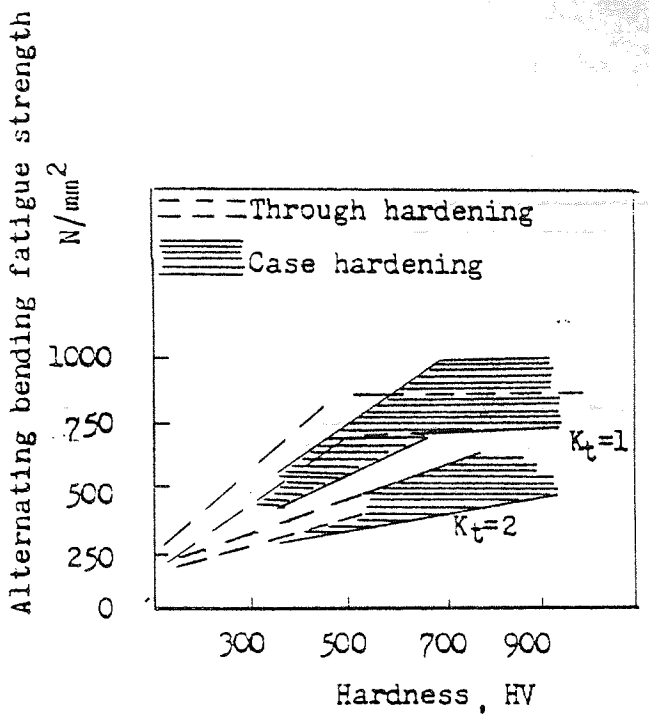

Fig. 23 Rotating bending fatigue strength of case-hardening, through hardening and tool steels as a function of surface hardness.(42)

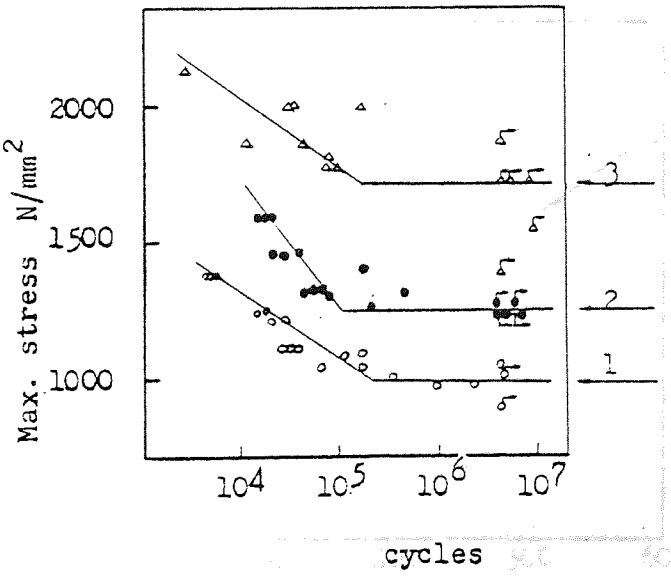

Fig. 24 Bending fatigue strength of SAE 8620
1. Direct quench; 2. Single reheat and 3. Double reheat, after carburising. (44)

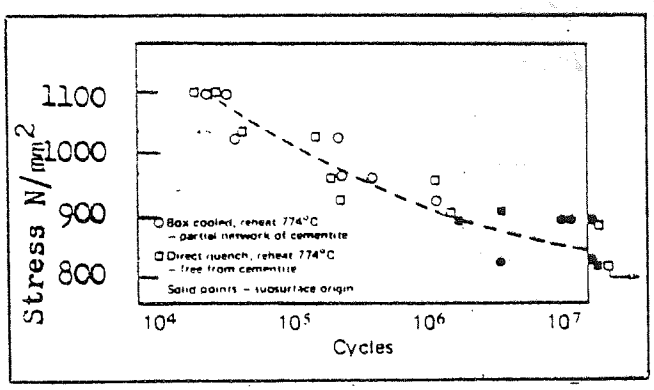

Fig.25 The bending fatigue strength of carburised samples of SAE 6120, comparing those containing a partial network of cementite with those free from cementite.(48)

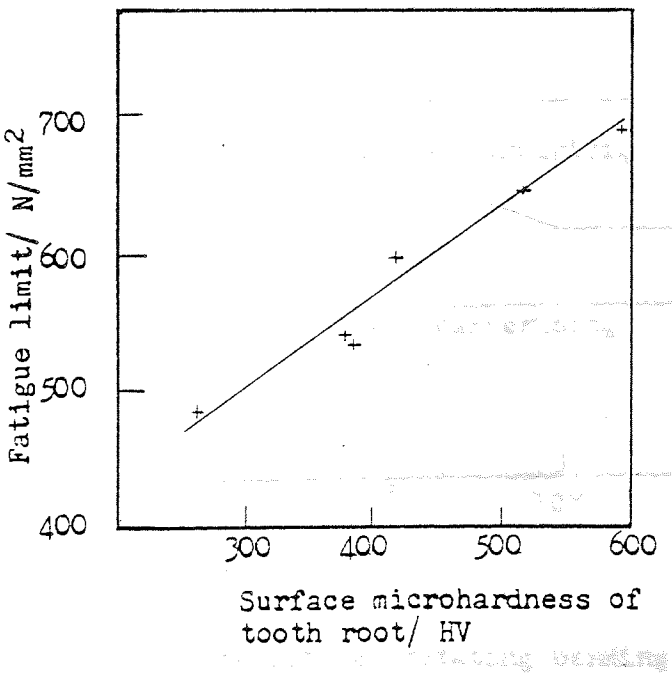

Fig. 26 The effect of tooth root surface hardness on the bending fatigue strength of 4mm modulus gear.(52)

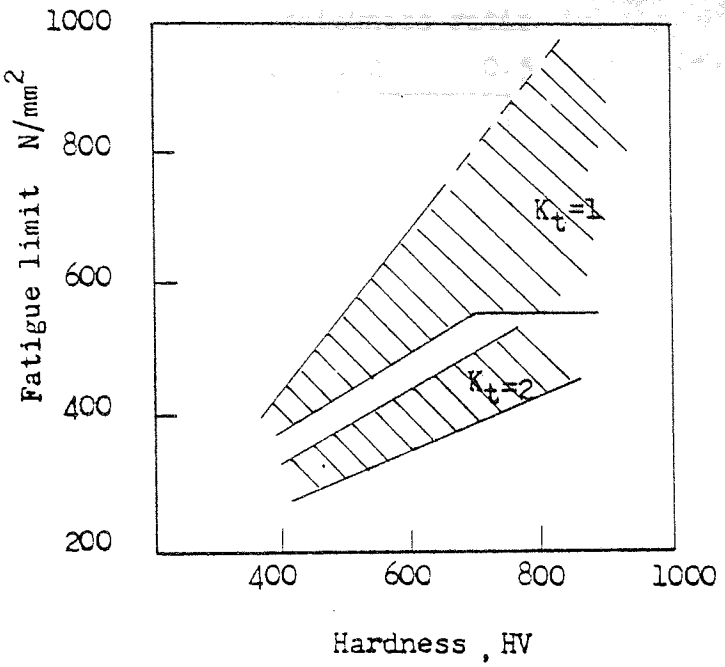

Fig.27 The rotating bending fatigue strength of case hardened 12mm dia. specimens notched and unnotched.(42)

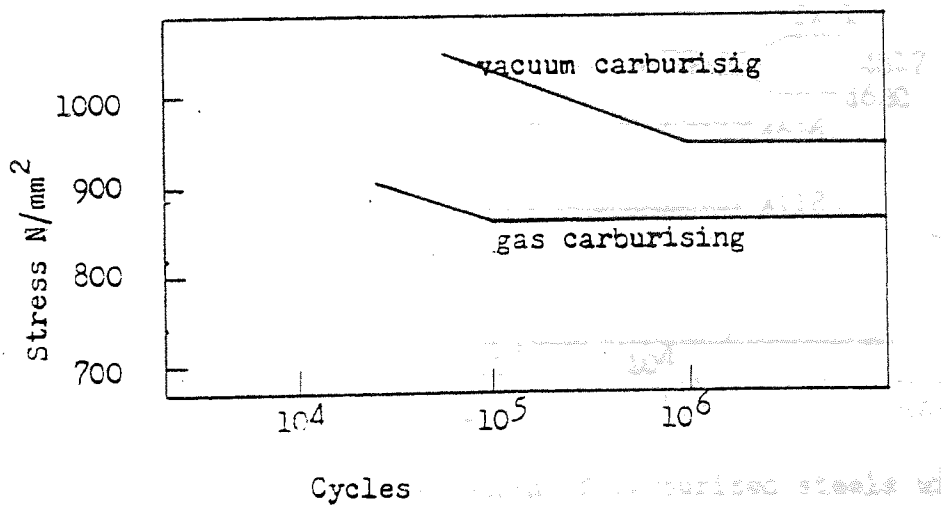

Fig.28 Fatigue chracteristics (rotating bending), of SAE 4320 with vacuum and conventional carburising (Tempered at 160°C for 4 hrs.)(56)

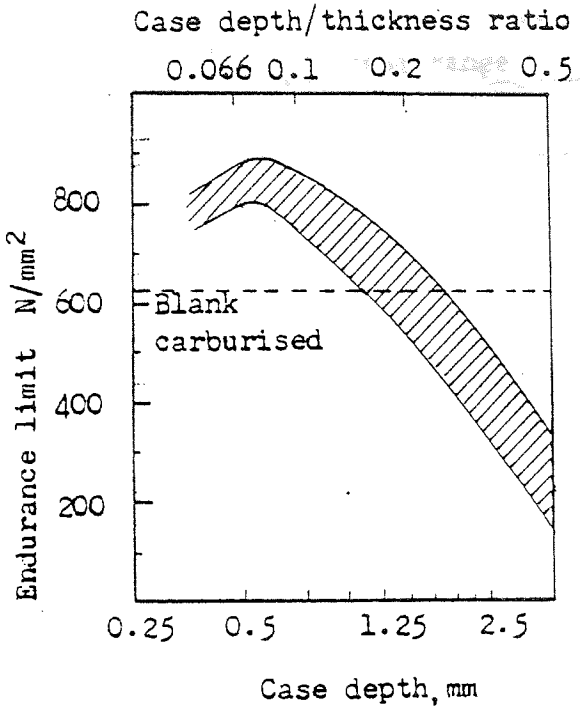

Fig.29 The relationship between fatigue strength and case depth for En 353 and 354 case hardening steels.(5)

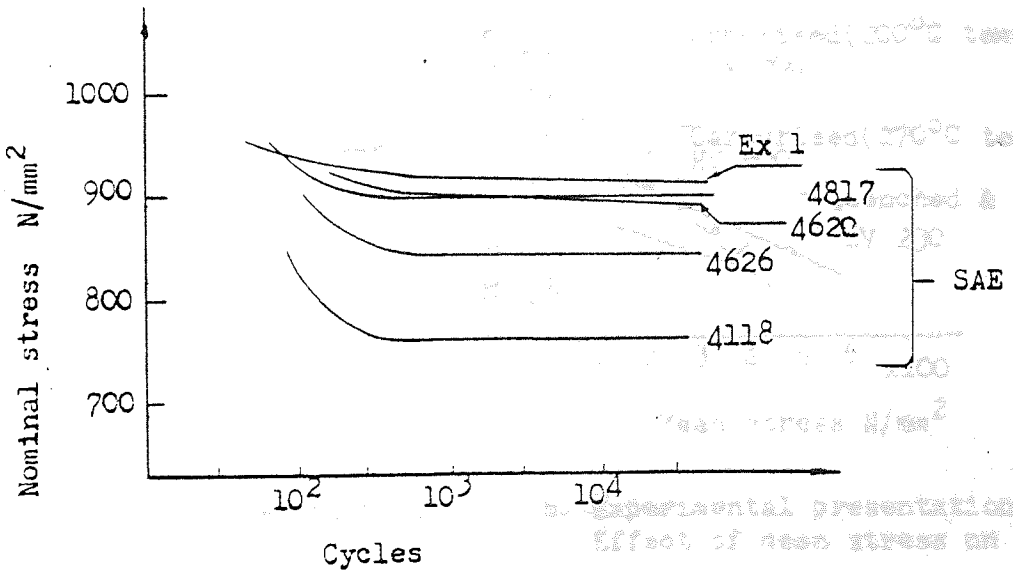

Fig.30 Bending fatigue strength of carburised steels with a case depth of about 1.0 mm .(69)

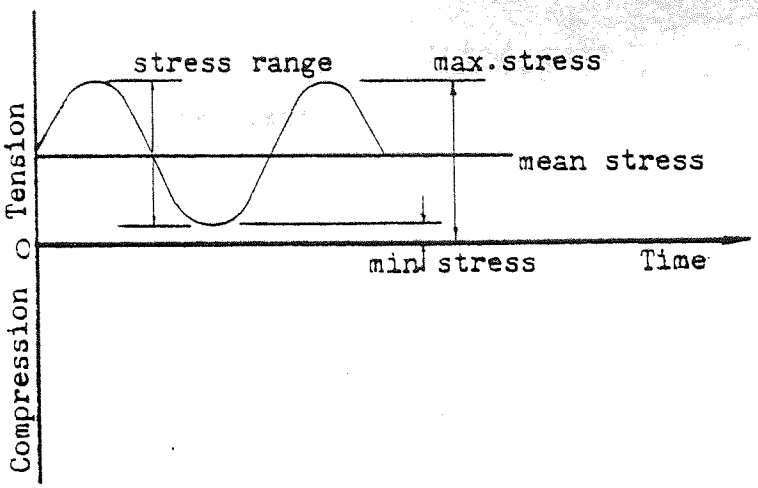

Fig.31 Tensile stress cycle

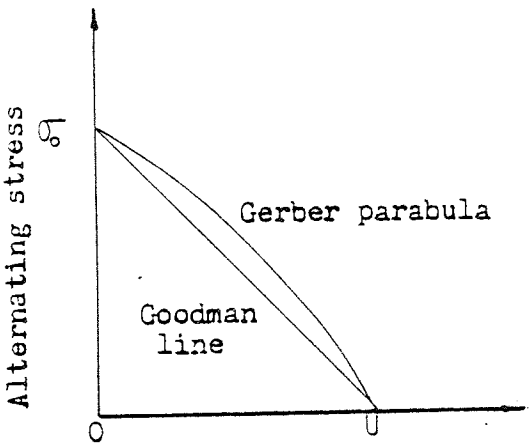

a. Theoretical presentation.
(U) tensile strength
(σ_o) fatigue strength

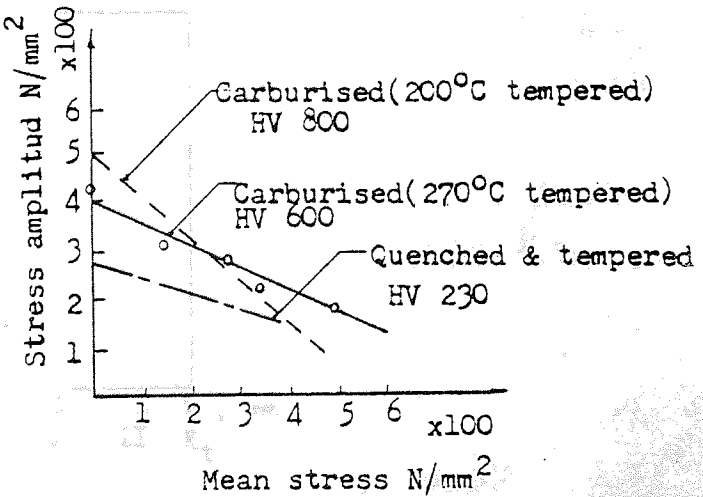

b. Experimental presentation,
Effect of mean stress on the fatigue strength of carburised , quenched and tempered specimens.

Fig.32 Mean stress effect on fatigue strength.(71)

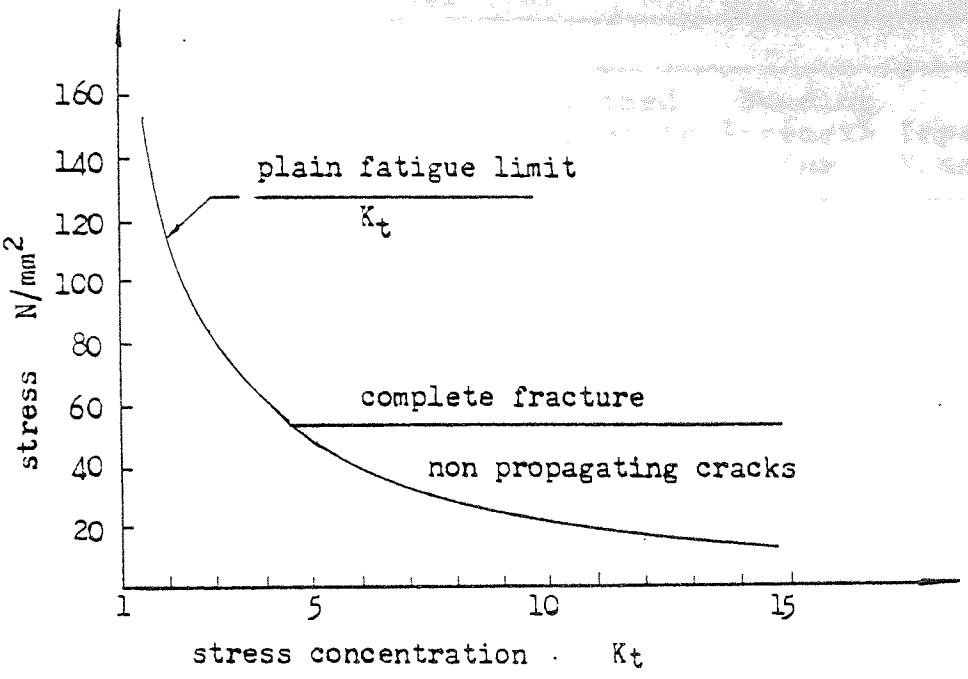

Fig. 33 Nominal alternating stress versus K_t for reversed direct stress mild steel specimens.(65)

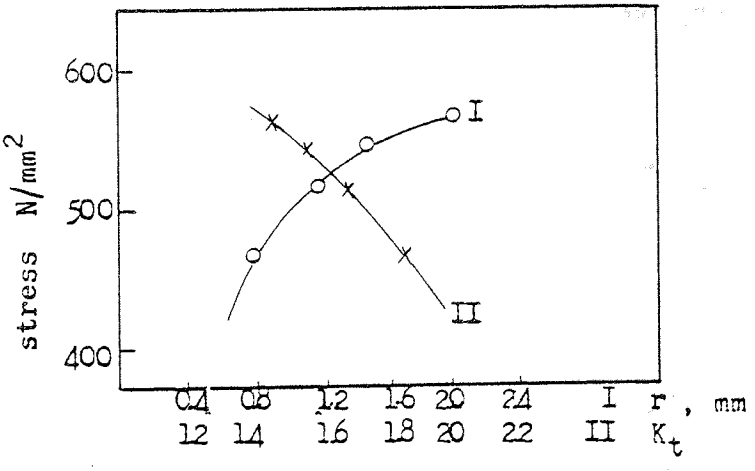

Fig. 34 The effect of stress concentration factor (K_t) - notch root radius (r) - on rotating bending fatigue strength of carburised steel specimens.(58)

TABLE 1

The effect of sub-zero treatment (-120°C) on the properties of carburised 18Kh2N4VA (30)

Heat treatment after Carburising	Condition	Retained austenite %	Bending Strength Nmm	Impact N/mm^2	Hardness H.V.
1. Oil quenched from 800°C; low temperature tempering	As quenched	62	1530	25.5	600
	Sub-zero	20	1442	19.5	790
2. Tempered at 650°C; oil quenched from 800°C, low temperature tempering	As quenched	34	1697	40	740
	Sub-zero	10	1608	-	790
3. Air cooled from 900-750°C oil quenched; low temperature tempering	As quenched	90	1618	59	470
	Sub-zero	20	1353	19.5	740

TABLE 2

The effect of depth of non-martensitic layer on hardness, residual stress and bending fatigue strengths in carburised and tempered 4 mm modulus gear (52)

Steel	Case depth mm	Depth of non-martensitic layer µm	Microhardness in tooth root H.V.	Residual stress at 10µm depth N/mm^2	Bending fatigue limit N/mm^2
20 Kh NM	1.2	7	560/720	0-(+ 50)	695
25 MO5Kh 05	1.2	6	510/575	-	646
18 Kh GT	1.2	16	415/440	+(253-432)	598
30 Kh GT	1.0	30	375/440	+(139-185)	540
18 Kh GT	1.2	17	380/500	-	532
18 Kh 2N4VA	1±0.5	17	265/575	-	482

TABLE 3

Notch Sensitivities of Carbon and Alloy Steels

Carbon or Alloy steel	Stress concentration Factor K_f	Fatigue strength Factor K_f	Notch sensitivity Q	Reference
0.18% C	3.3	2.4	0.61	65
0.3% C	2.0	1.8	0.8	65
0.37% C	3.3	2.3	0.56	65
0.4% C	2.0	1.8	0.8	65
Ni-Mo	3.3	3.0	0.87	65
Annealed 20 Cr 10 Ni	2.6	0.8	0	74

NOTATIONS FOR SPECIMENS AND GROUP DESIGNATION

G	Gas Carburising
V	Vacuum Carburising
H	Only Hardening
R.B.	Rotating Bending
3.P.B.	Three Point Bending
4.P.B.	Four Point Bending (Notched Condition)

4.0 Experimental Procedure and Techniques

4.1 Design and Production of Test Pieces

A range of test pieces were designed to meet various requirements in the project. Design was carried out according to testing machine capacity, section size to provide a reasonable case to diameter ratio and finally a span to diameter ratio of 6.6 [82] for three-point bending test pieces.

Test pieces were produced according to the required dimensions, however slight variation in the dimensions were found. This was taken care of in the calculations.

4.1.1 Material and Test Piece Geometry

Three types of carburising steels were used as the material for the test pieces in this work. Basically 635 A14 steel was used for preparing the majority of specimens for fatigue testing, in the programme, however test pieces of 835 A15 steel were also used in a primary stage of the test programme.

In addition steel type 080 M15 was used for:

1. The estimation of residual stresses
2. Investigating the effect of stress concentration factor
3. Skimming bar for determining the carbon profile by chemical analysis.

The chemical compositions of the steels involved with their designations are listed in the following table.

Steel	C	Si	Mn	Ni	Cr	Mo
635 A14	0.15	0.24	0.67	0.75	0.52	-
080 M15	0.15	0.12	0.64	-	-	-
835 A15	0.16	0.24	0.23	3.89	0.9	0.21

Cylindrical specimens were selected for the fatigue testing programme in order to produce uniform carburising and on subsequent hardening a uniform residual stress distribution. This geometry is preferred to rectangular. Corner effect in rectangular geometry is likely to result in carbide formation [83] in the corners and create a complicated stressing situation.

4.1.2 Test Pieces Preparation

1. Three-point bending (3-P.B) test pieces were turned from stock round bar of 635 A14 steel. Flat surfaces at the loading points were milled - see Fig. 35a - to avoid twist and specimen movement during the test. Finally specimens were polished by emery cloth. For full dimensions and geometry see Fig. 35a.

2. Four-point bending (4-P.B) test pieces were turned from 635 A14 steel bars, then notched in the middle circumferentially with a stress concentration factor of 1.5. Values between 1.2 and 2 for gears were reported by Vallance et al [73]. Flat surfaces at

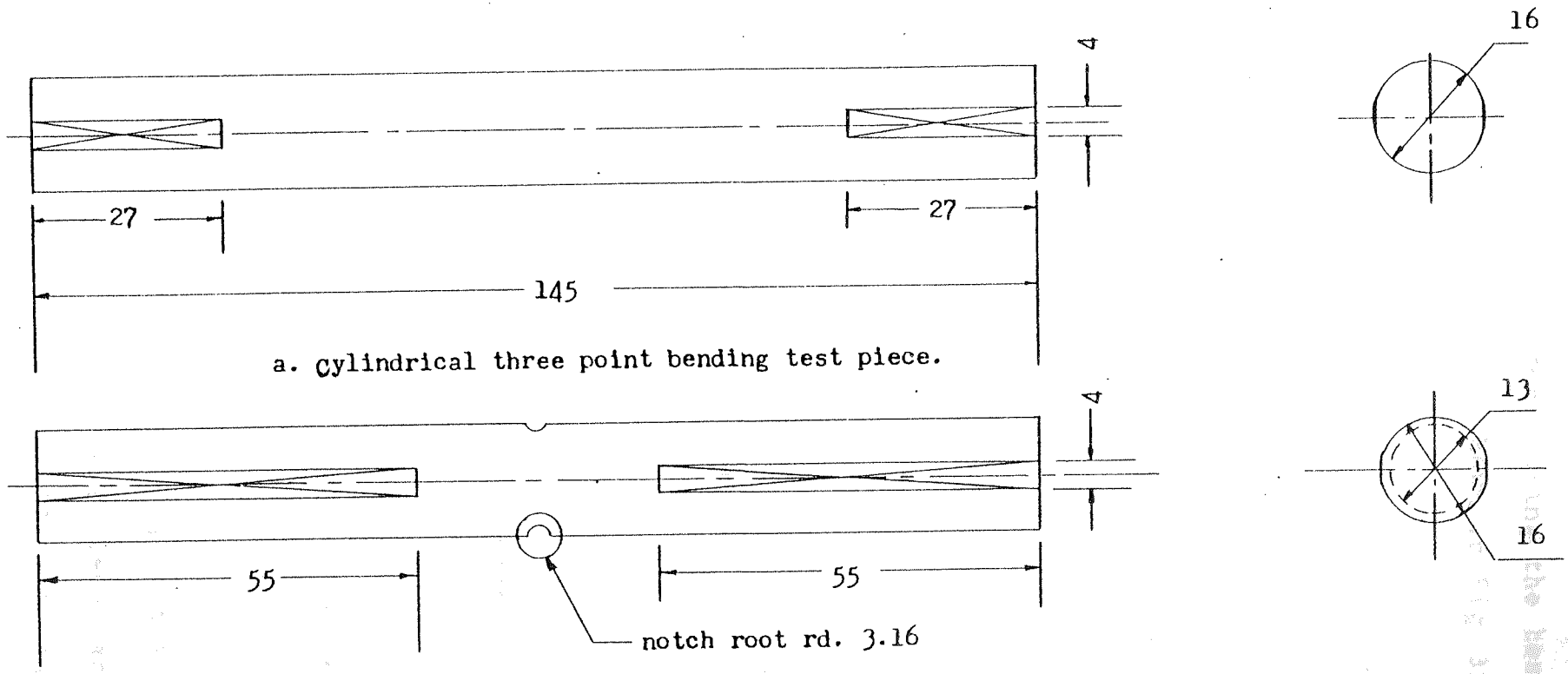

a. Cylindrical three point bending test piece.

b. Cylindrical four point bending test piece.

Fig. 35 Geometry and dimensions (mm).

the loading points were milled to avoid twist and specimen movement during the test. Full dimensions and geometry are shown in Fig. 35b .

3. Rectangular section specimens of 080M15 steel were shaped and notched as shown in Fig. 36a. See appendix 1 for full dimensions and notch root radius. Notch geometry, root radius, and the design dimensions were according to Peterson [84], as well as considering case depth to section ratio.

   Specimens were copper plated on the sides so as carburising will take place on the notch side and the one parallel as can be seen in Fig. 36a. The notch roots were given a final polish to eliminate any irregularities at the root of the notch.

4. Flat bars of 080M15 steel were shaped to dimensions, then ground to obtain flat surfaces. Copper plating was applied to allow carburising to occur on one side only, see Fig. 36b.

5. Skimming bars of 080M15 steel were turned on the lathe to dimensions as can be seen in Fig. 36c.

6. Round bar of 635A14 and 835A15 steel were turned into rotating bending test pieces according to the dimensions illustrated in Fig. 37a. Notched test pieces were also produced with the same gauge diameter and at a stress concentration of 2.8.

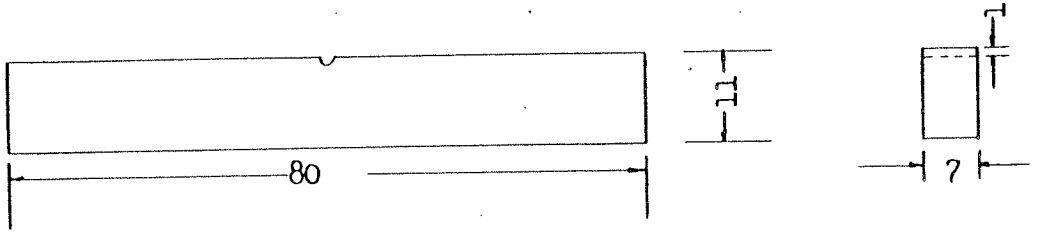

Fig.36 Geometry and dimensios (mm)

a. Three point bending test piece.

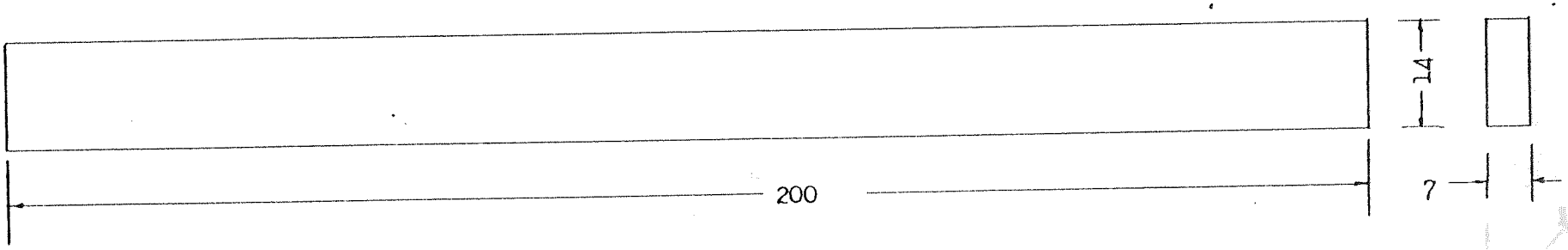

b. Residual stress measurement piece.

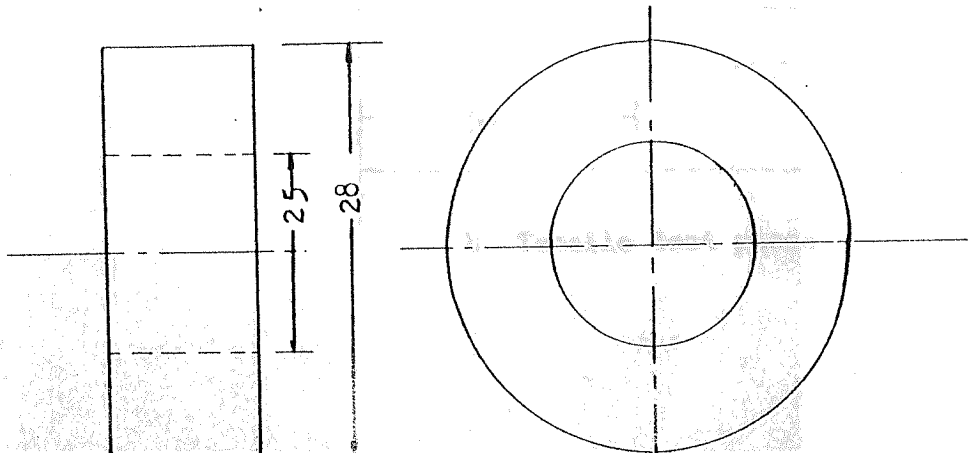

c. Skimming bar sample.

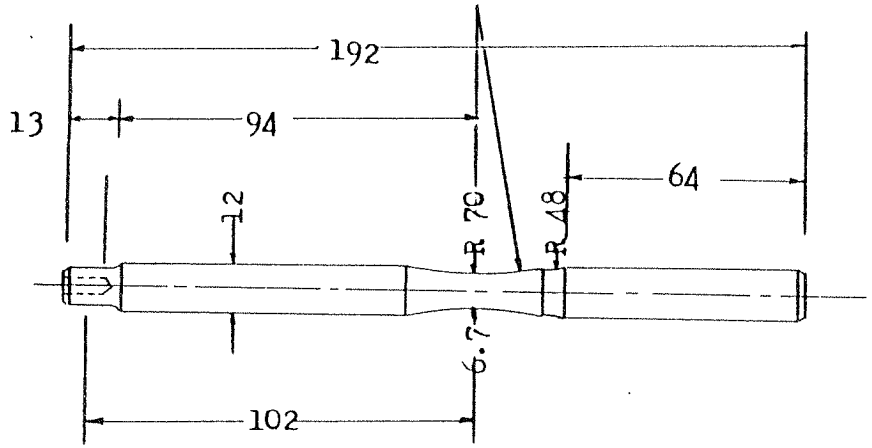

Fig . 37, Geometry and dimensions (mm).

a. Rotating bending test piece.

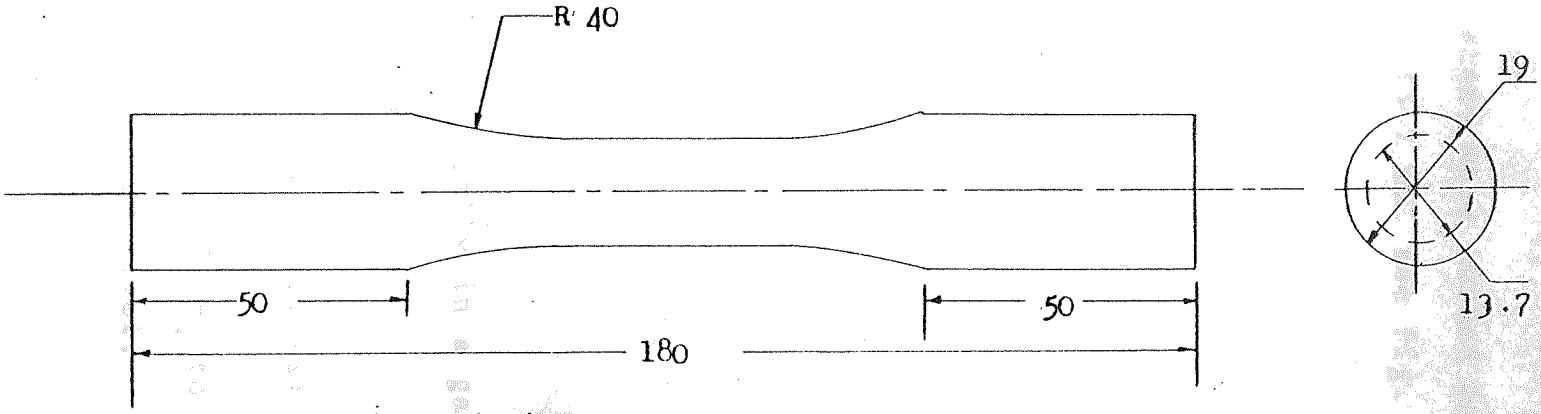

b. Tensile test piece

7. Tensile test pieces of 635A14 steel were turned on the lathe to a test diameter of 13.7 mm, see Fig. 37b for full dimensions and geometry.

4.1.3 Carburising and Hardening

Test pieces were divided into groups for carburising and hardening. Seven groups were selected for gas carburising and two more were vacuum carburised. Gas carburised pieces were hardened by oil quenching from carburising temperature. However vacuum carburised pieces were hardened by reheating to 810°C for 45 minutes, then oil quenched. One additional group (H) was hardened in the uncarburised condition to represent the core properties, see table 4A.

4.1.3.1 Gas Carburising

Methane CH_4 is burned with air catalystically in a gas producing unit to produce a carrier gas

$$2CH_4 + O_2 \rightarrow 2CO + 4H_2 \qquad \ldots\ldots\ldots\ldots(1)$$

The carrier gas is given an extra addition of CH_4 to adjust the carbon potential to the required level, e.g. ∿0.8% C.

$$CH_4 + CO_2 \rightarrow 2CO + 2H_2 \qquad \ldots\ldots\ldots\ldots(2)$$

$$CH_4 + H_2O \rightarrow CO + 3H_2 \qquad \ldots\ldots\ldots\ldots(3)$$

However the water-gas reaction, which is the fastest of the furnace reactions, maintains equilibrium between CO, H_2, H_2O and CO_2 according to:

$$CO + H_2O \rightarrow CO_2 + H_2 \quad \text{.....(4)}$$

and the main gas carburising reactions are:

$$2CO \rightarrow [C]_{Fe} + CO_2 \quad \text{.....(5)}$$

$$CH4 \rightarrow [C]_{Fe} + 2H_2 \quad \text{.....(6)}$$

$$CO + H_2 \rightarrow [C]_{Fe} + H_2O \quad \text{.....(7)}$$

Fig. 38 shows a schematic illustration of the furnace used at Lucas for gas carburising.

Carburising was carried out either in a single stage or in boost/diffusion process.

In the single stage technique the carbon potential is fixed over the carburising cycle, and the carburising time will control the case depth. While boost/diffusion is split into two stages. The boost stage which is carried out at high carbon potential, followed by a diffusion stage at a lower carbon potential, which will give the required surface carbon concentration.

However, in the present work both techniques were used to carburise the test pieces and produce the required carbon profiles.

Carburising temperature was about 925°C, and quenching from carburising temperature was always adopted. See table 4A for carburising conditions of different batches.

TABLE 4 CARBURISING AND HARDENING

A. Thermal and thermochemical (carburising) treatments in conventional gas carburising atmosphere at 925°C

Group	Technique	Time/minutes	% Carbon Potential	Nature of carbon profile
H	-	45	Neutral to the steel	-
G_1	Boost diffuse	300 60	1.2 0.8	Flat plateau near surface
G_2	Boost diffuse	255 24	1.2 0.35	Decarburised
G_3	Single stage	300	0.88	Steep
G_4	Single stage	280	1.0	Steep
G_5	Single stage	480	1.2	Over carburised
G_6	Boost diffuse	240 60	1.1 0.8	Relatively flat
G_7	Boost diffuse	300 60	1.1 0.8	Relatively flat

B. Vacuum Carburising

Group	Technique	Time minutes	Time/ pulse minutes	No. of pulses	Pressure Torr	Nature of carbon profile
V_1	Boost diffuse	14 37	2	5	50 10^{-3}	Flat plateau near surface
V_2	Boost diffuse	52 47	1.5	15	50 10^{-3}	Over carburised

4.1.3.2 Vacuum Carburising

This process was utilised so as to produce carburised test pieces free from internal oxidation. The process is carried out under vacuum by direct introduction of hydrocarbon. Propane C_3H_8 was used, which on contacting the steel surface is cracked releasing carbon atoms for solution with the steel, and the carburising reaction taking place at the hot steel surface is:

$$C_3H_8 \rightarrow 3[C]_{Fe} + 4H_2 \qquad \ldots\ldots\ldots\ldots (8)$$

It is a two-phase process.

1. Propane is introduced by pulses to supply carbon to the steel and causing it to be absorbed according to reaction (8)

2. Diffusion is allowed to take place at the same temperature and under vacuum.

Carburising temperature was 1040°C and gas quench was used to cool the charge. Post vacuum hardening treatment was carried out at G.K.N. Industries by heating the charge to 810°C, which is soaked at that temperature for about 45 minutes, and finally oil quenched. See table 4B for carburising details.

Many carburising boost/diffuse combinations were attempted then it was decided to carburise for four pulses, each pulse duration was 2 minutes at 50 Torr, and then diffused for about 37 minutes. Full details and description of the cycle are shown in Fig. 39. The vacuum furnace used for carburising is shown in Fig. 40.

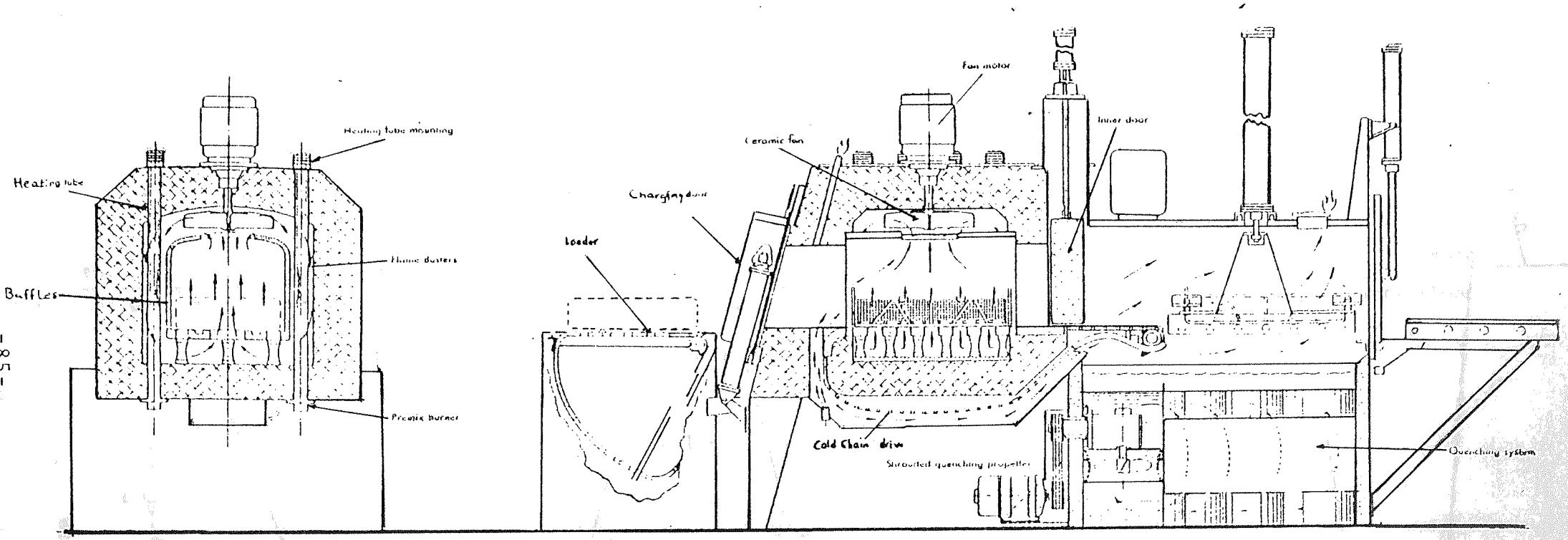

Fig. 38 Gas carburising furnace.

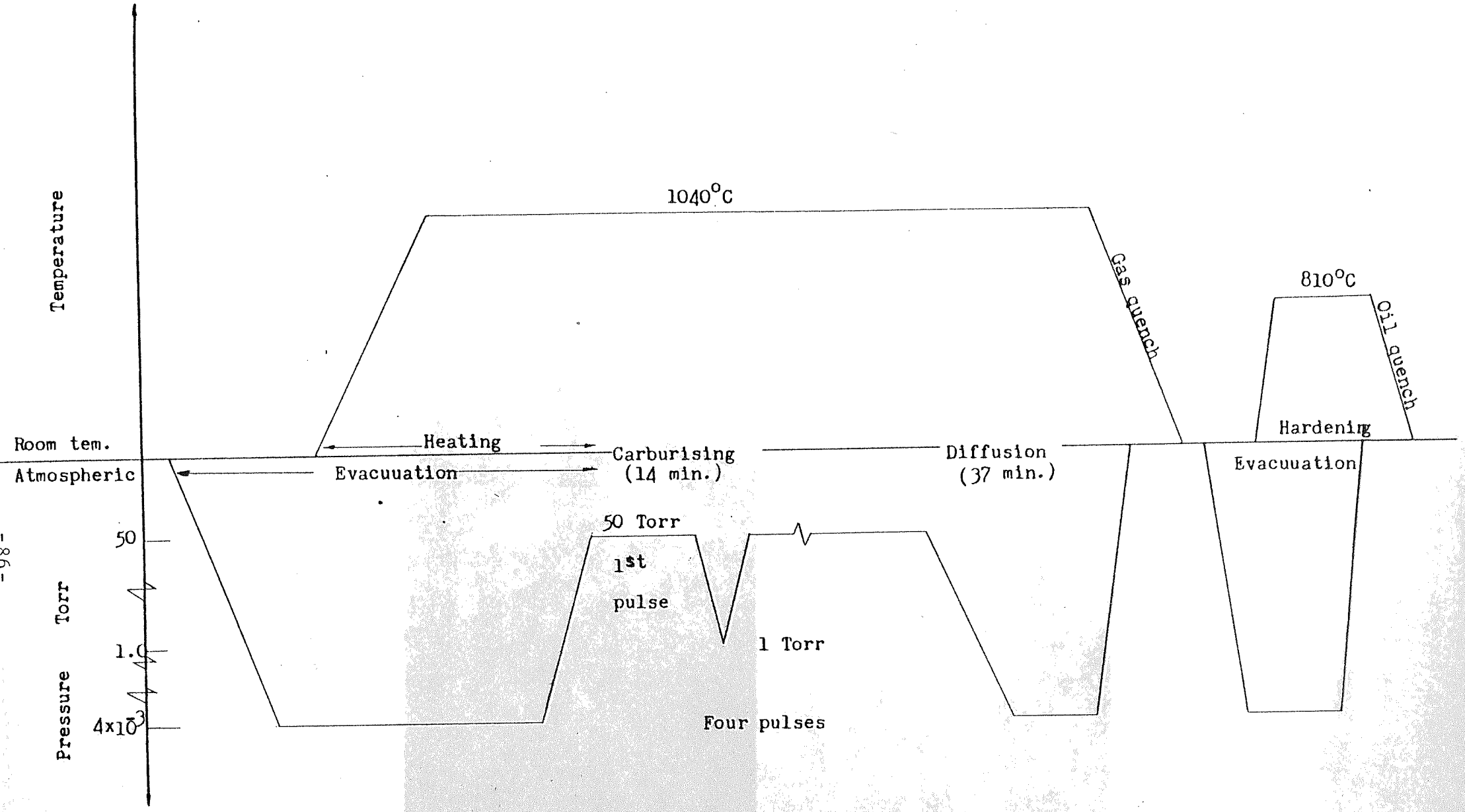

Fig. 39 Schematic illustration of Vacuum carburising and hardening.

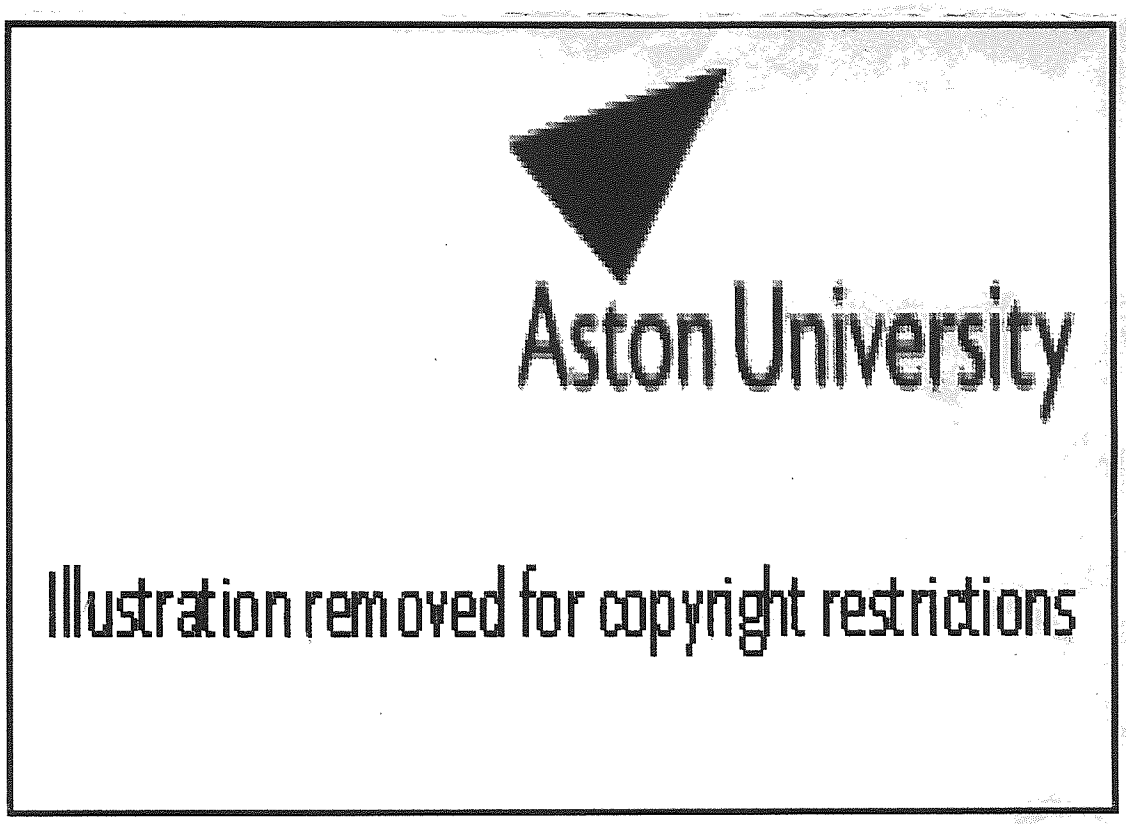
Aston University
Illustration removed for copyright restrictions

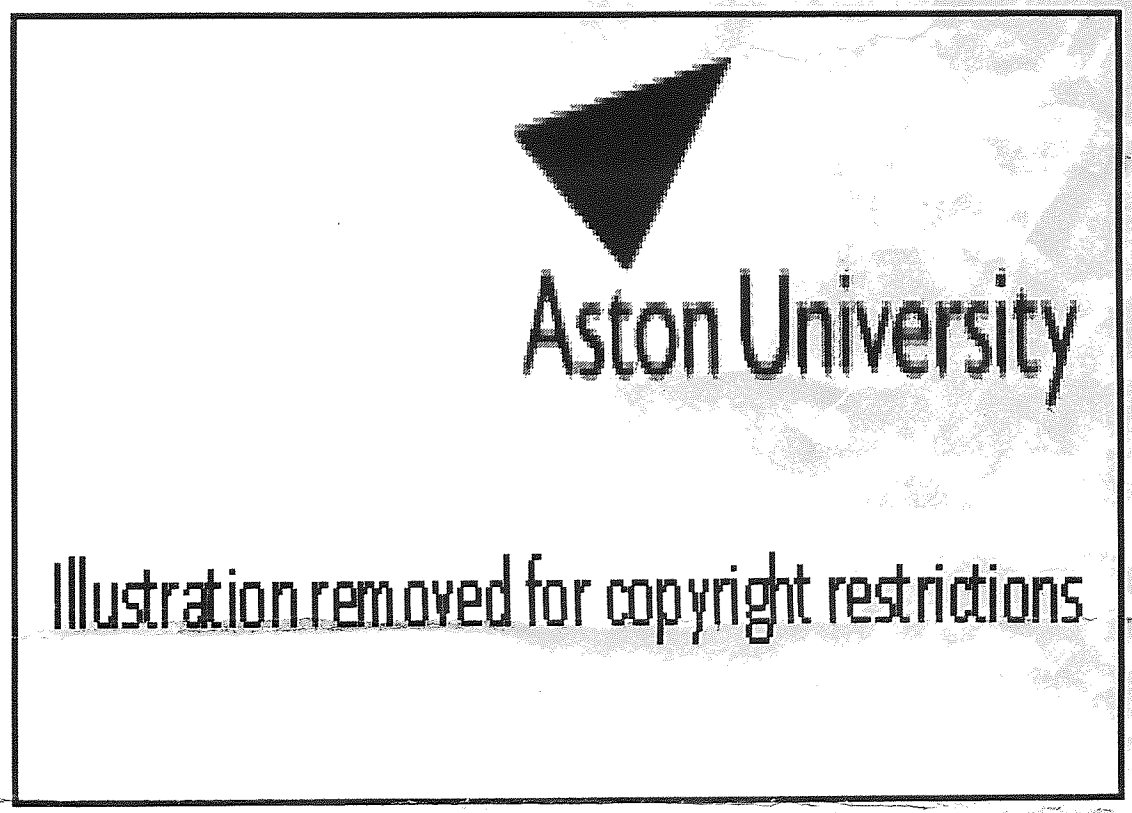
Aston University
Illustration removed for copyright restrictions

It has been mentioned that three types of steels were used in producing the test pieces required for the testing programme. They were subjected to either of the carburising conditions listed in table 4. However, full details about type, number, geometry and steel of test pieces at their particular carburising treatments are shown in table 5.

TABLE 5

Specimens, Steels and Treatment for Fatigue Testing

Group	Thermal treatments	Steel	Test Piece		
			Type	Number	Geometry*
G1	Gas carburised and hardened	635 A14	3PB	4	Plain
		"	4PB	4	Notched
G2	" "	635 A14	3PB	6	Plain
		"	4PB	5	Notched
G3	" "	635 A14	3PB	10	Plain
		"	4PB	7	Notched
		"	RB	6	Plain
		080 M15	3PB	16	Notched-flat
		"	3PB	2	Plain
G4	" "	635 A14	3PB	7	Plain
		835 A15	RB	6	Plain
		"	RB	6	Notched
G5	" "	635 A14	3PB	4	Plain
		"	4PB	5	Notched
G6	" "	835 A15	RB	3	Plain
		"	RB	4	Notched
G7	" "	835 A15	RB	4	Plain
		"	RB	4	Notched
V1	Vacuum carburised and hardened	635 A14	3PB	4	Plain
		"	4PB	5	Notched
V2	" "	635 A14	3PB	4	Plain
H	Uncarburised hardened	635 A14	3PB	4	Plain
		"	4PB	4	Notched

* Unless mentioned is cylindrical

4.2 Testings, Measurements and Techniques

4.2.1 Rotating Bending

This was carried out to produce fatigue strength data, based on failure while the mean stress is zero, i.e. stress ratio of -1. The nature of loading is a cantilever with triangular bending moment. The fibre stress was calculated according to:

$$\sigma = \frac{32}{\pi} \frac{PS}{d^3} \qquad \ldots\ldots\ldots\ldots (4)$$

where P is the Load

S is the span length - the distance between the centre of the bearing and the fracture point

d is the gauge diameter.

Figure 41 shows a test piece under loading.

4.2.2 Unidirectional Bending

(i) Three-point bending (3-P.B)

Plain cylindrical specimens were designed to be tested in 3-P.B. in order to determine the fatigue strength based on failure. Stress calculation was carried out using:

$$\sigma = \frac{16}{\pi} \frac{PS}{D^3} \qquad \ldots\ldots\ldots\ldots (5)$$

where P is the load applied

D is the diameter

$S \leqslant 53$ mm depending upon the location of fracture.

Distance between the two support points, i.e. total span length, was chosen to be 106 mm.

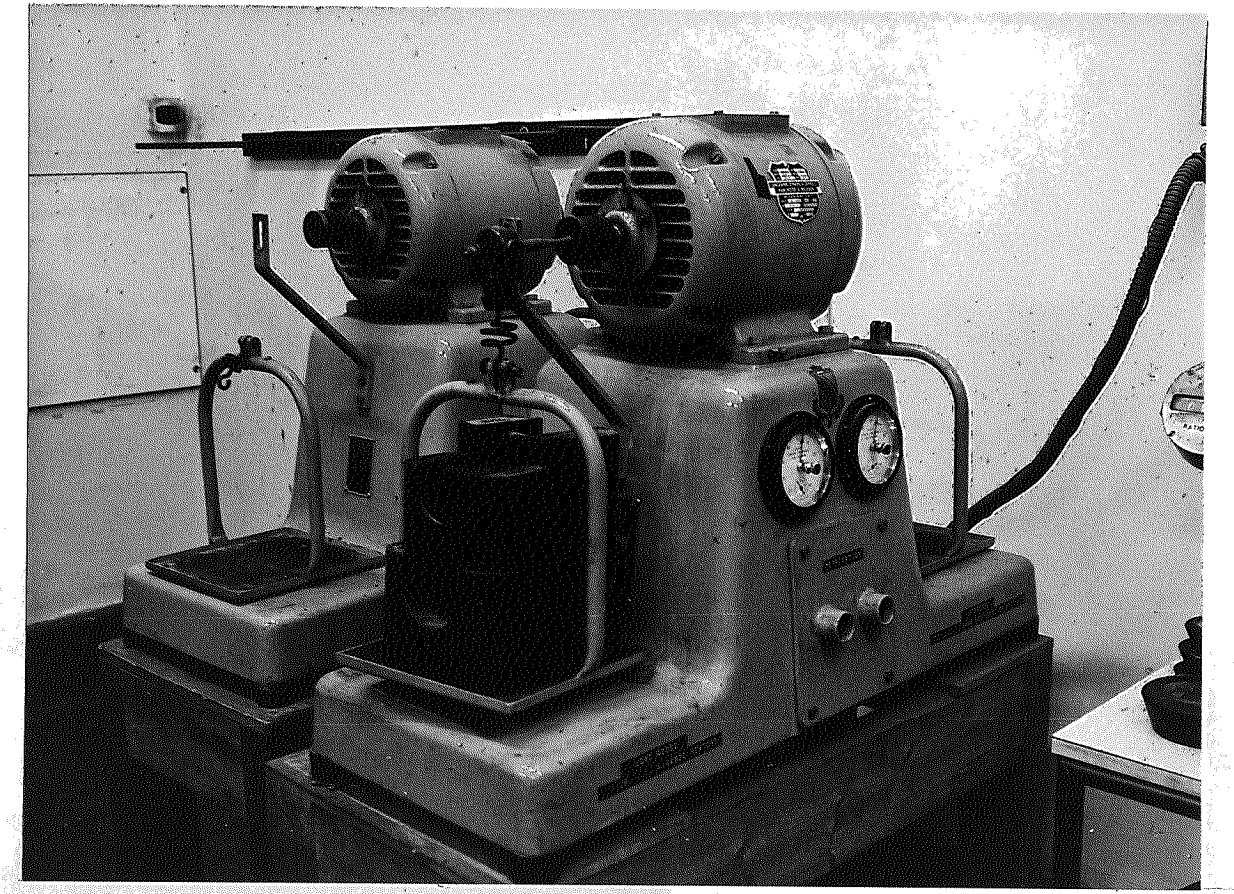

Fig, 41 Test piece subjected to traingular moment , in rotating bending.

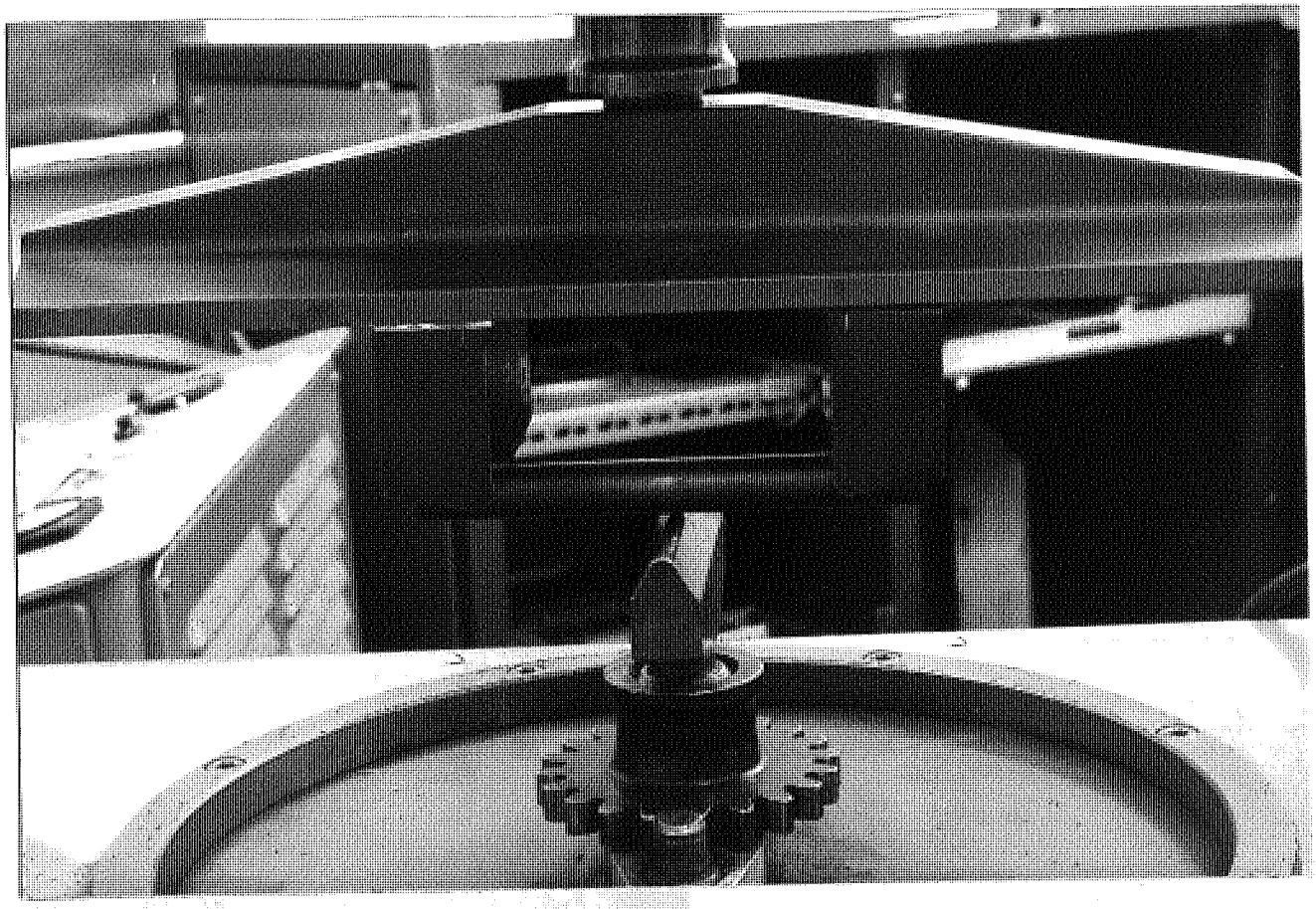

Fig.42, Test piece in three point bending.

Test piece in 3-P.B. is shown in Fig. 42.

Moreover, notched rectangular section pieces were also tested in 3-P.B. However, span length was 60 mm and stress to initiation was determined using:

$$\sigma = 1.5 \frac{PS}{bh^2} \qquad \ldots\ldots\ldots\ldots (6)$$

where b is the thickness

and h is the width of the test piece

(ii) Four-point Bending (4-P.B)

Practically it was not possible to determine the initiation stress on plain cylindrical specimens in 3-P.B. loading. Crack detection needed the use of potential drop equipment. Initiation was always occurring at the spot weld. Consequently the initiation stress bears no relevance to the true stress to initiate a crack. The damage caused by the spot weld was not reproducible.

However 4-P.B. loading was ultilised to test notched cylindrical samples (with circumferential notch at a stress concentration of 1.5). In this case the stress concentration factor and the test section diameter will act more effectively and ensure crack initiation at the notch. Consequently that will facilitate incorporating the potential drop attachment to decide the stress level at crack initiation.

The stress to initiation was calculated according to the equation:

$$\sigma = \frac{16}{\pi} \frac{Pa}{d^3} \qquad \text{.....(7)}$$

where P is the load

a is the outer span length which was 26 mm, while the inner span was 64 mm

d is the gauge diameter.

Test piece in 4-P.B. loading is shown in Fig. 43a. Stress ratio of 0.3 was used always except for investigating the mean stress effect, where a stress ratio of 0.1 and 0.7 were also used.

4.2.3 Fatigue Test Variables

4.2.3.1 Carbon Profile Effects

Notched and plain specimens were tested in rotating and unidirectional bending. The bending fatigue strength based on failure was derived from rotating and three-point bending. However that based on initiation was derived from four-point bending.

Bending fatigue strength was determined for seven types of carbon profiles produced by gas carburising and two types of carbon profiles produced by vacuum carburising. Accordingly a comparison of the fatigue strength to failure and initiation can be made for different carbon profiles and the associated metallurgical factors, and to enable an evaluation of vacuum carburised pieces due to the freedom from internal oxidation.

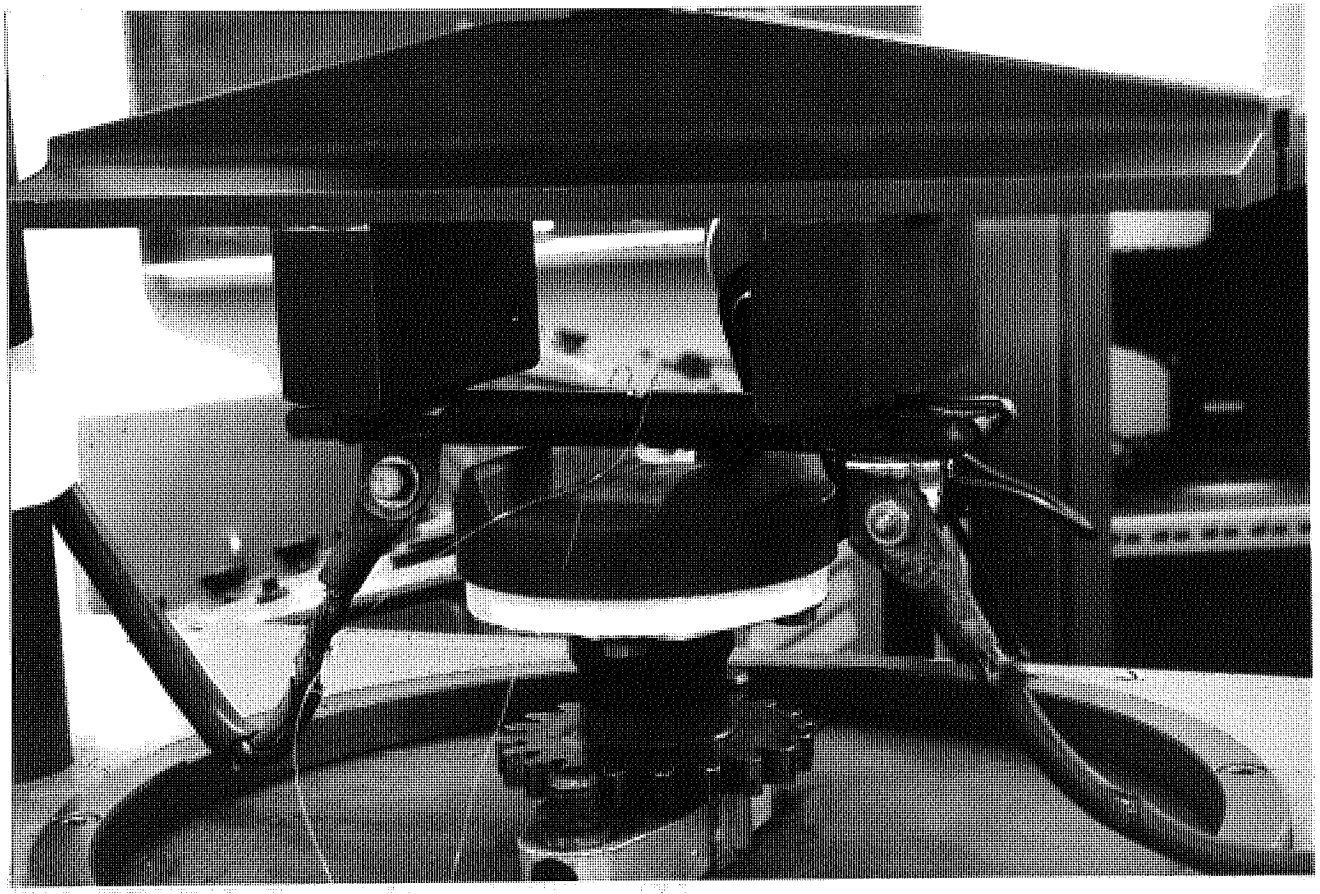

Fig. 43-a Test piece in four point bending.

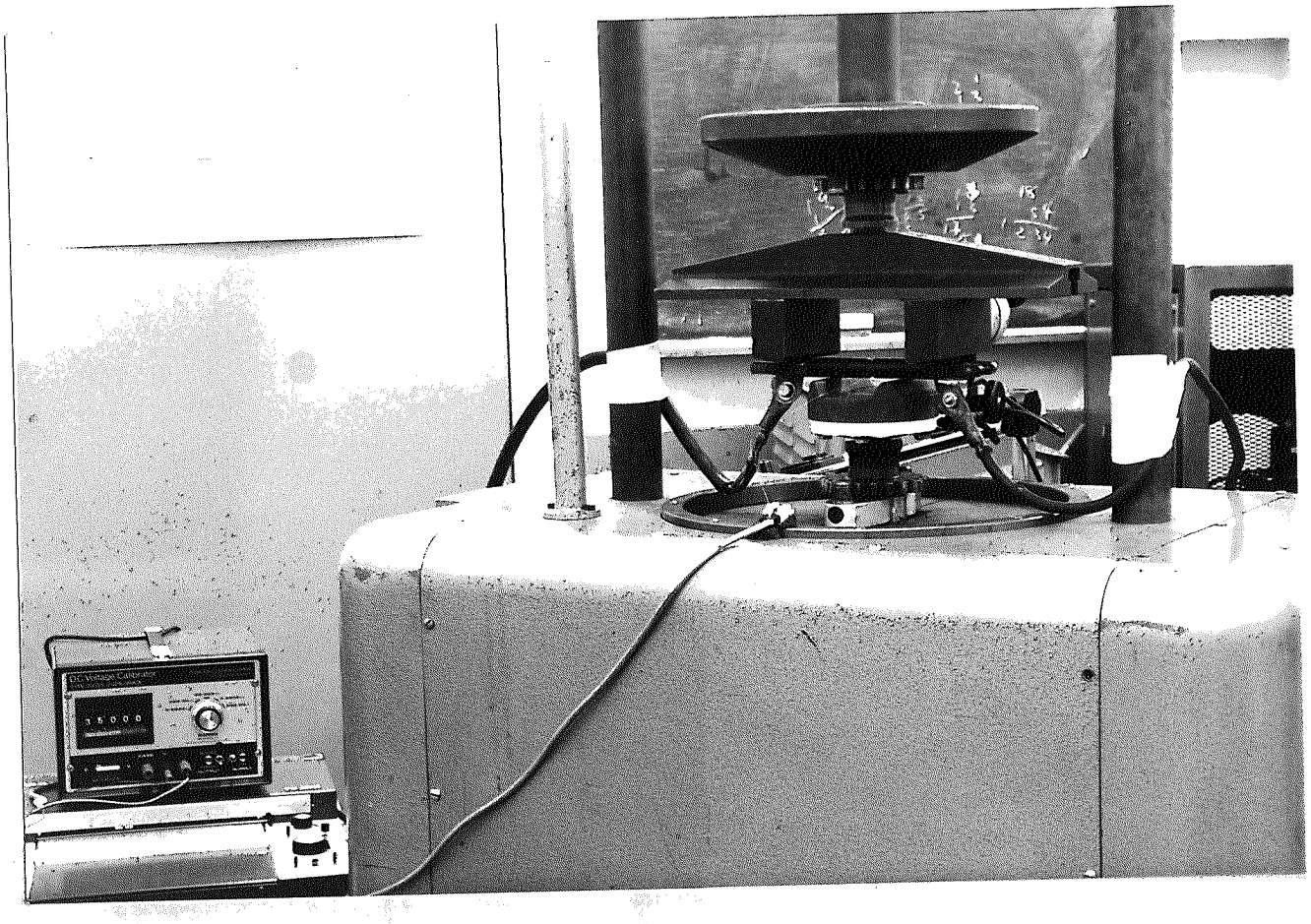

Fig. 43-b Potential drop connections on four point bending test piece.

4.2.3.2 Mean Stress Effect

One particular carbon profile, i.e. single stage G3, was chosen and produced on all test pieces designed for this investigation.

Fatigue testing was carried out on rotating bending at zero mean stress and in unidirectional bending, namely three-point bending, at three stress ratios:

(i) R = 0.1 low mean stress

(ii) R = 0.3 medium mean stress

(iii) R = 0.7 high mean stress

The fatigue strength at 10^6 based on failure was determined at the four levels of mean stress.

4.2.3.3 Stress Concentration Effect

The same carburising treatment, G3, was used for this purpose. Fatigue testing was carried out in unidirectional, three-point bending, with the potential drop attachment. The bending fatigue strength for different notch geometries and stress concentration factors was determined. Fatigue strength was based on the initiation of fatigue crack at the root of the notch. Initiation was assumed to have occurred when voltage increase of 3 to 5 μv is recorded by the potential attachment. However specimen was further cycled until a crack was observed visually.

4.2.3.4 Hardening in Comparison to Carburising and Hardening Treatment

Plain and notched hardened cylindrical samples were tested in three and four-point bending respectively, in order to

determine the fatigue strength at 10^6 cycles based on failure and initiation. Consequently a comparison can be made with those of carburised samples. Furthermore, the mean stress effect can be compared for both conditions. Since three-point bending tests of the hardened samples were carried out at two levels of stress ratio (0.3 and 0.1). Span length and stress calculation procedures were similar to those already mentioned.

4.2.4 Fatigue Strength

The main objective in the fatigue testing programme was to determine a mean value of the fatigue strength at 10^6 cycles. The step test method was used to limit the number of samples and the testing time. In this method each sample was tested until it actually failed, i.e. each sample is tested at a stress level, if it does not fail within 10^6 cycles it will be retested at a stress level higher than the previous step by 5% (of the estimated fatigue strength). This is continued until failure. The estimated fatigue strength is taken as the mean value between the stress at which failure occurred and that of the preceding step at which 10^6 cycles were completed without failure [80].

However an assumption is made that if sample fails at 1st testing stress level before completing 10^6 cycles, the fatigue strength is calculated assuming the specimen has survived 10^6 cycles at the step below, i.e. at 5% lower than the failure stress.

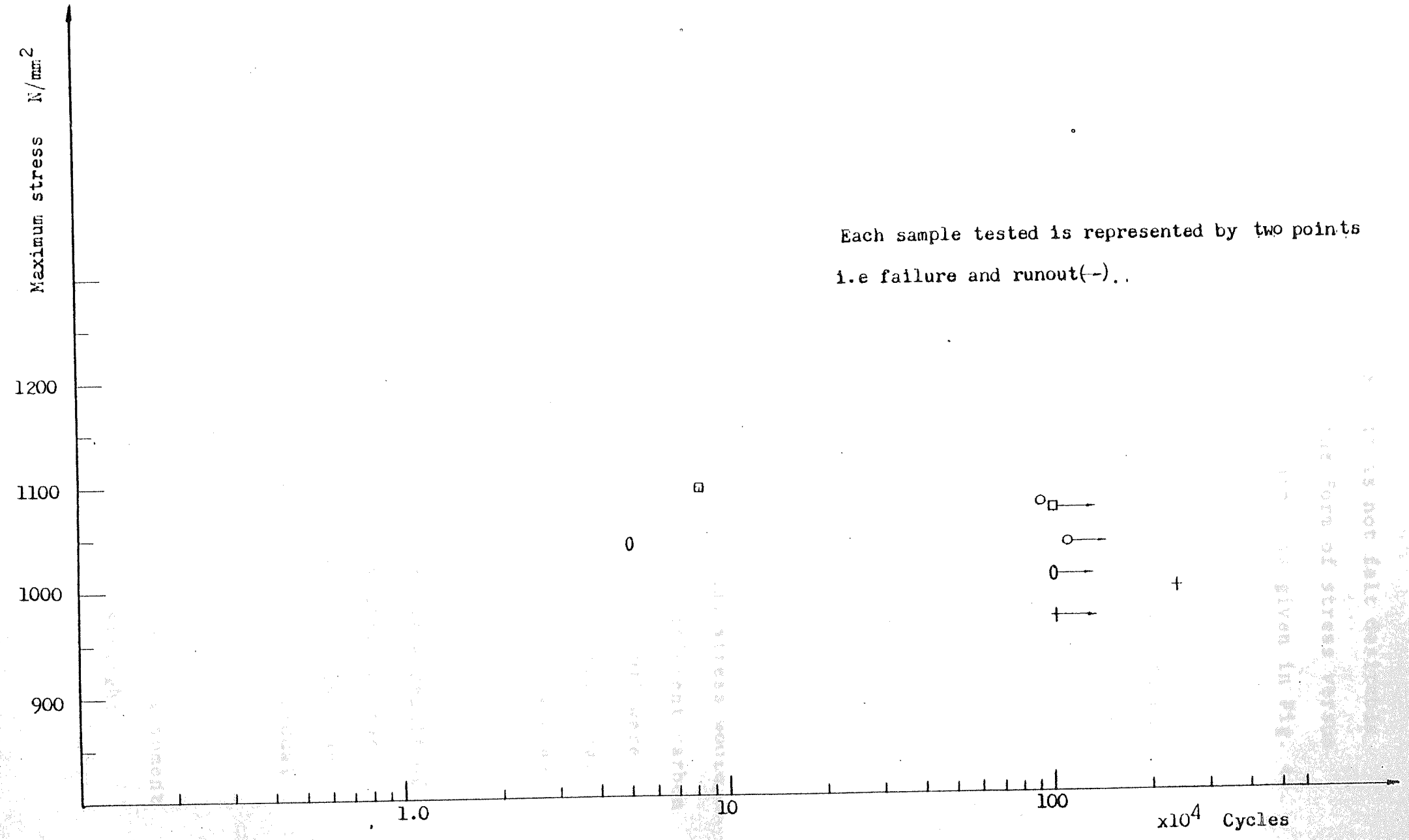

Fig. 44 (S-N) Fatigue behaviour of 635A14 : treatment G3.

In view of the method used, it is not felt desirable to represent the results in the form of stress versus number of cycles, however an example is given in Fig. 44.

4.2.5 Tensile Test

The tensile strength of carburised and uncarburised hardened samples was determined. Such data provided an indication of the mechanical static strength of the material tested as influenced by carburising and hardening. In addition tensile strength value helped in constructing a Gerber diagram.

4.2.6 Residual Stress Estimation

The wide aims of the project did not permit detailed measurement of the residual stress pattern. However it was felt that a mean value of the residual stress would be of use in assessing the effect due to different carbon profiles. For this purpose flat bars of 080 M15 were provided with some of the batches for gas carburising. Only one side was exposed to the gas metal reaction as others were protected by copper plating.

The deflection produced in the flat bars as a result of carburising and hardening treatment was utilised for estimating a mean value of the residual stresses. An assumption is being made that the majority of residual stresses have relaxed to produce the deflection.

Deflection has occurred due to a negative bending moment M_r. Therefore if the beam is to stay in straight

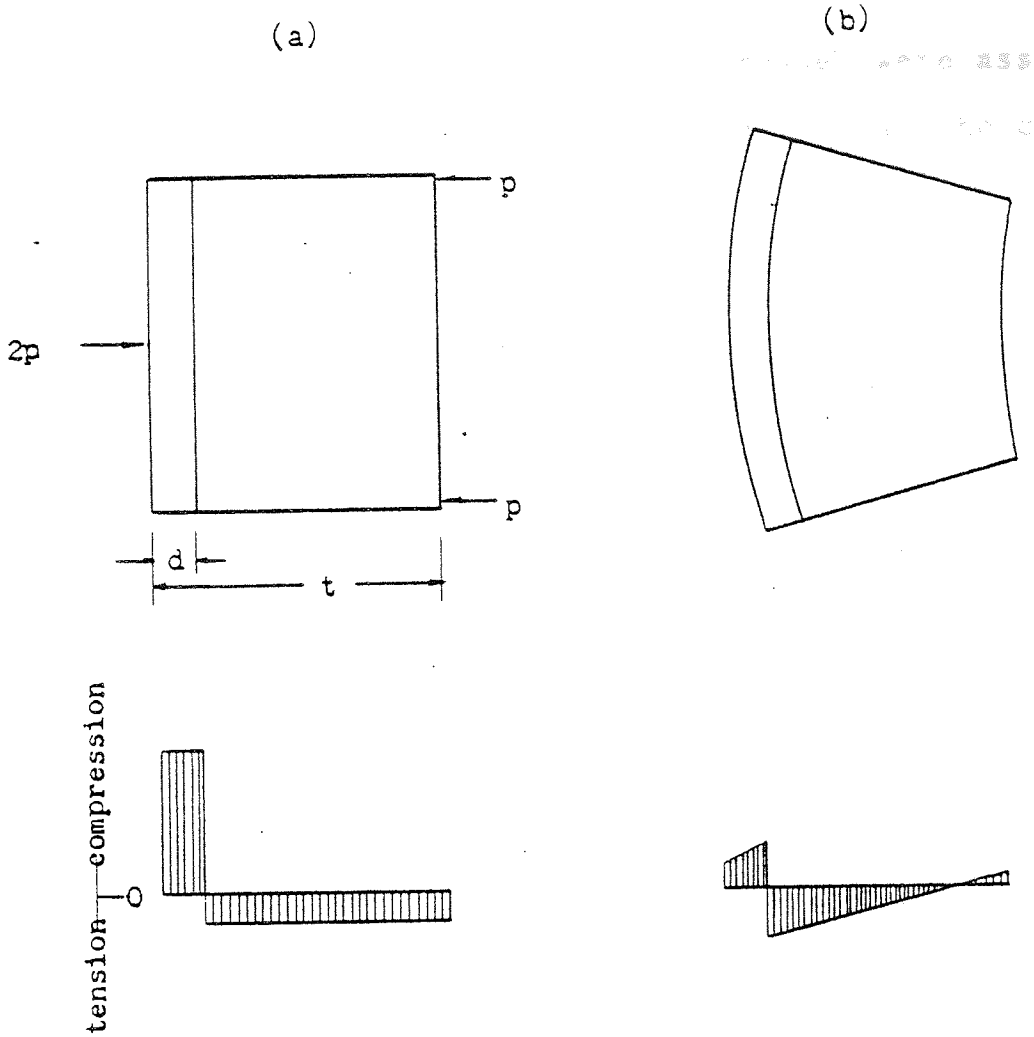

Fig. 45 Schematic illustration of residual stress and distortion; Panel (a) shows the beam in a balanced state, under the effect of both residual & applied stresses, panel (b) shows the beam distorted with the resulting stress distribution.

condition an equivalent bending moment with opposite sign is required, M.

In reference to Fig. 45 residual stresses were assumed uniform, compressive in the case, tensile in the core:

$$\sigma_s \cdot d = (t-d)\sigma_c$$

$$\sigma_c = \sigma_s \frac{d}{t-d}$$

where σ_c is the core stress

σ_s is surface stress

d is the case depth

t is the thickness

assuming W is the width

It follows that the bending moment due to residual stresses M_r

$$M_r = \int_o^d \sigma_s W x dx - \int_d^t \sigma_s \frac{d}{t-d} W x dx$$

$$= \sigma_s W \left(\frac{x^2}{2} \Big]_o^d - \left(\frac{d}{t-d}\right) \frac{x^2}{2} \Big]_d^t \right)$$

$$= \sigma_s W \left(\frac{d^2}{2} - \frac{d(t+d)}{2} \right)$$

$$M_r = -\sigma_s W \frac{dt}{2} \qquad \ldots\ldots (I)$$

An external bending moment which would bring the deflection to zero should have the same magnitude but an opposite sign. This externally applied bending moment due to the three-point loading will be associated with a fibre stress σ

$$\therefore \quad M = \frac{\sigma I}{Y}$$

$$= \frac{\sigma}{t/2} \frac{wt^3}{12}$$

$$M = \frac{\sigma wt^2}{6} \qquad \ldots\ldots(II)$$

equating (I) and (II) it follows that:

$$\sigma_s W \frac{dt}{2} = \frac{\sigma wt^2}{6} \qquad \ldots\ldots\ldots\ldots\ldots\ldots\ldots\ldots(8)$$

$$\therefore \quad \sigma_s = \frac{\sigma t}{3d}$$

where σ is the applied fibre stress.

Data and dimensions for residual stress determinations are given in Appendix 3. The measured load in bending, is that required to bring the beam deflection to zero.

4.2.7 Carbon Profile Determination

A piece of test sample was randomly taken from each batch. A spark erosion machine was employed to slice a sample of each piece, which was then mounted in a conductive bakelite.

Samples were polished on emery paper grade 100, 200, 320, 400 and 600 respectively, followed by 6 and 1 μ diamond. Any bevelling which is likely to be found after such

polishing procedure would reduce the accuracy of carbon measurement. Therefore the samples were vibratory polished on $\frac{1}{4}$ μ diamond until a shiny polished bakelite around the sample is achieved. This ensured reasonable flatness at the zone where the carbon is to be measured.

Ultimately samples were given a final polish on γ-alumina to clean them from any residual diamond. They were ultrasonically cleaned in an acetone bath and dried instantly. Then they were analysed immediately or kept in a vacuum desiccator until required.

The same samples were used afterwards for microhardness measurements and further metallographic investigations.

4.2.7.1 Carbon Analysis by EPMA Technique

Basically a beam of electrons hits the surface of the sample. Generated X-rays are collected and converted into pulses in terms of counts/sec. Consequently the carbon distribution through the case is represented by a count/rate plot.

Three carbon standards were used to produce a calibration line which assisted converting the count/rate plot into a carbon presentage.

4.2.7.2 Carbon Tracing by Chemical Analysis

A skimming bar of 080 M15 steel was carburised with some of the batches for this purpose.

The skimming bar was machined on the lathe and turned at 0.05 mm intervals, chip material was collected and chemically analysed. The analysis was carried out by a volumetric method using Strȍhlein apparatus.

Skimming bar was cleaned by sand blast and chip materials were handled with a high degree of cleanness.

4.2.7.3 Carbon Profile Plot

The electron probe microanalyser (EPMA) output was in counts per 25 seconds. As the specimen was travelling at 30 μm/min., i.e. 0.5 μm/sec., in each 25 seconds, therefore the count rate reading will be the mean value over the 12.5 μm, and so represented by a point midway across the 12.5 μm.

The count rate is then plotted versus depth in Fig. 46 for 080M15 carburised by G3, as an example of the probe output. A band of about 95% confidence limit was then drawn, and the mean curve was plotted. The count rate was read from the mean curve at various depths and converted into carbon content with the aid of calibration line (produced by three standards containing known amounts of carbon). The resulting carbon profile can be seen in Fig. 48. Similarly, carbon profiles for different batches gas and vacuum carburised are produced.

The carbon profile was also traced using results from chemical analysis. This was carried out for a few batches, to provide a reference for the EPMA results.

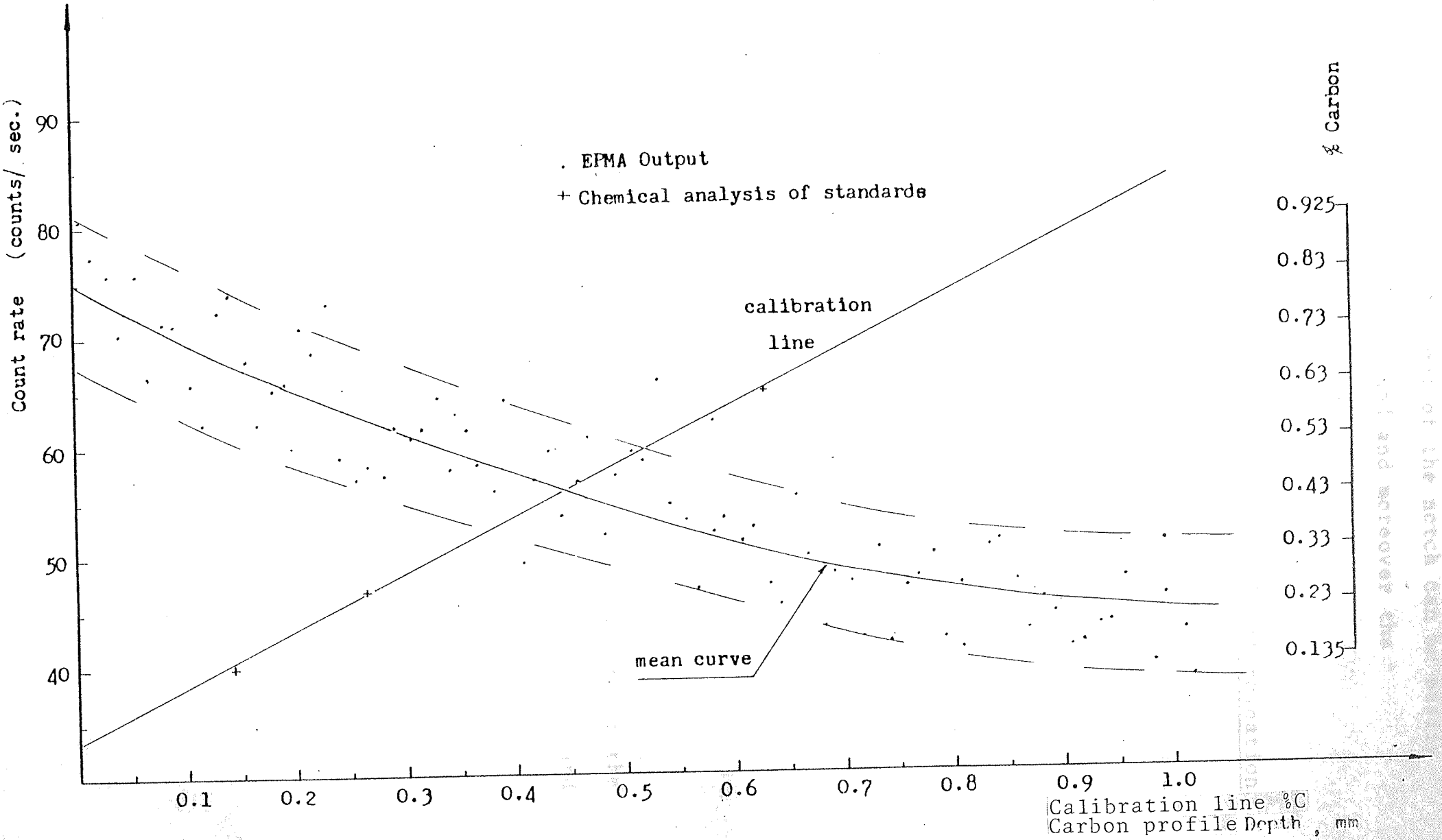

Fig 46 Carbon profile determination from the electron prob microanalyser out-put of 080M15 carburised by 03.

The carbon profile at the root of the notch can be easily determined using the EPMA method and moreover the technique is not time consuming.

4.2.8 Microhardness Profile and Case Depth Determination

4.2.8.1 Microhardness Values

Microhardness values were obtained at 0.05 mm intervals for the first ½ mm. Such measurements were continued at greater intervals until 2.5 mm depth. However microhardness at the centre of the specimen was also measured to represent core hardness. The best curve fit through the resulting point was then plotted to represent the hardness profile. This was carried out for all the batches involved.

4.2.8.2 Case Depth

Effective case depth was deduced from the microhardness profile [5].

Referring to Fig. 47 and assuming that the boundary of the case is at 500 HV (BH), by similarity of triangles Abc and ABC, in terms of hardness and depth, it follows:

$$\frac{H_1 - BH}{CD - t} = \frac{H_1 - H_2}{t_2 - t_1}$$

$$CD = t_1 + \frac{(H_1 - BH)(t_2 - t_1)}{H_1 - H_2}$$

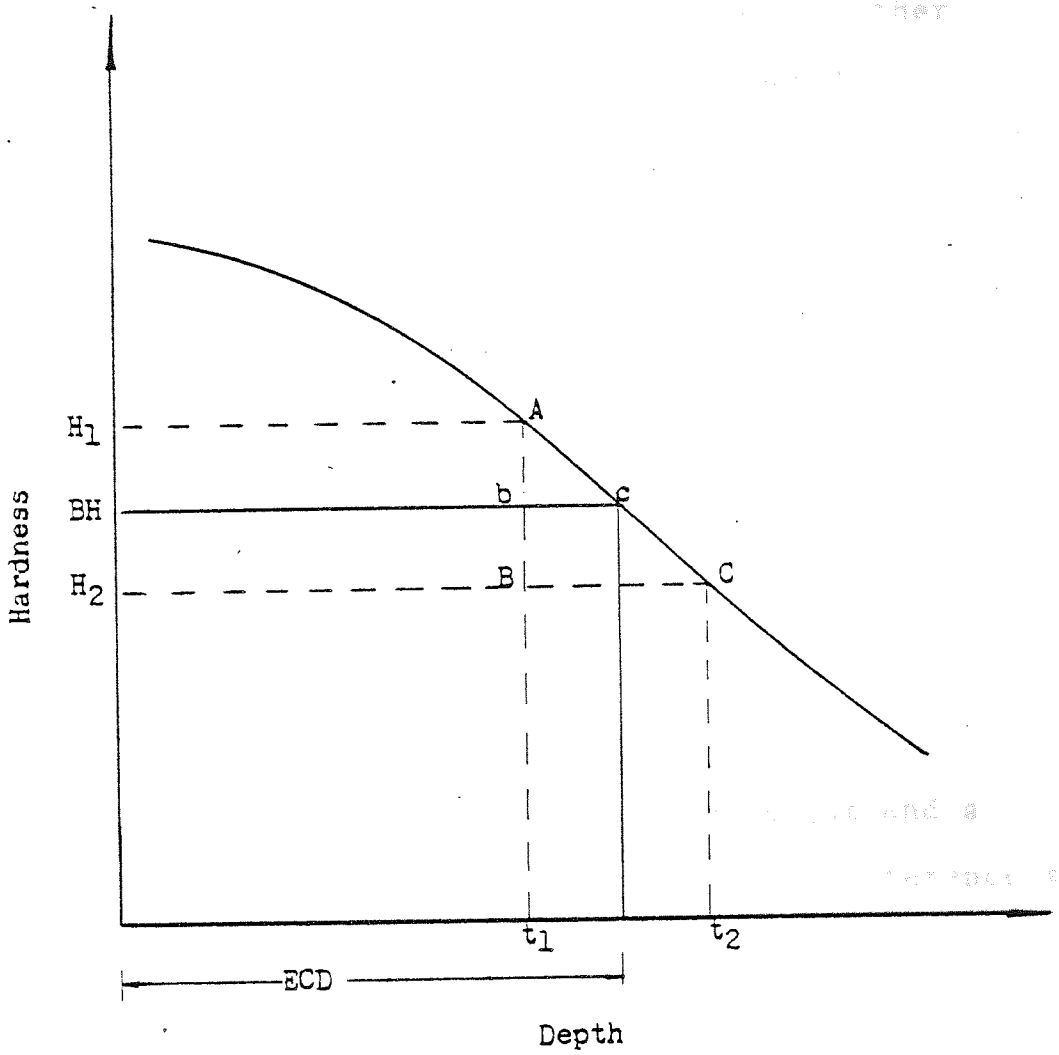

Fig. 47 Effective case depth from hardness profile.

4.3 Equipments

1. Fatigue

   Fatigue test was carried out on two machines,

   a) Rotating bending, 3000 RPM

   b) $\pm$ 20 kN Vibrophor, Amsler type, with either three or four point bending attachment.

2. Electron Probe Micro-Analyser

   An EPMA Cambridge Microscan 5 was employed at 15 kV, for determining carbon profiles. Three carbon standards were cleaned and traced at every session on the equipment. A barium stearate crystal was used.

3. Microhardness Tester

   Microhardness measurements were carried out on a Leitz Miniload Tester, using 300 gm weight and a standard calibration piece was used as a reference at each session on the instrument.

4. Scanning Electron Microscope

   An SEM Cambridge S150 was employed for fracture surface investigation and fatigue crack initiation, as well as correlating the microstructure to the fracture topography.

5. Tensile Testing

   This was carried out using a 500 KN Dennison type machine or a 20 KN Instron.

6. Surface Roughness

A Talysurf Model 3 was employed for surface roughness measurement. All tested samples were checked and controlled within 0.3 to 1.0μm roughness (centre line average).

7. Alignment

Rotating bending samples were checked for alignment and for this a Universal Measuring machine MO 214B with feeler microscope was used.

8. Vickers Projector Microscope

Metallugraphical investigation was carried out on a Vickers Projection microscope. This equipment was also used in a macroscopic investigation of fracture surfaces.

9. Potential Drop

This equipment was used to provide a constant direct current through the test piece and as $V = I R$. The voltage across two points on the specimen is constant unless the resistance (R) changes and that can only happen on crack initiation. The above equipment was used whenever crack initiation investigations were carried out.

The potential drop electrical attachment can be seen in Fig. 43b on a 4 P.B. loading attachment on the Vibrophore.

10. Shadow Microscope

A shadow microscope was employed to check the notch root, and suggest if it needed a final polish at the root to eliminate any irregularities due to machining.

5.0 Results

5.1 Fatigue

Fatigue strength in both rotating and unidirectional bending of the three steels, namely 635A14, 835A15 and 080M15, were determined. A few examples of calculations are given in Appendix 2.

Fatigue results are listed in tables 6 to 9; it should be noted that they include all details of stressing steps prior to failure or initiation.

Values of the maximum cyclic applied stress at failure (or initiation) are listed in the first column, while two other stress levels are quoted to indicate the first and last (step below failure or initiation) stress levels, the number of steps used in testing any one sample are also listed bearing in mind that if the number of steps is (n), the number of increments is (n-1). Values in brackets are 5% lower than "first step" stress at which failure (or initiation) unfortunately occurred. These results have been considered on individual basis.
The estimated fatigue strength column include the mean value between failure (or initiation) stress and that of the preceeding survival run (see 4.2.4)

The statistical mean of the estimated fatigue strength is determined for each group of tables 6 and 7 and then listed in table 10. However estimated fatigue strength results are presented in Figs. 60 and 64, where the highest and lowest estimated fatigue strength in each

group are shown as a range with the statistical mean of the estimated fatigue strength also shown.

Table 8 includes three additional columns where the stress ratio, mean stress and stress amplitude are listed, however calculations concerning mean stress and stress amplitude are shown in Appendix 2. Stress amplitude versus mean stress is plotted in Fig. 71.

The estimated fatigue strength results, table 9, at different stress concentration factors are plotted in Fig. 75.

Statistical comparison of fatigue results, between plain and notched conditions, carburising treatments as well as direct comparison between gas and vacuum carburising, were carried out at 95% confidence limit, by analysis of variance. Results of such comparisons will be considered in the discussion.

TABLE 6a

Plain Fatigue Strength (rotating bending) of Carburised 835A15

Specimen Code	Failure Stress N/mm^2	No. of cycles at failure	No. of steps	Starting stress N/mm^2	Stress step below failure N/mm^2	Estimated fatigue strength N/mm^2
G4 1	715	720000	3	652	683	699
G4 2	769	450000	5	641	737	753
G4 3	826	15000	7	641	795	810
G4 4	720	550000	4	600	680	700
G4 5	729	20000	4	638	698	713
G4 6	707	870000	3	646	676	692
G6 1	834	210000	7	649	803	819
G6 3	652	50000	2	618	618	635
G6 4	764	630000	3	644	704	634
G7 1	785	90000	6	636	755	770
G7 2	645	45000	1	645	(613)	629
G7 3	692	250000	3	633	663	678
G7 4	695	800000	3	633	664	680

TABLE 6b

Notched Fatigue Strength (rotating bending) of Carburised 835A15

Specimen Code	Failure Stress N/mm^2	No. of cycles at failure	No. of steps	Starting stress N/mm^2	Stress step below failure N/mm^2	Estimated fatigue strength N/mm^2
G4 1	437	1080000	2	402	402	420
G4 2	426	200000	2	395	395	411
G4 3	426	160000	2	395	395	411
G4 4	519	100000	5	387	486	502
G4 5	469	540000	4	381	440	455
G4 6	477	3000	3	414	445	461
G6 1	494	475000	2	434	434	464
G6 2	537	340000	6	439	517	527
G6 3	491	200000	4	432	471	481
G6 4	473	500000	3	432	453	463
G7 1	463	1400000	2	432	432	448
G7 2	494	300000	3	432	463	479
G7 3	463	50000	2	432	432	448
G7 4	432	420000	1	432	(410)	421

TABLE 7a

Plain Fatigue Strength (three-point bending) of Carburised 635A14

Specimen Code	Failure Stress N/mm^2	No. of cycles at failure	No. of steps	Starting stress N/mm^2	Stress step below failure N/mm^2	Estimated fatigue strength N/mm^2
G1 1	1076	903000	10	723	1037	1057
G1 2	1044	50000	4	942	1010	1027
G1 3	995	2500000	3	942	968	982
G1 4	1093	82000	4	971	1052	1073
G2 9	1033	138000	6	712	969	1001
G2 10	903	387000	1	903	(858)	880
G2 11	863	689000	1	863	(820)	841
G2 12	1075	113500	10	689	1032	1054
G2 13	1050	131000	7	788	1006	1028
G2 14	869	920000	1	869	(826)	847
G3 1	1191	190000	10	785	1146	1169
G3 2	1174	110000	4	1054	1134	1154
G3 3	1104	243000	1	1104	(1049)	1076
G3 25	1025	981000	3	950	988	1007
G4 1	1069	22000	5	893	1025	1047
G4 2	971	320000	5	807	930	951
G4 3	1004	816000	4	869	959	982
G4 4	975	122000	7	687	927	951
G4 5	874	320000	5	714	834	854
G4 6	992	335000	4	860	948	970
G4 7	948	214000	3	850	899	924

TABLE 7a (continued)

Specimen Code	Failure Stress N/mm^2	No. of cycles at failure	No. of steps	Starting stress N/mm^2	Stress step below failure N/mm^2	Estimated fatigue strength N/mm^2
G5 5	1050	33000	1	1050	(998)	1024
G5 6	834	145000	4	714	794	814
G5 7	988	23000	1	988	(939)	963
G5 8	888	170000	4	771	849	869
V1 5	1203	10900	7	856	1145	1174
V1 6	1161	89000	4	1042	1121	1141
V1 7	1137	26000	4	1019	1098	1118
V1 14	1208	36000	4	1095	1170	1189
V2 1	1202	26000	6	924	1146	1174
V2 2	1086	32000	3	979	1033	1060
V2 3	1189	495000	4	1032	1137	1163
V2 4	1109	57000	3	999	1054	1082
H 2	1191	228000	9	880	1152	1172
H 4	1205	261000	4	1021	1144	1175

TABLE 7b

Notched Fatigue Strength (four-point bending) of Carburised 635A14

Specimen Code	Initiation Stress N/mm^2	No. of cycles to initiation	No. of steps	Starting stress N/mm^2	Stress Step below Initiation N/mm^2	Estimated fatigue strength N/mm^2
G1 2	891	620000	1	891	(846)	869
G1 4	964	50400	4	843	924	944
G1 7	1158	77220	6	868	1100	1126
G1 8	1036	77000	4	891	988	1012
G2 1	916	13000	1	916	(870)	893
G2 2	988	75000	7	723	944	966
G2 3	1134	25740	6	868	1081	1108
G2 4	939	79000	1	939	(893)	916
G2 5	1024	272000	17	308	979	1002
G3 1	1013	294680	3	940	977	995
G3 2	988	240240	1	988	(939)	963
G3 3	1061	205920	4	965	1029	1045
G3 4	1013	223080	1	1013	(962)	988
G3 5	1086	334620	5	940	1050	1068
G3 6	988	120000	1	988	(939)	963
G3 7	1013	497460	3	940	977	995
G5 1	798	93240	5	638	758	778
G5 2	737	164800	4	597	691	714
G5 3	695	150000	7	542	669	682
G5 4	701	331200	4	560	654	678
G5 5	701	170000	6	551	671	686

TABLE 7 b (Continued)

Specimen Code	Initiation Stress N/mm^2	No. of cycles to initiation	No. of steps	Starting stress N/mm^2	Stress Step below Initiation N/mm^2	Estimated fatigue strength N/mm^2
V1 1	1097	16848	4	916	1037	1067
V1 2	1194	519000	6	916	1138	1166
V1 5	1097	10179	5	880	1043	1070
V1 6	1097	21760	5	880	1043	1070
V1 8	1097	66690	5	880	1043	1070
H 1	885	50000	8	610	845	865
H 2	1027	388800	11	613	986	1007
H 3	1027	103000	1	1027	(976)	1001
H 4	934	71280	9	613	894	914

TABLE 8

Effect of Mean Stress on the Bending Fatigue Strength of Carburised 635A14

Specimen Code	Failure stress Nmm^{-2}	No. of cycles at failure stress	No. of Steps	Starting Stress Nmm^{-2}	Stress step below failure Nmm^{-2}	Estimated fatigue strength Nmm^{-2}	Stress Ratio	Mean Stress Nmm^{-2}	Stress Amplitude Nmm^{-2}
G3 RB1	834	2090000	3	765	799	817	-1	0	817
G3 RB2	806	4400000	1	806	(766)	786	-1	0	786
G3 RB3	869	30000	3	806	838	854	-1	0	854
G3 RB4	886	310000	4	780	851	869	-1	0	869
G3 RB5	830	1580000	11	386	786	808	-1	0	808
G3 RB6	888	3244000	5	772	859	874	-1	0	874
G3 19	1137	27000	3	981	1059	1098	.07	587	511
G3 21	1198	218000	4	1001	1132	1165	.06	617	548
G3 4	1112	289000	1	1112	(1056)	1084	.12	607	477
G3 5	1195	41000	3	1087	1141	1168	.15	672	496
G3 25	1025	981000	3	950	988	1007	.3	654	353
G3 1	1191	190000	10	785	1146	1169	.35	789	380
G3 2	1174	110000	4	1054	1134	1154	.32	762	392
G3 3	1104	243000	1	1104	(1049)	1076	.3	700	376
G3 13	1219	194000	4	1035	1158	1189	.69	1004	185
G3 14	1249	199000	1	1249	(1187)	1217	.7	1036	182
H 1	1107	94000	1	1107	(1052)	1079	.09	588	491
H 3	1184	458000	13	684	1142	1163	.14	663	500
H 4	1205	216000	4	1021	1144	1175	.32	775	400
H 2	1191	228000	9	880	1152	1172	.33	779	393

TABLE 9

Bending Fatigue Strength of Carburised 080M15, at Different Stress Concentration Factors

Specimen Code	K_t stress Concentration Factor	Stress to Initiation Nmm^{-2}	No. of Cycles to Initiation	No. of Steps	Starting Stress Nmm^{-2}	Stress step below Initiation Nmm^{-2}	Estimated Fatigue Strength Nmm^{-2}
1A	1.96	613	108000	5	490	582	598
1B	1.93	567	300000	3	506	537	552
1C	1.91	619	88920	6	472	590	605
1D	1.93	589	359732	5	471	560	575
2A	2.52	610	185220	7	411	578	594
2B	2.5	493	106000	3	431	462	476
3A	2.21	622	59400	4	481	575	599
3B	2.21	584	42720	3	494	539	561
4A	1.89	751	10860	3	600	676	713
4B	1.87	614	364140	3	490	553	584
4C	1.89	757	50000	4	568	694	726
4D	1.91	695	143640	3	569	632	664
5A	2.8	527	41400	7	284	488	508
5B	2.82	483	124200	3	405	444	464
6A	2.8	523	2500	5	324	474	499
6B	2.93	530	243600	4	362	474	502
7A*	1.0	977	1083000	4	875	942	960
7B*	1.0	897	329000	5	731	855	876

* Plain cylindrical specimens tested to failure

5.2 Carbon Profile

Carbon profile determined by chemical analysis of 080M15 would be expected to occur at a lower carbon level than that of an alloyed steel, such as 635A14 [47]. This was shown by the present results, despite the fact that carbon profile on 635A14 was determined by the E.P.M.A. In this respect carbon profile due to G3 was determined by chemical analysis and Electron-probe microanalyser (E.P.M.A.) techniques on two samples of a piece of 080M15. The resulting profiles were found to be similar, see Fig. 48.

A slight drop in the carbon profile was observed due to the presence of the notch (in 4-P.B. pieces), however the shape of the profile is similar. This is illustrated in Fig. 49 for 635A14, carburised by G1, however carbon profile by chemical analysis of 080M15 carburised by G1 is also shown for comparison purposes. The presence of the notch in vacuum carburised pieces did not influence the resulting carbon profile, see Fig. 50. The effect of notch geometry on carbon profile is shown in Fig. 51.

Carbon profiles were determined by the E.P.M.A. unless otherwise stated. It should be noticed that carbon distribution was determined to a depth of about 1.0 mm, however the core carbon content was determined at greater depth and was found to correspond to the base steel carbon content.

Carbon profile results are presented in Figs. 51, 56, 61 and 66.

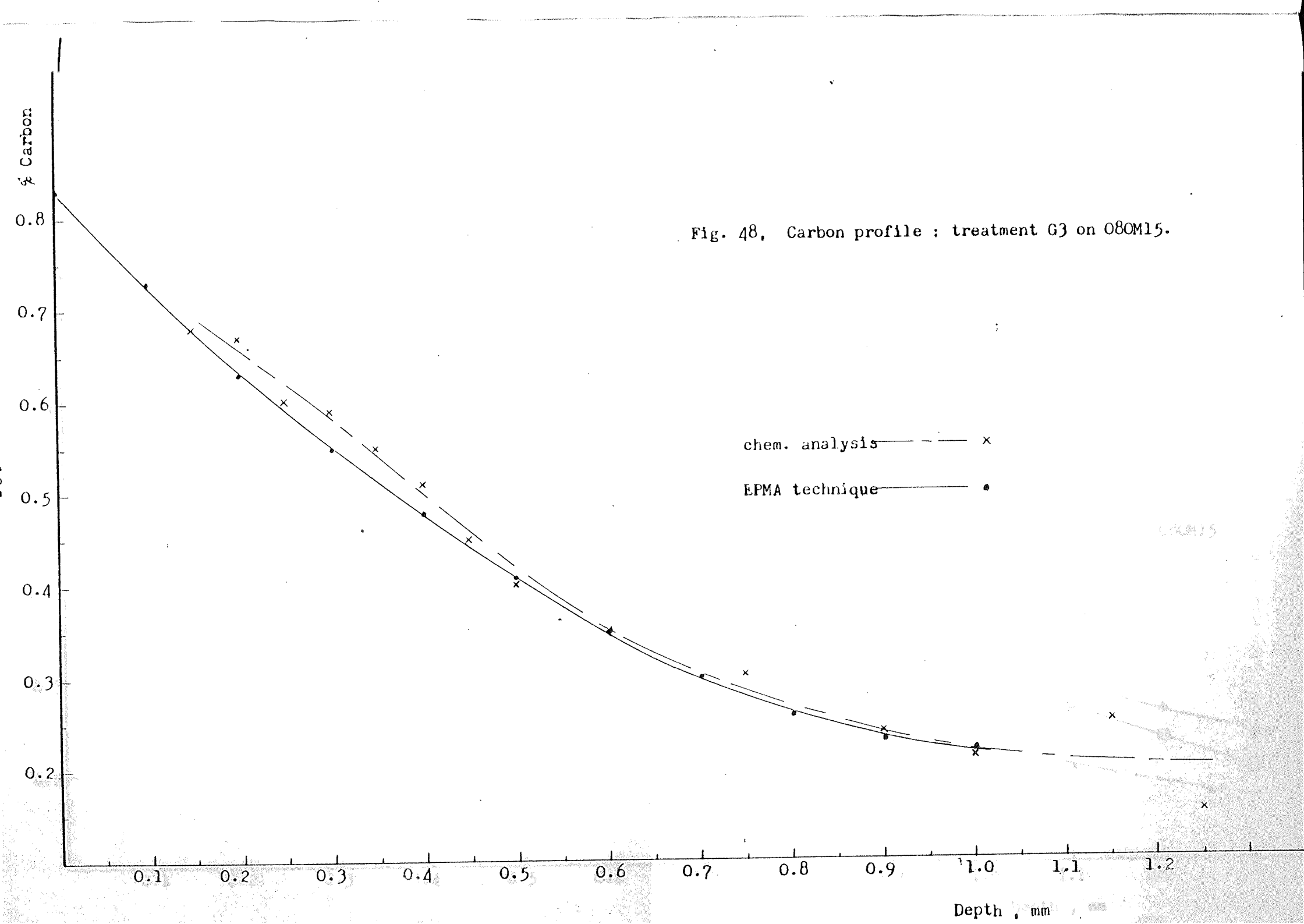

Fig. 48, Carbon profile : treatment G3 on O8OM15.

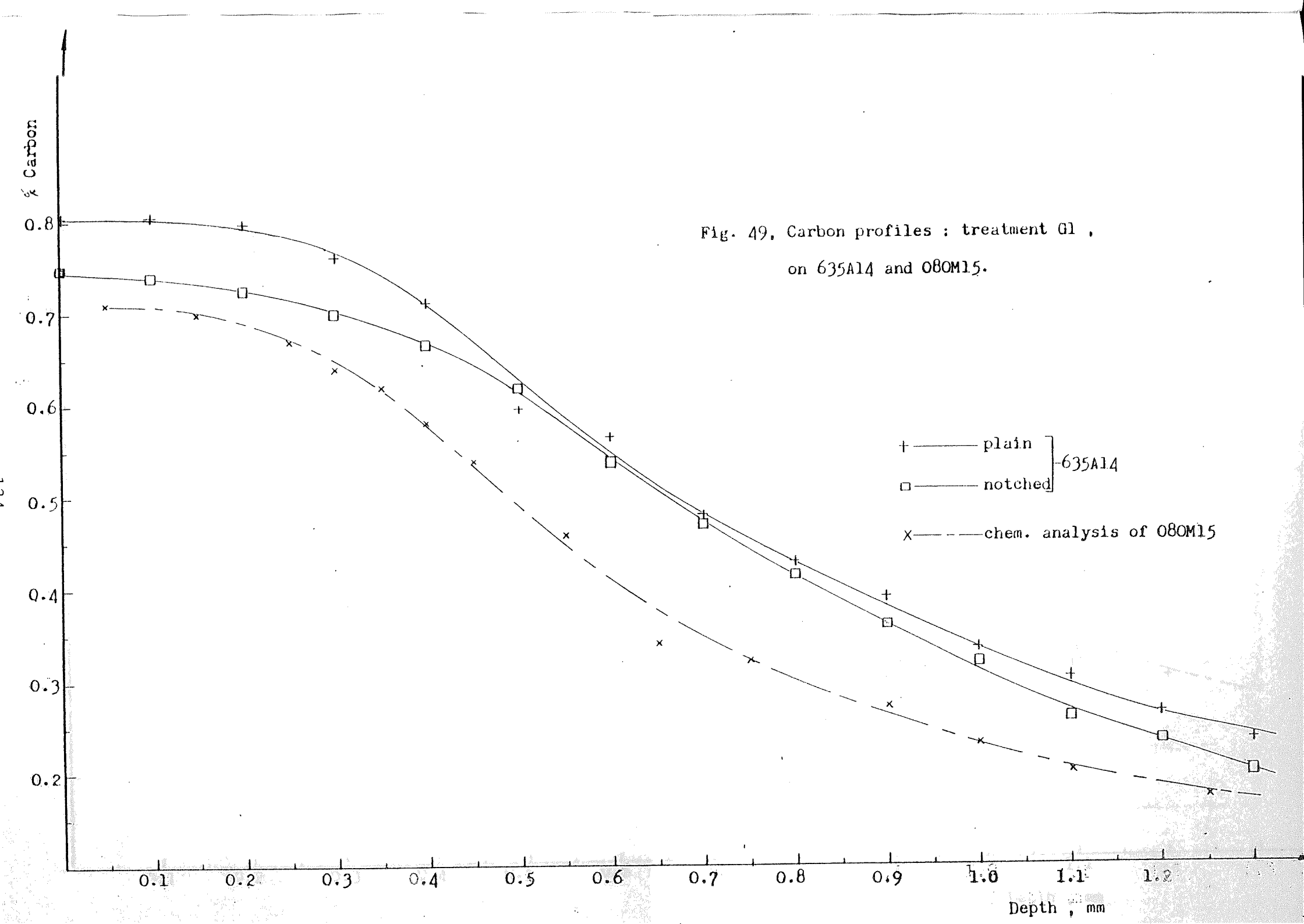

Fig. 49, Carbon profiles : treatment G1 ,
on 635A14 and 080M15.

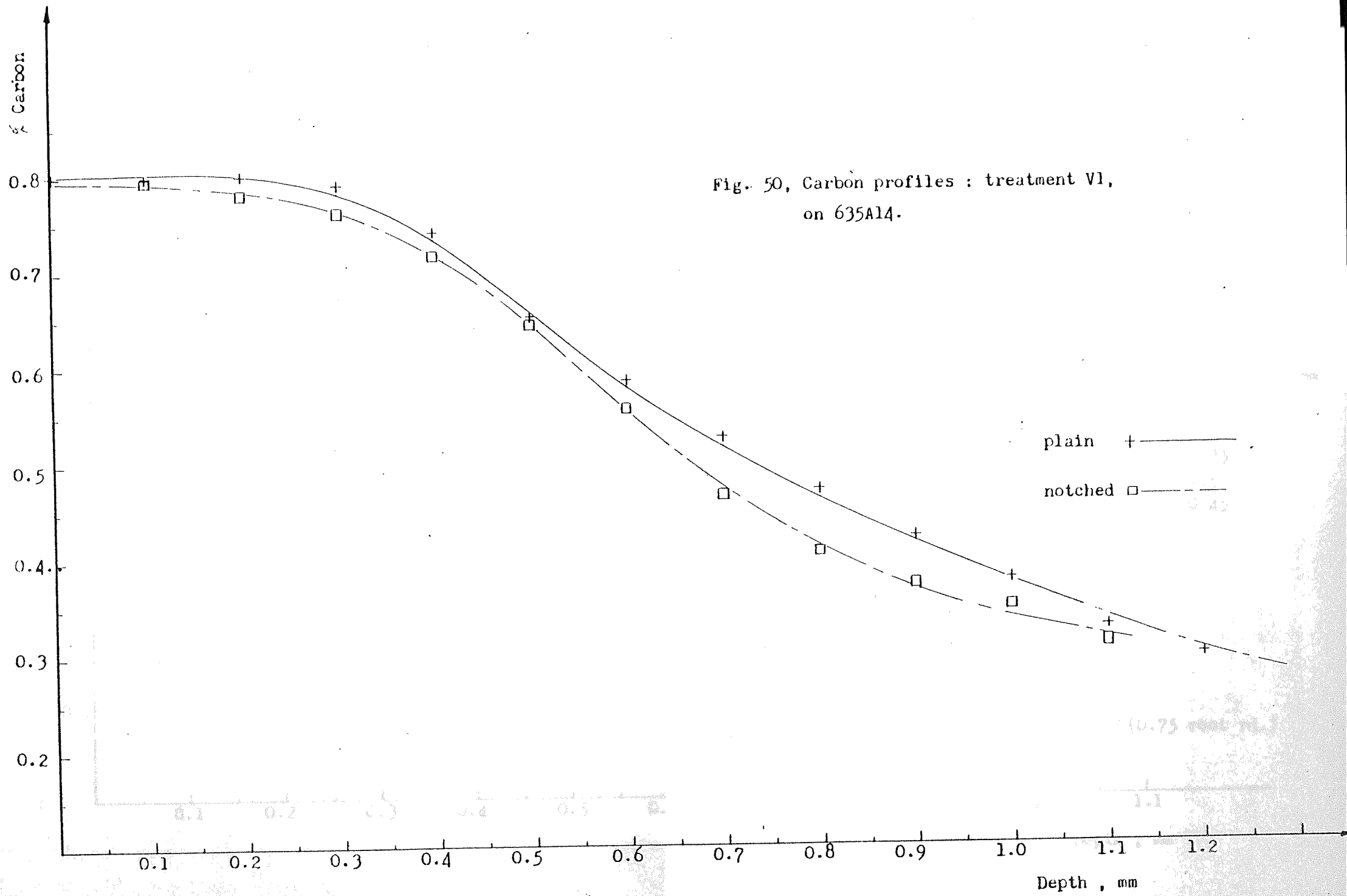

Fig. 50, Carbon profiles : treatment V1, on 635A14.

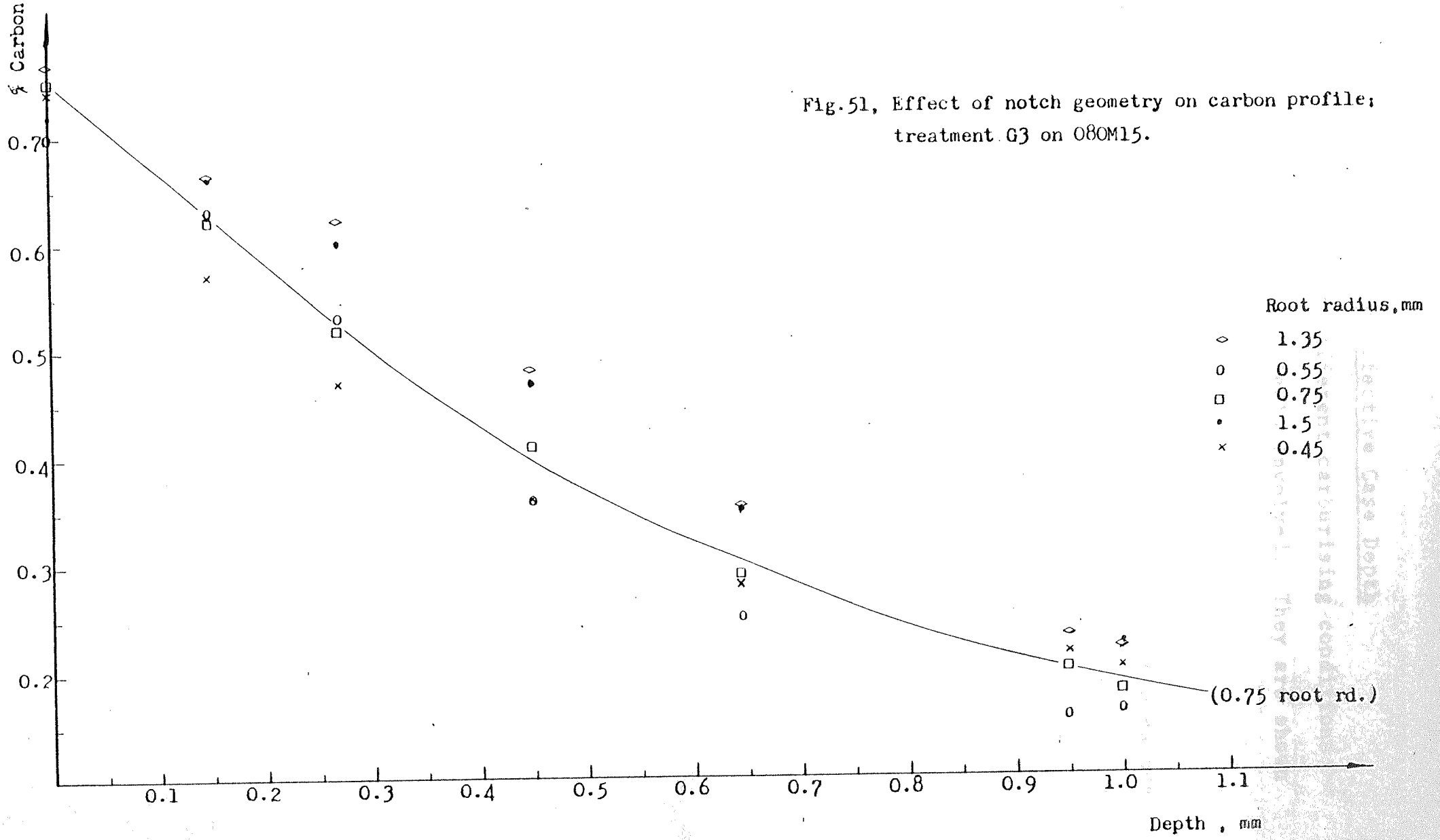

Fig.51, Effect of notch geometry on carbon profile; treatment G3 on 080M15.

5.3 Microhardness and Effective Case Depth

Hardness profiles for different carburising conditions were determined for the steels involved. They are shown in Figs. 57, 62, 67 and 73.

The slight drop of the carbon profile, due to the presence of the notch, may result in slight changes in the hardness profile and perhaps influence the effective case depth. Such a limited variation is not expected to influence the fatigue behaviour. Case depth, hardness and carbon content are listed in table 10 a,b along with the mean fatigue strength of each group.

TABLE 10a

Effect of Carburising on the Unidirectional Bending Fatigue Strength of 635A14

Group Design-ation	Geometry	Surface Hardness HV	Core Hardness HV	Effective Case depth mm	Surface Carbon %	Mean Fatigue Strength Nmm^{-2}
G1	Plain	870	283	1.11	0.8	1035
G1	Notched	960	308	1.03	0.75	987
G2	Plain	560	307	1.08	0.5	942
G2	Notched	560	280	1.0	0.45	977
G3	Plain	850	439	1.3	0.81	1101
G3	Notched	800	241	0.82	0.76	1002
G4	Plain	780	366	1.2	0.96	954
G5	Plain	980	300	1.8	1.2	917
G5	Notched	870	300	1.6	1.02	708
V1	Plain	860	250	1.03	0.8	1155
V1	Notched	840	250	1.06	0.8	1089
V2	Plain	950	383	2.0	1.12	1120

TABLE 10b

Effect of Carburising on the Rotating Bending Fatigue Strength of 835A15

Group	Geometry	Surface Hardness HV	Core Hardness HV	Effective case depth mm	Surface Carbon %	Mean Fatigue Strength Nmm^{-2}
G4	Plain	625	400	1.3	0.97	728
G4	Notched	860	380	1.2	0.88	443
G6	Plain	880	430	1.1	0.87	696
G6	Notched	850	430	1.06	0.89	484
G7	Plain	930	450	1.4	0.81	689
G7	Notched	770	435	1.36	0.76	449

5.4 Residual Stresses

Residual stresses, as a result of carburising and hardening treatments G1, G2, G3 and G5, were determined, see appendix 3. Results are shown in table 11 along with the estimated fatigue strength of 635A14. It should be noted that residual stresses were determined on 080M15 steel specimens, which may be of higher magnitude than on 635A14 or 835A15, depending upon the surface and core carbon contents and other metallurgical variables arising from carburising. Only longitudinal stresses are considered.

martensitic case,

pearlite and/or

TABLE 11

The effect of Carbon Profiles on the Residual Stresses of Carburised 080M15

Thermochemical Treatment	Residual stress N/mm^2	Fatigue Strength N/mm^2
G1	-661	1037
G2	+103	942
G3	-507	1101
G5	-306	917

5.5 Microstructural Investigations

Microstructure examinations showed the martensitic case, however core microstructure consisted of martensite and/or bainite and ferrite depending upon the steel and the austenitising temperature. Retained austenite, carbides and oxides were observed due to particular carburising conditions. Microstructural variations will be discussed later. However, typical case and core microstructures are shown in Fig. 52.

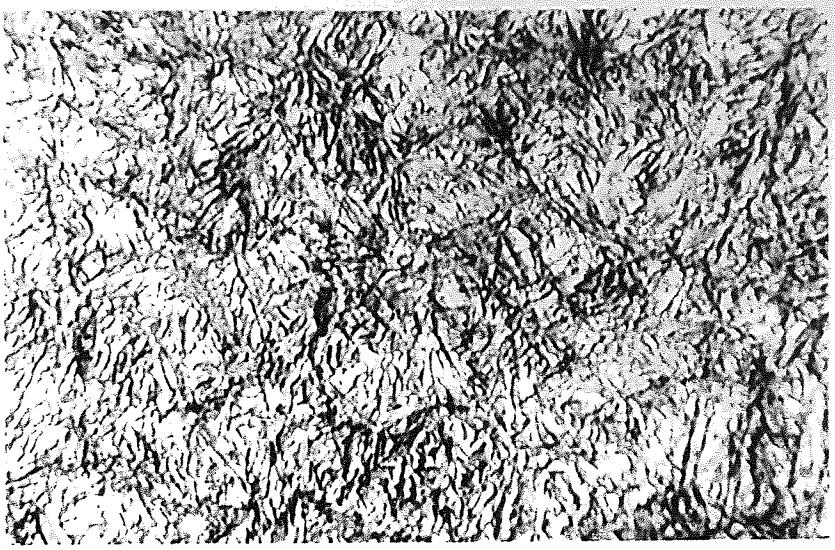

Case

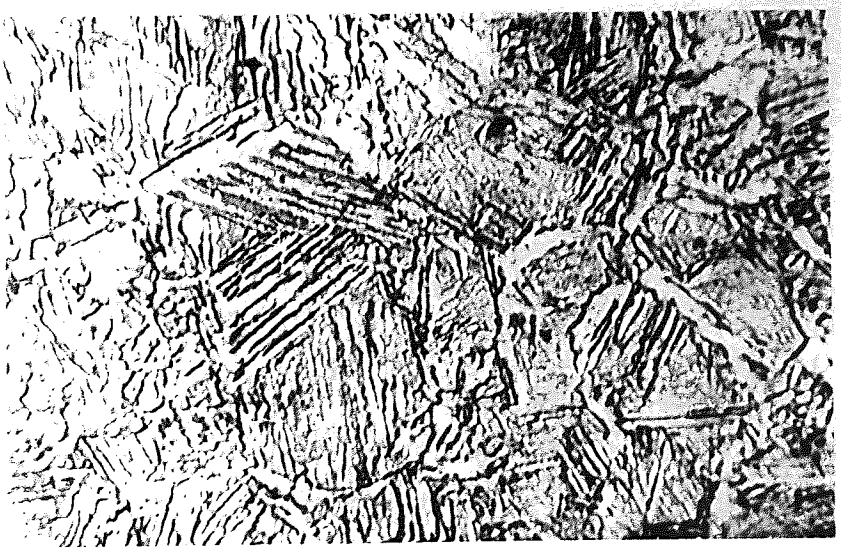

Core

Fig.52 , Typical case & core microstructure of carburised-oil quenched 635A14.(x 1000).

5.6 Fracture Surface Observations

Examination of fracture surfaces showed the brittle intergranular fracture in the high carbon case, while the low carbon core fracture was ductile, Fig. 53. This will be considered in more detail in the discussion.

In an attempt to relate microstructure to fracture topography, few fracture surfaces were examined with part of the fracture surface in the polished etched state, see Fig. 54. However micrographs produced by the scanning electron microscope can be seen in Figs. 55 and 86.

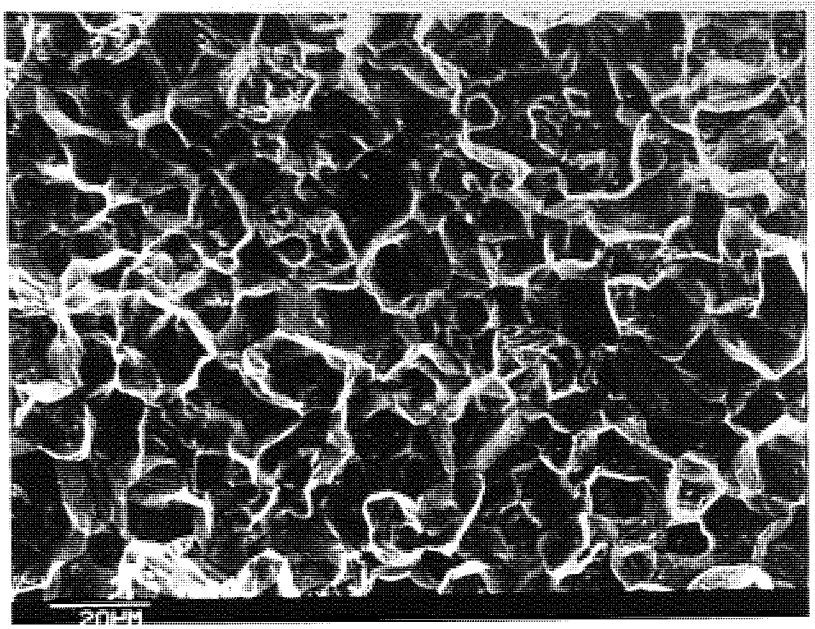

Case

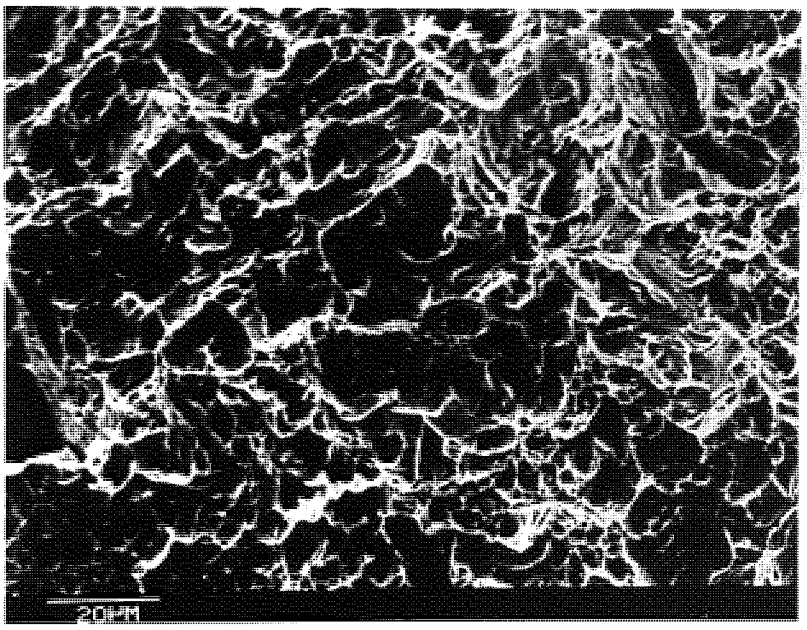

Core

Fig.53, Fracture surface topography of carburised 635A14.

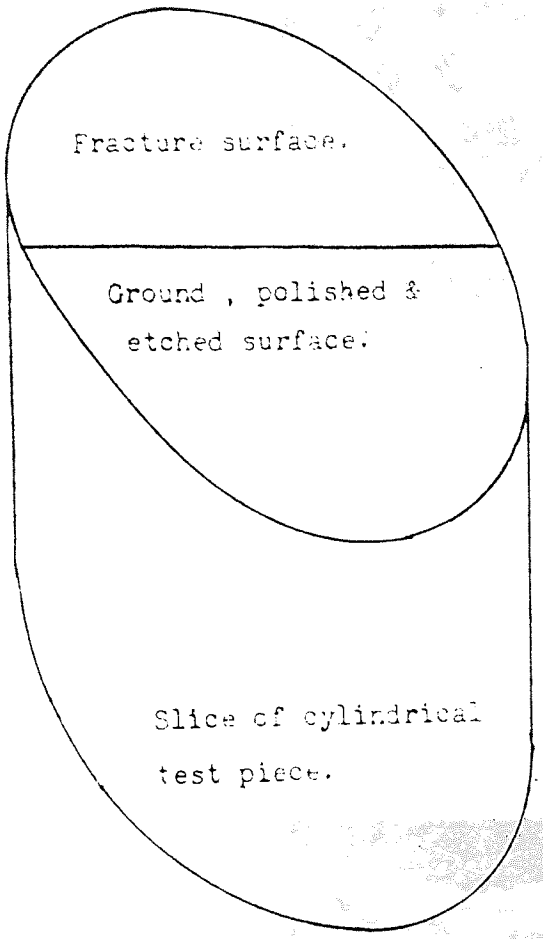

Fig.54. Fracture surface, partly ground to relate microstructure to fracture topography.

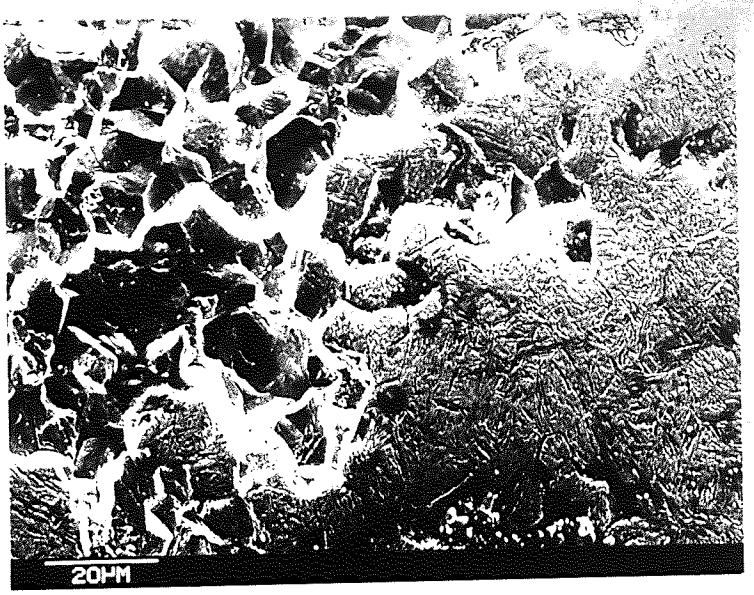

(a)

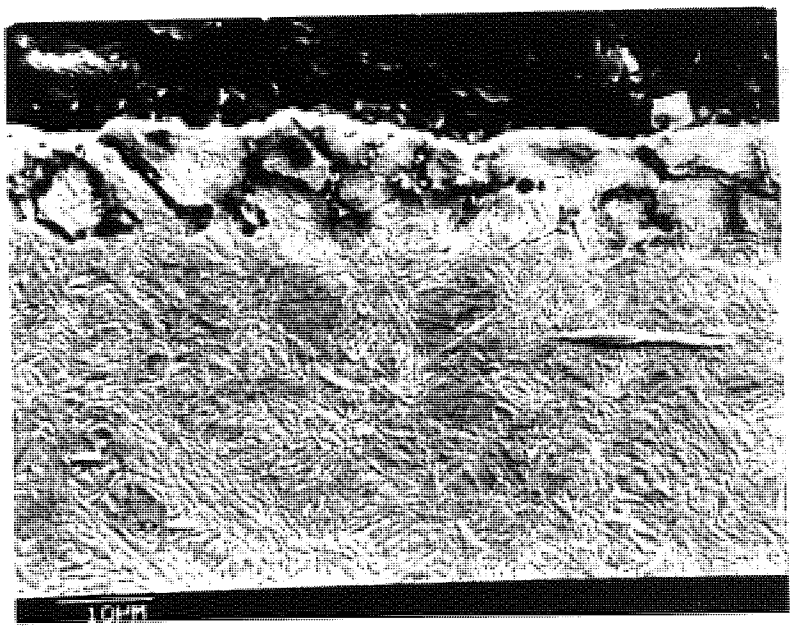

(b)

Fig. 55 , Scanning electron micrographs, (a) Fracture; (b) Microstructure and internal oxidation, in carburised 635A14.

6.0 Discussion

The fatigue behaviour of carburised steel under reversed bending has been given more consideration by other workers than that in unidirectional bending.

The mechanical and in particular the fatigue behaviour of a carburised component is complicated because of strength gradient and triaxiality of stresses at the case-core interface, as well as the wide variation of factors arising from different carburising conditions and the dependent nature of those factors. However the fatigue performance may also be influenced by the type of loading and mean stress. In this respect most fatigue results quoted in the literature are for rotating bending.

Compressive residual stresses are one of the main objectives of carburising. The literature has covered residual stresses and their variation due to other factors such as internal oxidation, carbides, etc.. The detrimental effect of tempering on compressive residual stresses and subsequently on the fatigue strength is well documented. Despite that most of the results are for tempered test pieces.

It is intended to discuss the influence of different carburising conditions on the fatigue strength, mainly under unidirectional bending. Metallurgical variables will be considered in conjunction with each carbon profile. However residual stresses are discussed in light of the present results, and as influenced by other metallurgical variables.

6.1 Residual Stresses

The importance of residual stresses in the fatigue performance of a carburised component is most pronounced in the untempered condition. Residual stress sign and magnitude is expected to be influenced by the carburising procedure and the subsequent carbon profile.

The experimental determination of residual stresses due to four gas carburising treatments are shown in table 11. Where a single value represents the mean of the residual stress in the carburised case. These values do not allow assessing the effect of residual stresses on the initiation and subsequent propagation of a fatigue crack for which a knowledge of residual stress distribution is essential. However they may be used in discussing fatigue strength results.

It can be seen from table 11 that residual stresses are compressive in all cases except for the group subjected to surface decarburisation (G2). Maximum compressive stresses have resulted from boost diffuse-plateau (G1), residual stress of 661 N/mm^2 was determined. Single stage carburising (G3), showed a slight loss of compressive stress. Their value is found to be 507 N/mm^2 compressive. The relatively higher amount of retained austenite due to G3 may be responsible for the mentioned loss in residual stress.

Single stage over carburised (G5) has resulted in 306 N/mm^2 compressive. This is less than half that due to G1 and about two thirds that of G3. The reduced compressive stresses due to G5 may be attributed to the combined effect of retained austenite and carbides.

Surface decarburisation (G2) has resulted in the complete loss of compressive stress, and tensile stresses of about 103 N/mm^2 has resulted instead. In this case surface decarburisation is responsible for the resulting tensile stresses, by the early transformation at the lower carbon immediate surface layer on one hand and the severe internal oxidation associated with it on the other.

Internal oxidation is expected to exert its effect on residual stresses, however carburising parameters were comparable in all cases. The only exception is the fact that during decarburisation, air was introduced rapidly in the furnace to allow decarburisation to occur. Consequently severe internal oxidation has resulted and influenced the residual stresses. The freedom of vacuum carburised pieces from internal oxidation must have a bearing upon their superior fatigue strength, as will be shown later, however in this respect residual stresses in the absence of internal oxidation and tempering might have exerted their full effect.

As it has been mentioned earlier, residual stresses were determined on 080M15 which is a plain carbon steel, in which the oxidation affinity would not be as high as in an

alloyed steel such as 635A14. Consequently residual stresses on the latter would be more influenced by internal oxidation. Also the higher surface carbon on 635A14 at any carburising potential would result in greater amounts of retained austenite and carbides, both of which will influence the resulting residual stresses. When considering fatigue strength results reference will be made to the residual stress results quoted in table 11 despite the above differences.

6.2 Rotating Bending

Despite the whirlling effect, due to specimen distortion by heat treatment (see appendix 4), a limited number of samples were designed and tested in rotating bending. Single stage and boost diffuse carburised 835A15 specimens were produced according to conditions G4 (single stage), G6 and G7 (boost diffuse). Both plain and notched fatigue strength were determined.

The three carburising conditions employed, i.e. G4, G6 and G7, have produced the carbon profiles shown in Fig. 56. The steep shape of the profile due to single stage (G4), becomes flatter by boost diffuse, G6 and G7. Carburising by G4, see Fig. 56, has produced 0.97% surface carbon. This, however, is likely to be associated with retained austenite. The hardness profiles are shown in Fig. 57, that due to G4 was indicative to the presence of retained austenite. On the other hand G6 and G7 produced lower surface carbon and the corresponding hardness profiles showed no similar behaviour to that found as a result of G4. Microstructure investigation showed and confirmed the hardness profile indications in that considerable amount of retained austenite is found in the case - near the surface - of pieces treated by single stage (G4), however, case microstructure due to both G6 and G7 showed no retained austenite, see Fig. 58, while Fig. 59 shows a typical core microstructure.

Retained austenite due to carburising by G4 was estimated by point count to be about 35%.

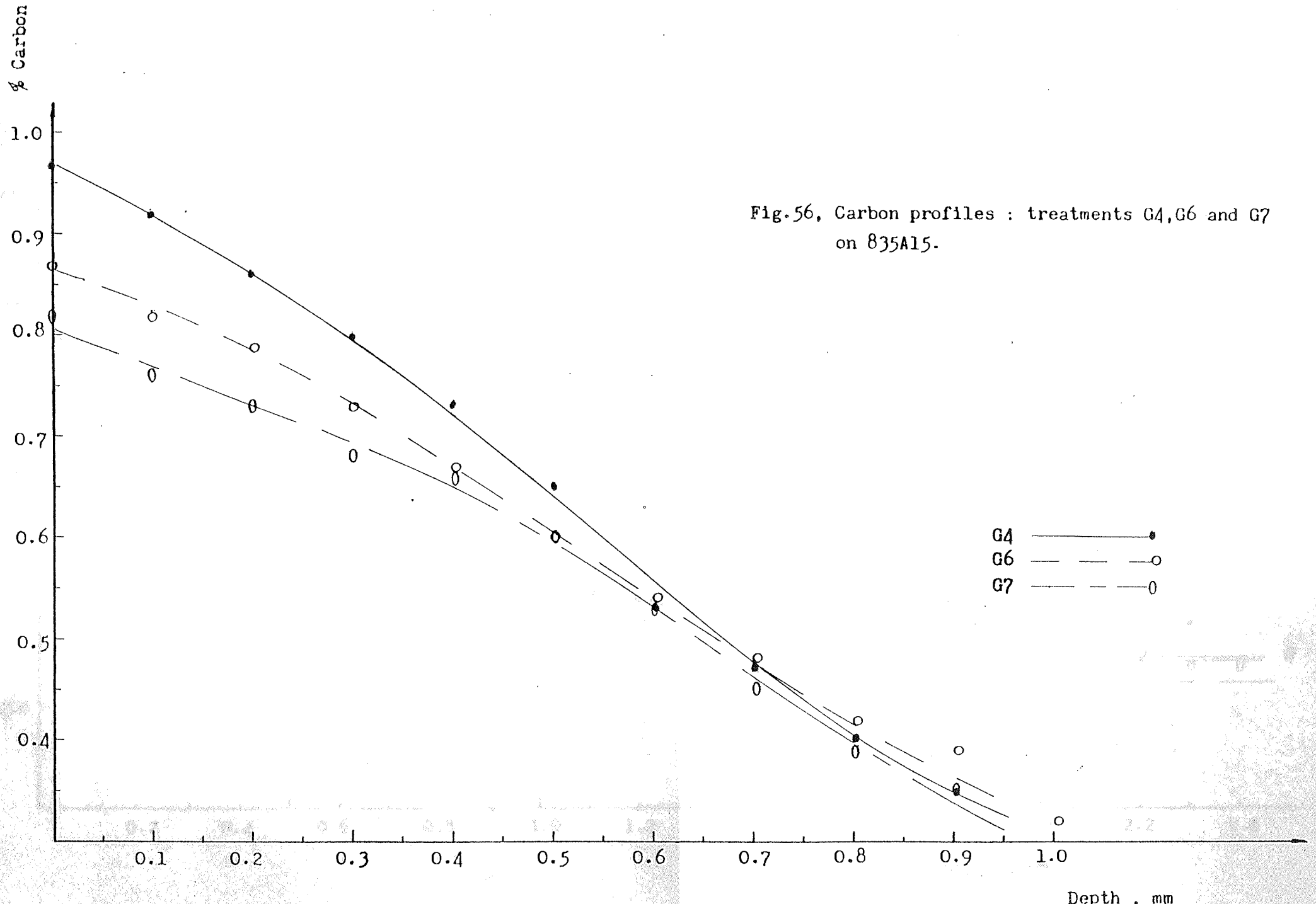

Fig.56, Carbon profiles : treatments G4, G6 and G7 on 835A15.

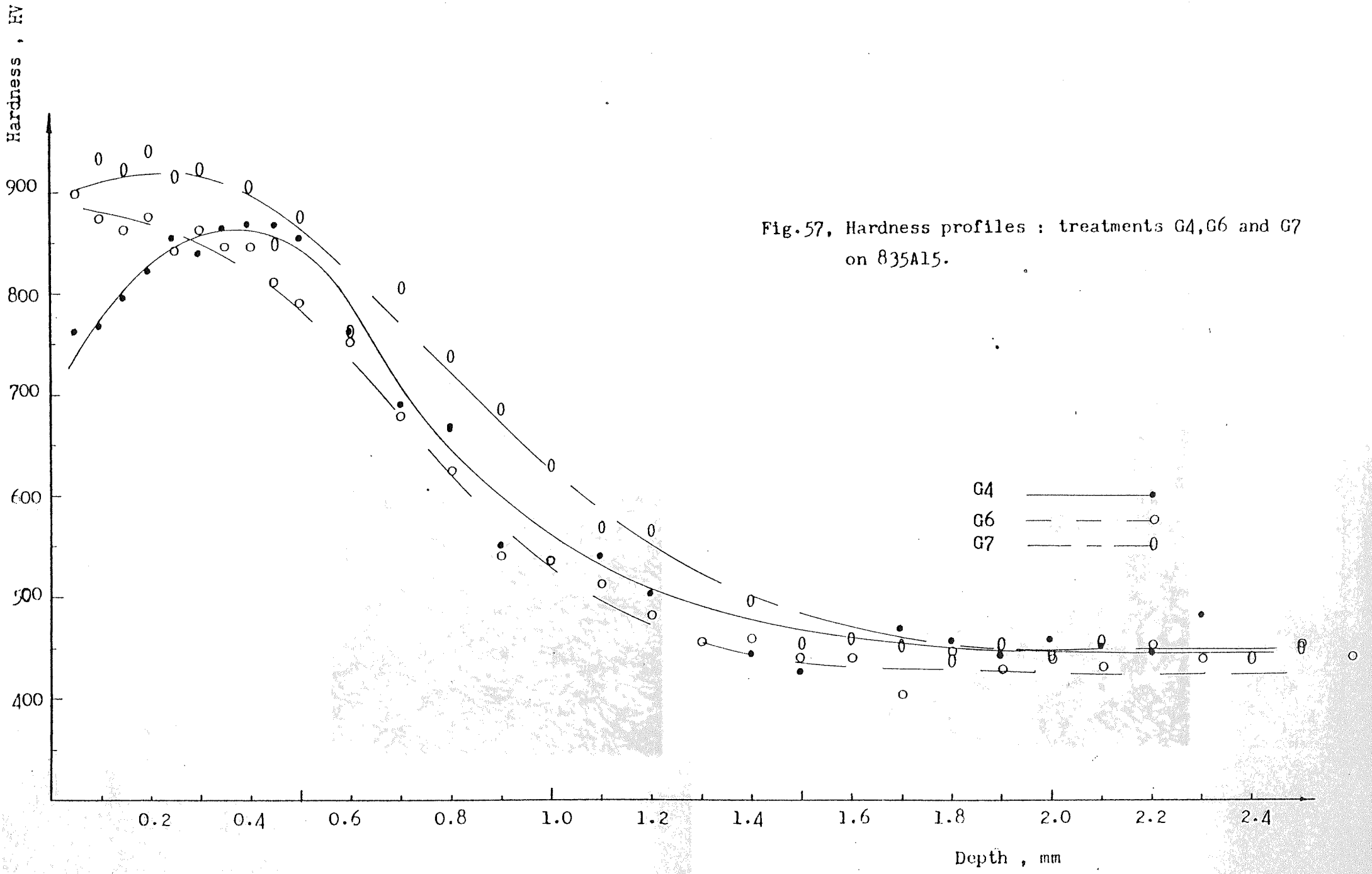

Fig.57, Hardness profiles : treatments G4,G6 and G7 on 835A15.

(a)

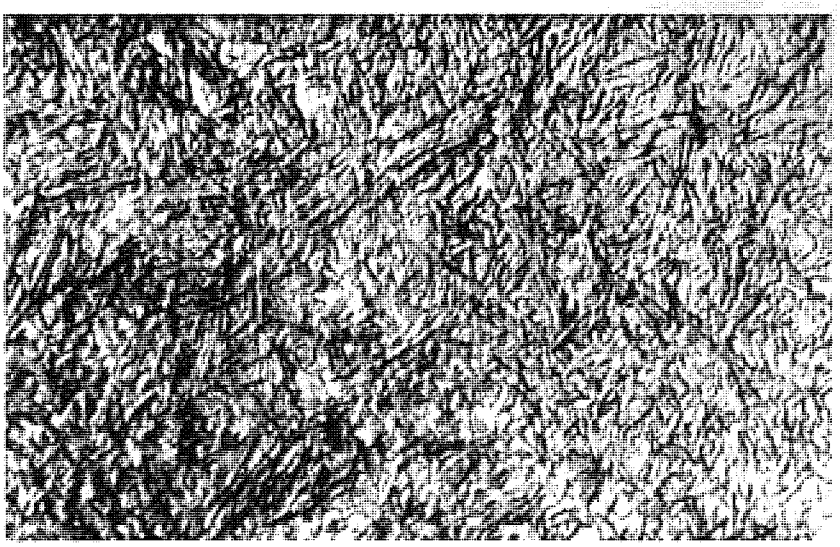

(b)

Fig.58, Case microstructure of 835A15 carburised by a.Single stage-G4;b.Boost diffuse-G6.(x 1000).

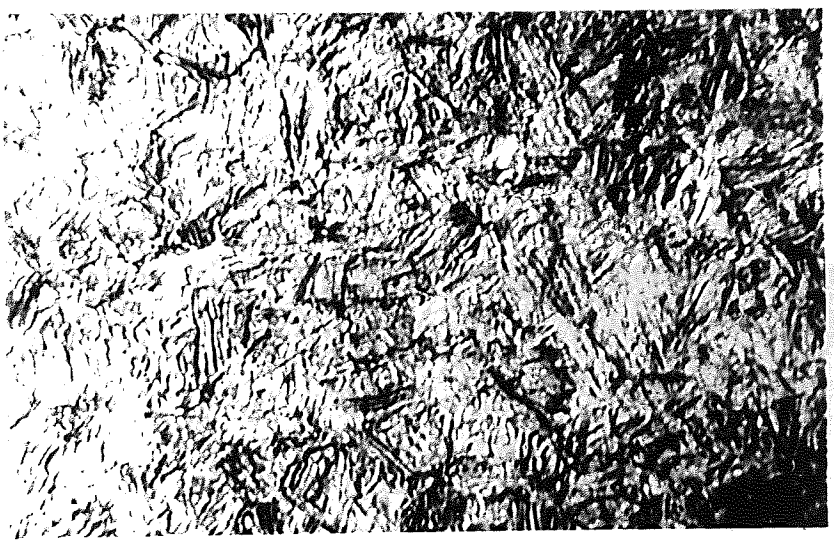

Fig.59, Typical core microstructure of carburised 835A15. (x 1000).

The results presented in table 10 show that slight variation in the case depth did not influence rotating bending fatigue strength. As far as fatigue results are concerned, Fig. 60 shows that single stage carburising G4 has resulted in 5% increase in the plain bending fatigue strength over that due to either G6 or G7. However, statistical analysis showed that the increase quoted above is not significant. Consequently this suggests that the retained austenite to the amount of 35% did not influence the plain fatigue strength in rotating bending.

The high level of retained austenite due to G4 in comparison to either G6 or G7 is expected to lead to lower level of compressive residual stresses than would be expected from G6 or G7. Although residual stresses were not determined for these conditions, it can only be suggested that the lower residual compressive stresses expected due to G4 did not significantly affect the plain bending fatigue strength.

As for the notched fatigue strength, Fig. 60, boost diffuse by G6 produced the highest, where 7 and 10% increase is observed over that due to G7 and G4 respectively. However statistical comparisons showed that the quoted increase is not significant. In fact case microstructure due to G4 at the root of the notch was found to be very similar to those due to G6 and G7 in the absence of retained austenite.

Notch sensitivity will be discussed later. Meanwhile, the similar notch sensitivities found due to G4, G6 and G7 treatments indicate the comparable effect of compressive residual stresses.

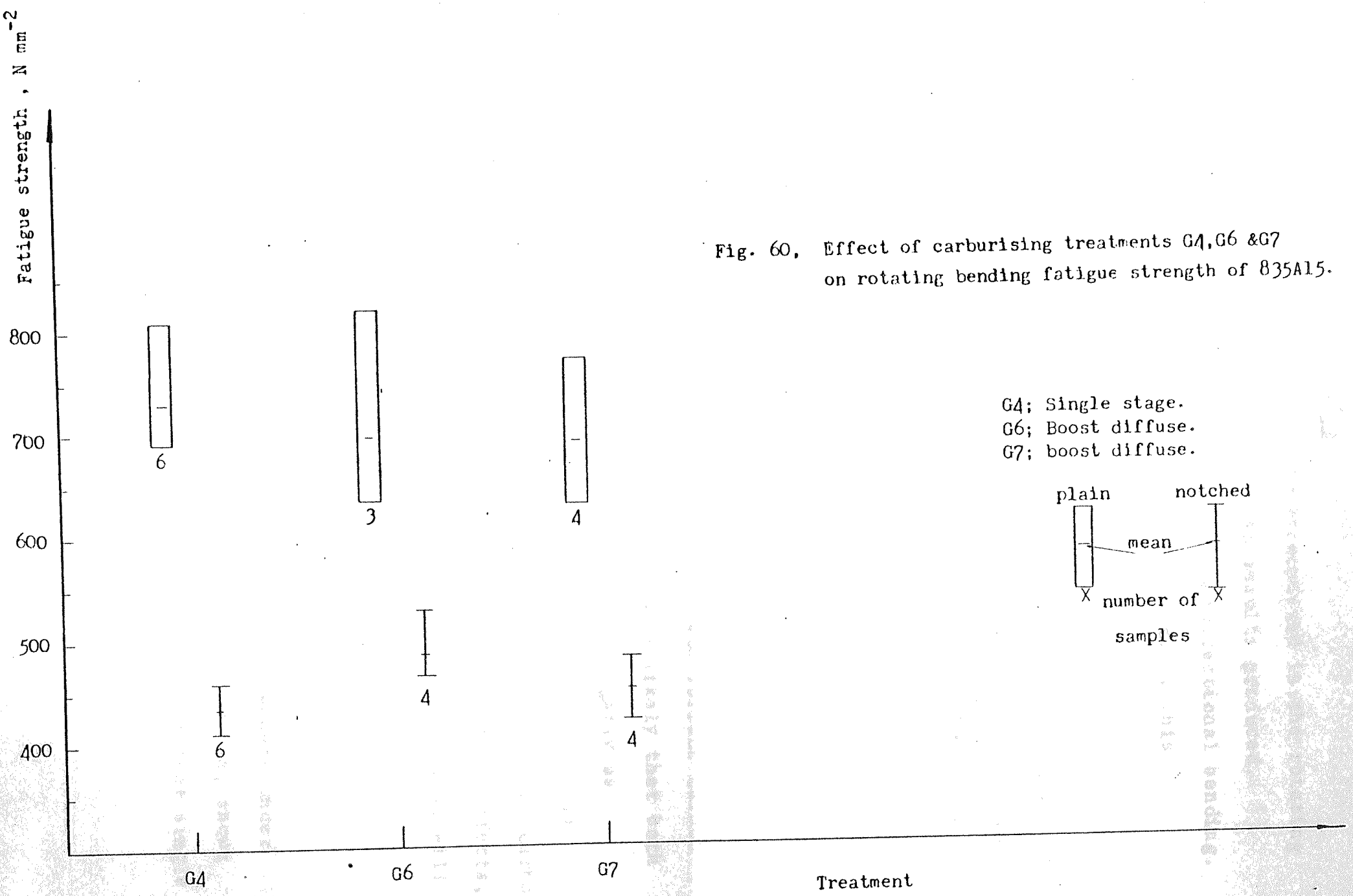

Fig. 60, Effect of carburising treatments G4, G6 &G7 on rotating bending fatigue strength of 835A15.

G4; Single stage.
G6; Boost diffuse.
G7; boost diffuse.

6.3 Unidirectional Bending

The unknown effect of whirling encountered in the rotating bending tests may have affected the results produced. Consequently the project used mainly unidirectional bending. This may help in assessing the significance of this stressing mode for practical applications.

The fatigue behaviour of 635A14 in different carburising conditions is investigated in unidirectional bending, where a stress ratio of 0.3 was used for the nature of the machine and specimens on one hand and to avoid crack closure once it is initiated.

6.3.1 Gas Carburising

Ideally carbon profiles can be produced by altering the carburising conditions to maintain the same surface carbon content and case depth. In practice it is likely that both surface carbon and case depth will change slightly as different carbon profiles are produced. Consequently it is difficult if not impossible to isolate the effect of carbon profile on the fatigue strength. Accordingly, these effects, i.e. microstructural differences and residual stresses, will be considered.

6.3.1.1 Single Stage - Steep Carbon Profile (G3)

Single stage carburising in conventional atmosphere under conditions G3 and G4 produced steep carbon profiles, shown in Fig. 61. However it can be seen from table 4 that single

stage G4 was carried out at higher carburising potential. Consequently, the surface carbon content and the whole carbon profile is higher than that due to single stage G3. The higher surface carbon of G4 is associated with some retained austenite. This is recognised from the hardness profile shown in Fig. 62, where it can also be seen that the profile due to G3 did not indicate comparable amounts of retained austenite. In fact this is also shown by the microphotographs of Fig. 63.

Retained austenite estimated by point count to be about 28% due to G4 and only 8% due to G3. The actual amount of retained austenite may be higher than that determined by the point count technique.

As far as plain fatigue strength is concerned, Fig. 64 illustrates that G3 has resulted in 15% increase over that due to G4. In this respect statistical analysis showed the significance of that superiority. Higher level of retained austenite, due to G4, is expected to lower the compressive residual stresses, although the residual stresses due to G4 were not determined. Their value due to G3 estimated to be 507 N/mm^2 (compressive) where the retained austenite was only 8%. This can only suggest that when retained austenite is 28% the compressive residual stresses could be much lower.

Therefore the higher bending fatigue strength due to G3 is an indication of the detrimental effect of the high retained austenite found in G4, on the compressive residual stresses and consequently on the plain fatigue strength in unidirectional bending.

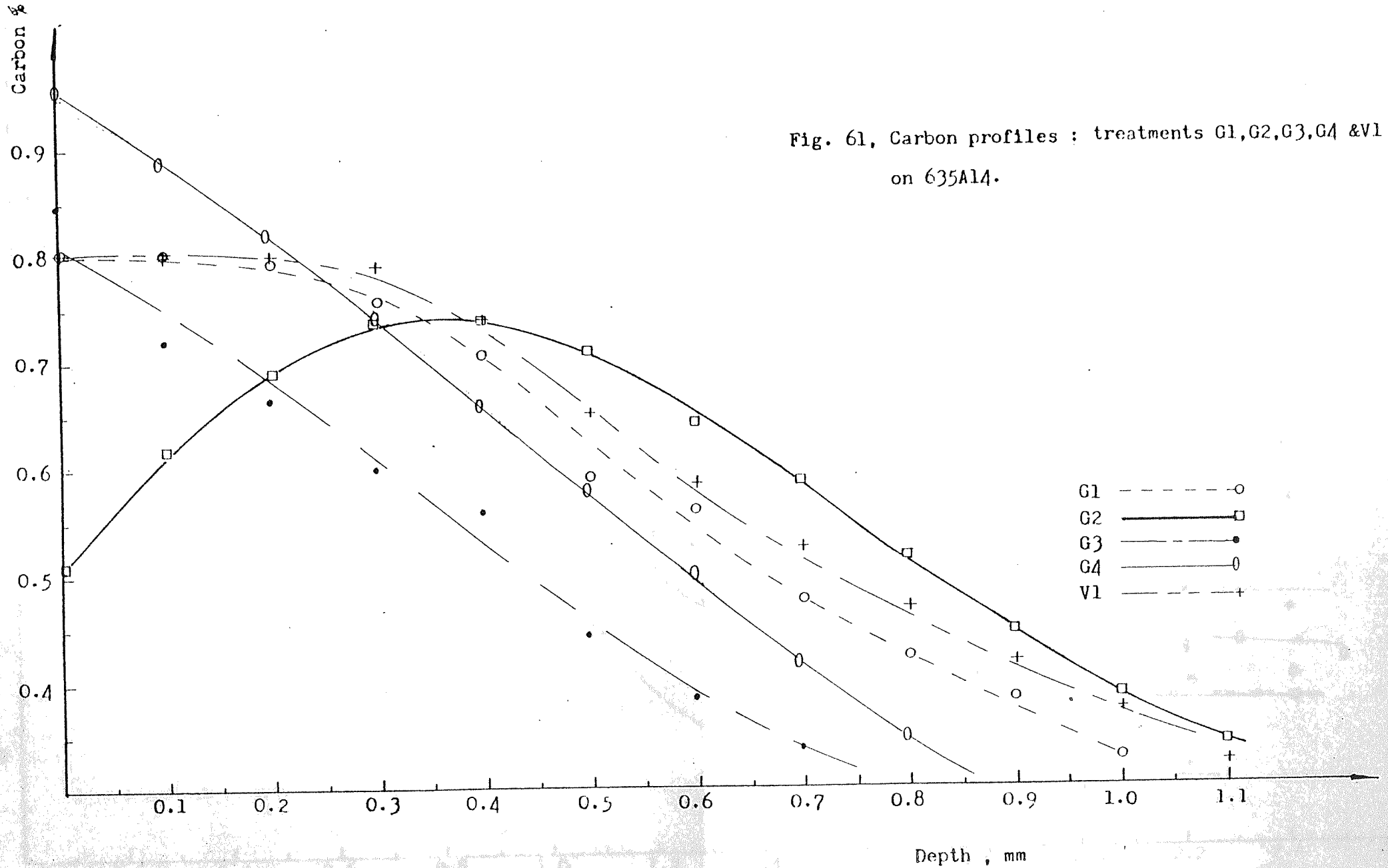

Fig. 61, Carbon profiles : treatments G1,G2,G3,G4 &V1 on 635A14.

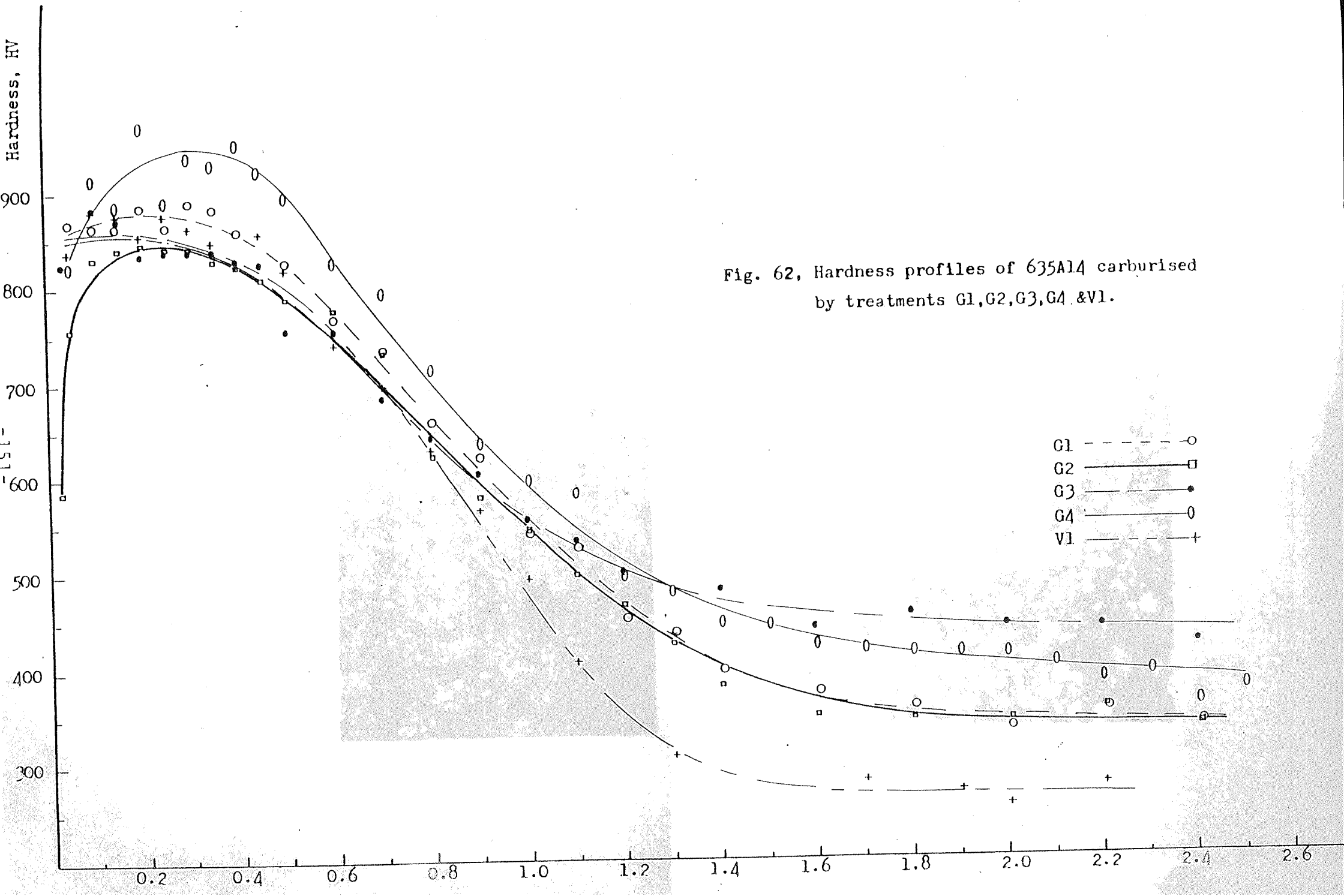

Fig. 62, Hardness profiles of 635A14 carburised by treatments G1,G2,G3,G4 &V1.

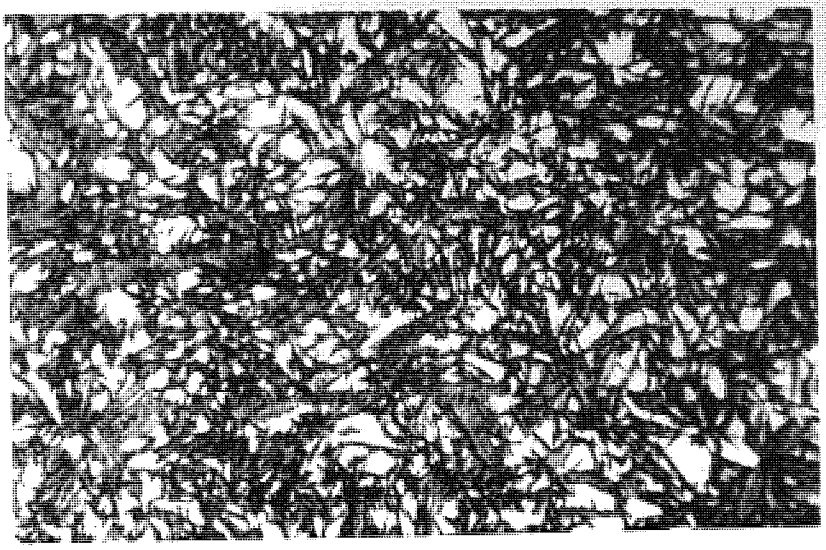

(a)

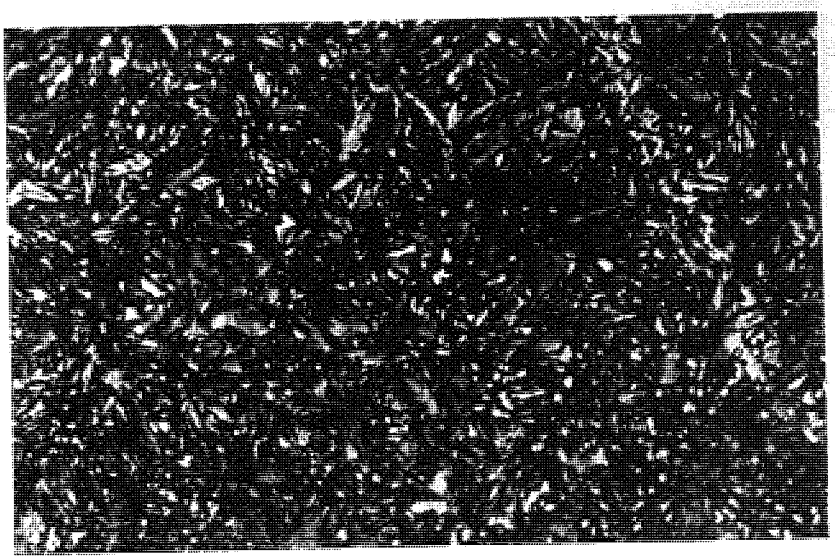

(b)

Fig.63, Case microstructure of 635A14 carburised by;

(a).Single stage - G4. (x 1000)

(b).Single stage - G3.

6.3.1.2 Boost-diffuse with Surface Decarburisation (G2)

Surface decarburisation of a carburised 635A14 resulted due to treatment G2, whose carbon profile is shown in Fig. 61. It can be seen that such surface decarburisation has caused the surface carbon content to decrease to about 0.5%, while 0.74%C is maintained at about 0.35 mm from the edge. This decarburisation is also indicated by the hardness profile shown in Fig. 62. It is to be expected that such surface decarburisation will result in softer low carbon martensite. In practice decarburisation takes place due to inaccurate control of the carburising conditions, or due to reheating for hardening. However this has not been the case here, as decarburisation was allowed to occur intentionally by dropping the carburising potential by rapid addition of air, which in doing so increased the oxidation potential.

Microstructural investigation of the case revealed internal oxidation associated with small amounts of ferrite, see Fig. 65. Residual stress estimated to be tensile to a value of 103 Nmm^{-2}, as shown in table 11. The tensile nature of the residual stresses underlines the detrimental effect of decarburisation on residual stresses.

Decarburisation was found to be associated with low carbon martensite as well as small amounts of ferrite, both are of lower strength than high carbon martensite. Furthermore, it is likely that the transformation of

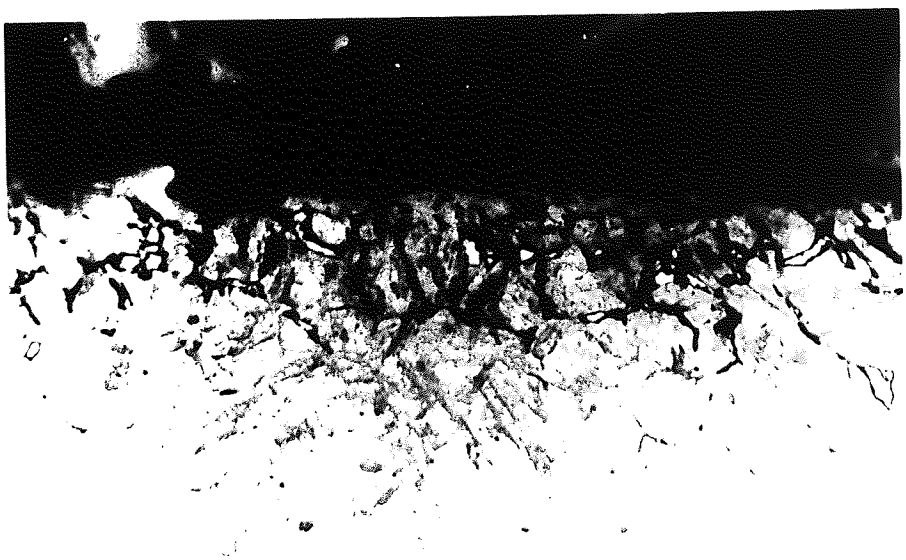

Fig.65, Ferrite associated with severe internal oxidation in decarburised 635A14. (x 1000)

the lower carbon martensite and the ferrite at the immediate surface along with the progress of transformation from the case-core interface has left the surface or near the surface in a state of tension.

Surface decarburisation due to G2 has resulted in 15% reduction in the fatigue strength in comparison to single stage G3, see Fig. 64. However the detrimental effect of decarburisation was proved by statistical analysis of variance which showed that the fatigue strength due to G2 is significantly lower than that due to G3.

It is apparent that the tensile residual stresses along with the lower strength surface layer, have acted in lowering the fatigue strength in unidirectional bending.

6.3.1.3 Boost-diffuse without Surface Decarburisation (G1)

Carburising by boost-diffuse techniques as we have seen resulted in a flatter carbon profile as compared to that due to single stage. However this technique was employed and the carbon profile was allowed to flatten near the surface by duffision treatment. The carbon profile due to boost-diffuse G1 is flat - plateau - near the surface, as can be seen in Fig. 61. The hardness profile shown in Fig. 62 indicates similar pattern. Microstructure investgations revealed typical case and core microstructure, retained austenite, if existing, very limited and was estimated to be about 4%.

The resulting carbon profile is expected to allow the right transformation sequence to take place. In turn it is to be expected that compressive residual stresses will be produced in the case. In fact the residual stress due to G1 are compressive, estimated to a value of 661 Nmm^{-2}.

The plain fatigue strength due to G1 is lowered by about 6% when compared with single stage G3, see Fig. 64. This reduction is surprising in the light of the compressive residual stress quoted above is higher than the value quoted due to G3 (507 Nmm^{-2}). Statistical analysis showed that the fatigue strength due to G1 is not significantly different from that due to G3 and consequently suggest that the quoted reduction has arisen by chance.

Previous workers underlined the fact that residual stresses did not correlate with the fatigue strength, besides that, estimated residual stresses do not give any detail about their pattern which is needed in visualising any possibility of local yielding due to high applied stresses. Therefore it is certain that for qualitative assessment of this type of boost-diffuse profile and accurate comparison with single stage, residual stress distribution is essential.

6.3.1.4 Single Stage - Over Carburised (G5)

The failure in controlling the required carburising potential in single stage carburising, and that in dropping the high potential during the boost stage to the required level for the diffusion stage in the boost-diffuse technique, would both bring the surface layer of the charge to the saturation level of austenite, consequently resulting in overcarburised surfaces.

The associated variation in microstructure, the formation of carbides in the main and their subsequent effect on the residual stresses and in turn on the fatigue strength (in unidirectional bending), are all of vital importance in the fatigue behaviour of a carburised component. Single stage over carburised profile will be discussed according to these effects.

Single stage (G5) gas carburising at high carbon potential has produced the carbon profile shown in Fig. 66. It should be noticed that the amount of carbon absorbed at the immediate surface is actually 1.2%C and, more than that, the whole carbon profile is shifted to a higher carbon content at any depth of penetration as compared to any of the other treatments. The saturation of the surface with carbon has resulted in the formation of carbides in globular and intergranular form, alongside with some retained austenite. The hardness profile shown in Fig. 67 with the hardness dropping gradually

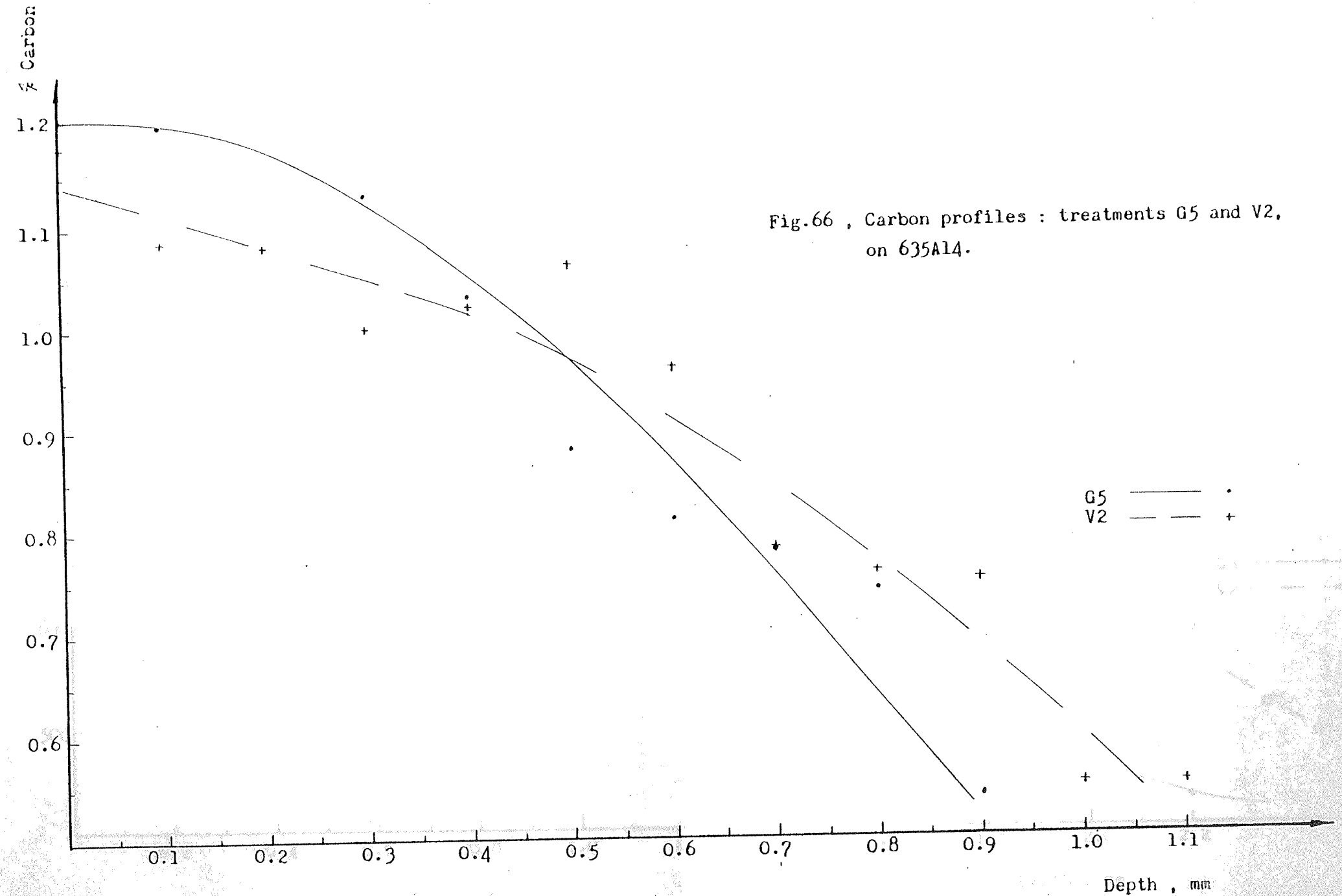

Fig.66 , Carbon profiles : treatments G5 and V2, on 635A14.

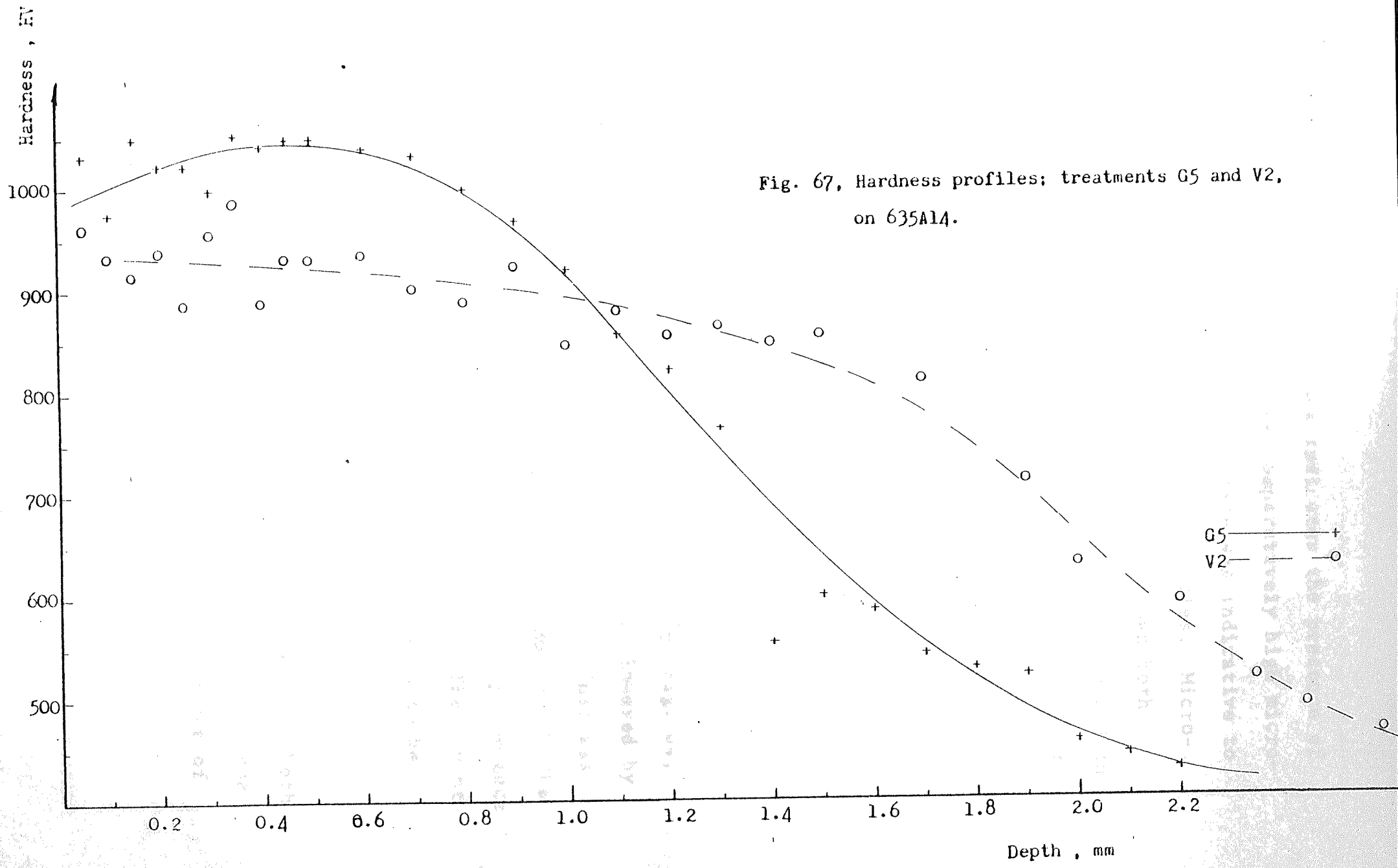

Fig. 67, Hardness profiles; treatments G5 and V2, on 635A14.

on approaching the surface indicates the presence of retained austenite, and the comparatively high micro-hardness measured near the surface was indicative to the presence of the hard carbide particles. Micro-structure investigation, Fig. 68, has shown both carbide particles and retained austenite contained in the martensite case microstructure. The presence of both retained austenite and carbides is expected to lower the inherent strength of the material adjacent to them as well as reducing the resulting compressive residual stresses. This was seen in the value of residual stresses estimated as 306 Nmm^{-2} compressive, which is less than half their magnitude quoted due to G1 and about two thirds that due to G3.

Fatigue strength in unidirectional bending, Fig. 64, due to this type of carbon profile (G5) is lowered by about 17% in comparison to that due to G3. This was proved to be significant by statistical analysis. The reduced fatigue strength is attributed to the presence of carbides as well as retained austenite. The amount of retained austenite due to G5 was estimated to be about 12%, whilst that of G3 was about 8%.

The amount of retained austenite is comparable in both cases, therefore the reduction in the bending fatigue strength may be attributed mainly to the presence of the carbides.

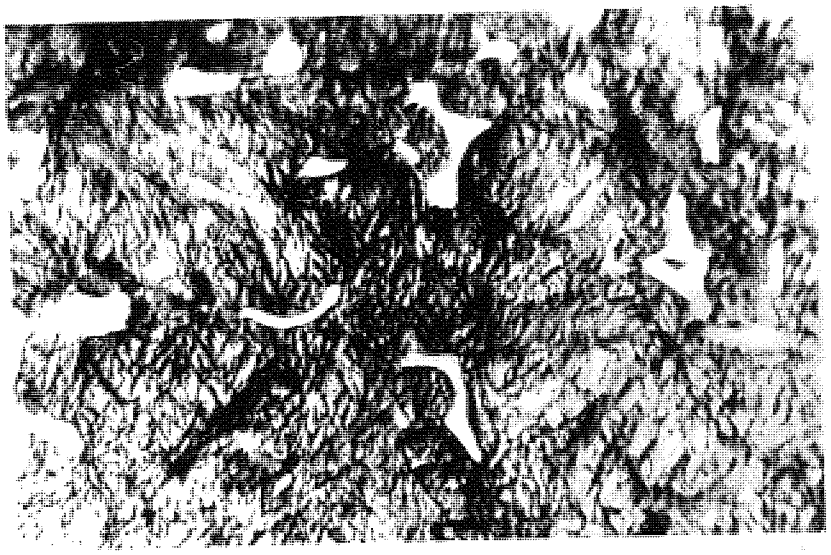

Fig.68, Carbides and retained austenite in the surface layer of 635A14, carburised by G5. (x 1000).

6.3.2 Vacuum - Partial Pressure-Carburising

Vacuum carburising in practice is basically attempted to ensure the freedom from internal oxidation encountered in conventional gas carburising. However in view of the present work, the resulting type of carbon profile may have a bearing upon the improved fatigue behaviour of a vacuum carburised piece. This process was used to avoid the formation of internal oxidation and carbon profiles similar to those due to gas carburised G1 and G5 were produced.

6.3.2.1 Boost/diffuse - Plateau - V1 (Similar to G1)

The carbon profile produced is shown in Fig. 51 where it can be seen that a surface carbon content of 0.8%C was maintained constant over the first 0.2 mm depth, then it starts to decrease. The carbon profile is similar to that produced by G1. The observed similarity in the shape of the profile and the surface carbon content would isolate the effect of internal oxidation found due to G1, so that direct assessment of the effect of internal oxidation can be made.

The hardness profile associated with this treatment, i.e. V1, is shown in Fig. 62, and it is, like the carbon profile, similar to that which was associated with G1. As both carbon and hardness profiles were similar, it is only to be expected that the same sort of similarity will be valid on the microstructural bases. In this

respect microstructural investigation showed similar microstructures, and retained austenite estimated to be 3% due to V1 (that due to G1 is 4%). While internal oxidation was found to occur up to a depth of 13 μm in test pieces due to G1, those due to V1 showed the freedom from internal oxidation, see Fig. 69.

As far as fatigue strength in unidirectional bending is concerned, Fig. 64 shows that vacuum carburising is superior to gas carburising under any of the discussed conditions. In particular an improvement of about 11% is shown over that due to the comparable G1. Statistical analysis of variance showed the significance of the quoted improvement. Which may all be attributed to the fact that vacuum carburising V1 produced oxide free surfaces as compared to gas carburising G1.

Although single stage carburising (G3) produced a higher fatigue strength than boost-diffuse carburising (G1), G3 has not been compared with vacuum carburising (V1) as the carbon profiles are different (see Fig. 61).

(a)

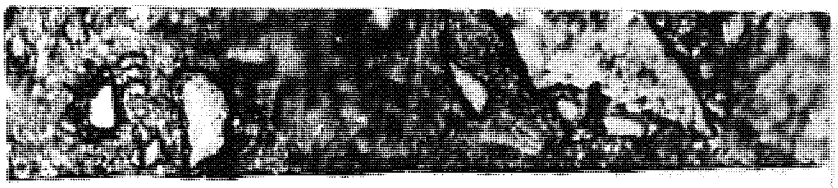

(b)

Fig.69, Polished samples of 635A14 : (a).Gas carburised, (b).Vacuum carburised. (x 1000).

6.3.2.2 Over Carburised V2 (Similar to G5)

Over carburising in conventional atmospheres has already been discussed on the bases of associated microstructure and residual stress variations, however the comparison was made with single stage G3. Vacuum carburising treatments V1 and V2 had been studied and certain differences were observed. One of these conditions, that of an over carburised carbon profile (V2) will be compared with similar one (G5) produced in conventional gas atmosphere.

Vacuum carburising to the saturation level of austenite produced the carbon profile (V2) shown in Fig. 66, where it can be seen that the surface carbon is greater than 1.1%C, and the carbon profile is shifted to higher carbon content at any penetration depth in comparison to V1.

Microstructural examination revealed the martensitic case with carbide particles, which appeared to be finely divided and uniformly distributed in the matrix, micro-photograph is presented in Fig. 70a.

Free oxide surfaces were absorved again due to this treatment (V2). The absence of internal oxidation due to both V1 and V2 has produced the highest fatigue strength among all the carburising conditions, the slight reduction, less than 3%, observed due to V2 in comparison to V1, may be attributed to the presence of carbides, assuming it is a genuine difference, and not due to

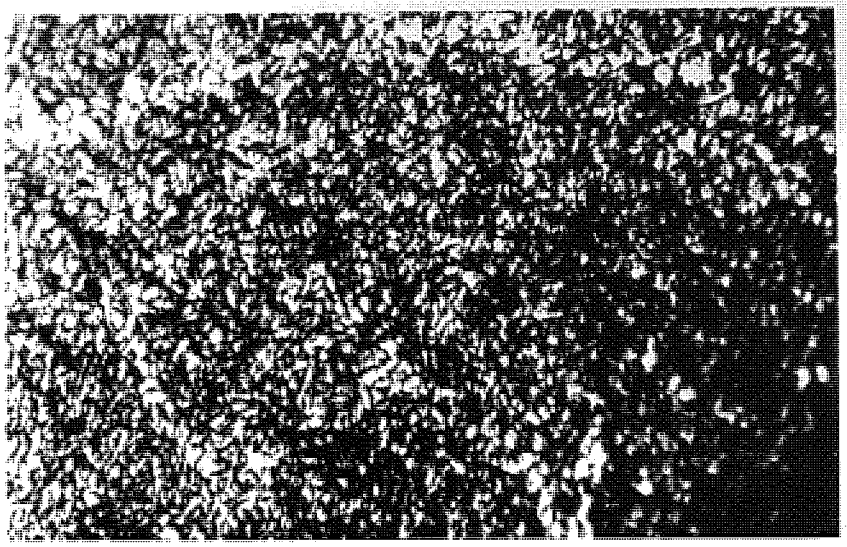

Fig.70-a, Fine carbide particles in the case of 635A14 vacuum carburised & oil quenched.(x 1000)

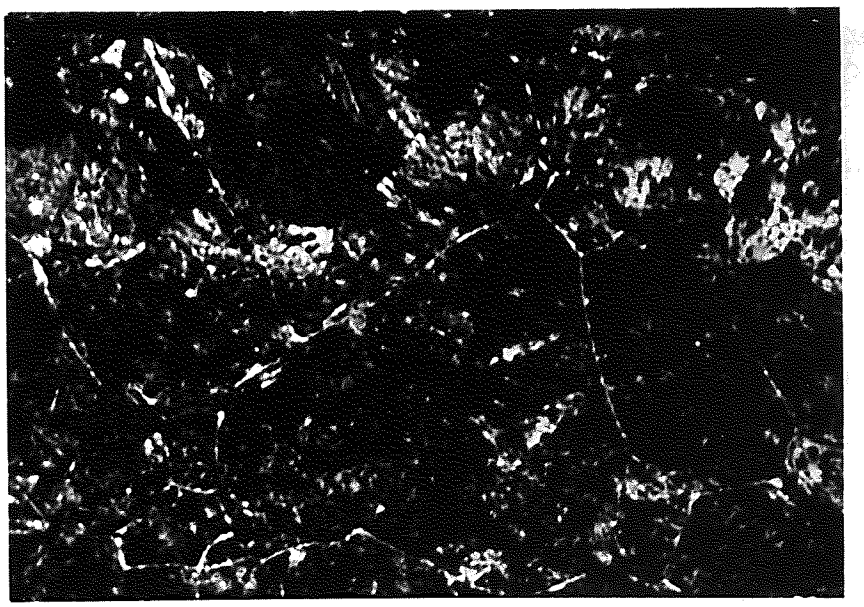

Fig.70-b, Carbide net-work in the case of 635A14 vacuum carburised & gas quenched.(x 400)

statistical scatter. Whatever the case is, internal oxidation seems to make all the difference.

In order to evaluate over carburised V2 over that due to G5, although they produced comparable carbon profiles, it must be borne in mind that they might be associated with different microstructures. Quenching by nitrogen after vacuum carburising produced the microstructure shown in Fig. 70b where the carbides are seen as a network around the prior austenite grain boundaries. For hardening, vacuum reheating to 810°C, and oil quench was finally employed to produce vacuum carburised and properly hardened pieces. In doing so the carbide network observed in the case is broken down into fine particles uniformly distributed in the matrix.

Austenite was seen to be retained in the case microstructure due to G5 along with the carbides, however the lower hardening temperature practiced in V2 would not allow the retention of austenite mentioned. In fact, the hardness profile in Fig. 67 shows no sign of retained austenite, neither does the microphotographs in Fig. 70. Looking back to Fig. 66 where the carbon profiles due to V2 and G5 are presented, it can be seen that the depth of penetration in V2 is slightly greater than that in G5. The two profiles are comparably similar. Test pieces produced by G5 showed the lowest fatigue strength, Fig. 64. Statistical analysis showed that plain fatigue strength due to G5 and V2 are significantly different. In fact plain fatigue strength due to V2 is superior to that of

G5 by about 20%. The superiority quoted may be explained on the grounds of the freedom from internal oxidation in V2, as well as the relatively large carbide - globular and/or intergranular - particles found due to G5. It is rather of importance here to underline the fact that the presence of the fine carbide particles as a result of V2 is not as detrimental as the coarser ones, whether globular or intergranular resulting from G5.

Therefore it is worth remembering the importance and the contribution of the carbide particles in V2 is not only limited towards the bending fatigue strength but also contributes towards better wear resistance. In effect overcarburising in vacuum may improve the fatigue behaviour of a component under simultaneously combined action of bending and contact loading, e.g. gear teeth.

6.4 Mean Stress

The fatigue behaviour of carburised 835A15 has been discussed in rotating bending, while that of 635A14 under different carburising conditions was discussed in unidirectional bending and at the particular stress ratio of 0.3. However, here, the fatigue behaviour of the 635A14, carburised by G3 is examined under the effect of mean stress. In fact the fatigue behaviour is assessed in unidirectional bending at low, medium and high stress ratio, as well as in rotating bending. Eventually fatigue strength-mean stress diagram is constructed and the behaviour is examined in comparison to the uncarburised hardened condition H. It should be noted that the ultimate tensile strength determined in the two conditions G3 and H, were used in constructing the mentioned diagram, Fig. 71. However it should be borne in mind that in the carburised condition, test pieces loaded in tension are different to that in bending. Actually it can be seen from the diagram that the tensile strength of uniformly hardened steel, treatment H is higher than that of carburised G3.

The diagram in Fig. 71, curve A, shows that the bending fatigue strength at zero mean stress is the highest, about 880 Nmm^{-2}, however as the mean stress increased the fatigue strength decreases, similarly curve B shows that for uncarburised hardened H, the behaviour is the same, i.e. decreasing with increasing the mean stress, although less significant than curve A. It can be noticed that at

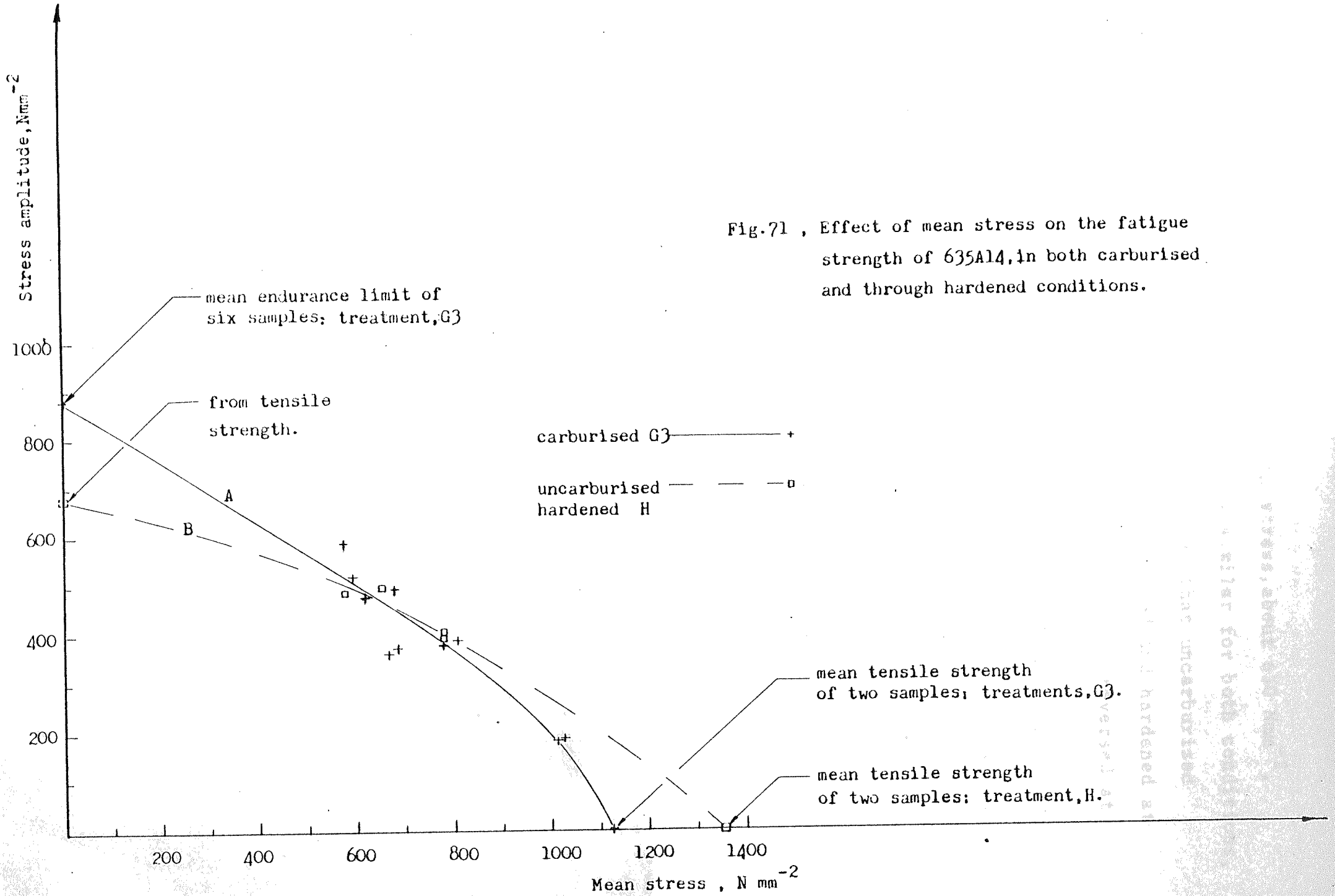

Fig.71 , Effect of mean stress on the fatigue strength of 635A14, in both carburised and through hardened conditions.

an intermediate value of mean stress, about 630 Nmm^{-2}, the bending fatigue strength is similar for both conditions, i.e. G3 and H. It can also be seen that uncarburised hardened steel is superior to carburised and hardened at high mean stresses. While the situation is reversed at low mean stresses.

The involved microstructure, carbon and hardness profiles of G3 are as has been shown earlier. However, microstructure due to H is shown in Fig. 72. The hardness was found to be about 440 Hv.

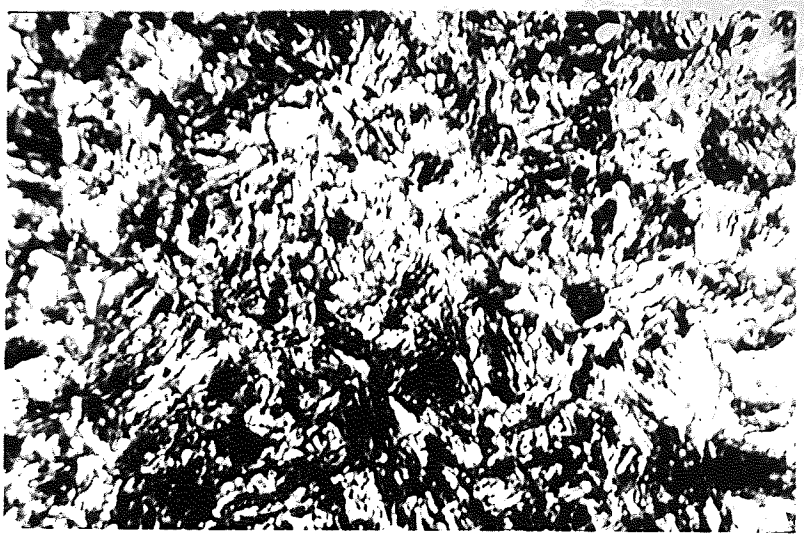

(a)

(b)

Fig.72, Microstructure of uncarburised-hardened 635A14;
(a).Surface layer.
(b).Core. (x 1000)

6.5 Stress Concentration

Carburised components under the effect of a stress concentration feature may behave different to the normal behaviour documented for most metals. In fact, the residual stress, microstructure variation may be of major importance in differentiating the effect of stress concentration. Variation of stress concentration factor is created by altering the geometry of the notch mainly the root radius. Conventional gas carburising under any conditions produced carbon profile, at the root of the notch, shifted slightly to lower carbon content in comparison to the unnotched geometry. Therefore it would be expected that carbon profile may undergo changes due to different root radius, i.e. different stress concentrations.

Conventional gas carburising was carried out on 080M15 test pieces. Carburising was according to G3. The carbon profile through the carburised layer at the root of different notch geometries can be seen in Fig. 51. In fact no major differences were found in the resulting profiles. One of them was plotted as an example. The surface carbon content varied between 0.7 and 0.77% for different notches. This however is not expected to produce significant differances in microstructure or hardness. A hardness profile is given as an example in Fig. 73. The hardness at the root of different notch geometries varied between 700 and 840 HV, while core hardness varied between 180 and 270 HV. Case depth, in effect, was found to vary between 0.3 and

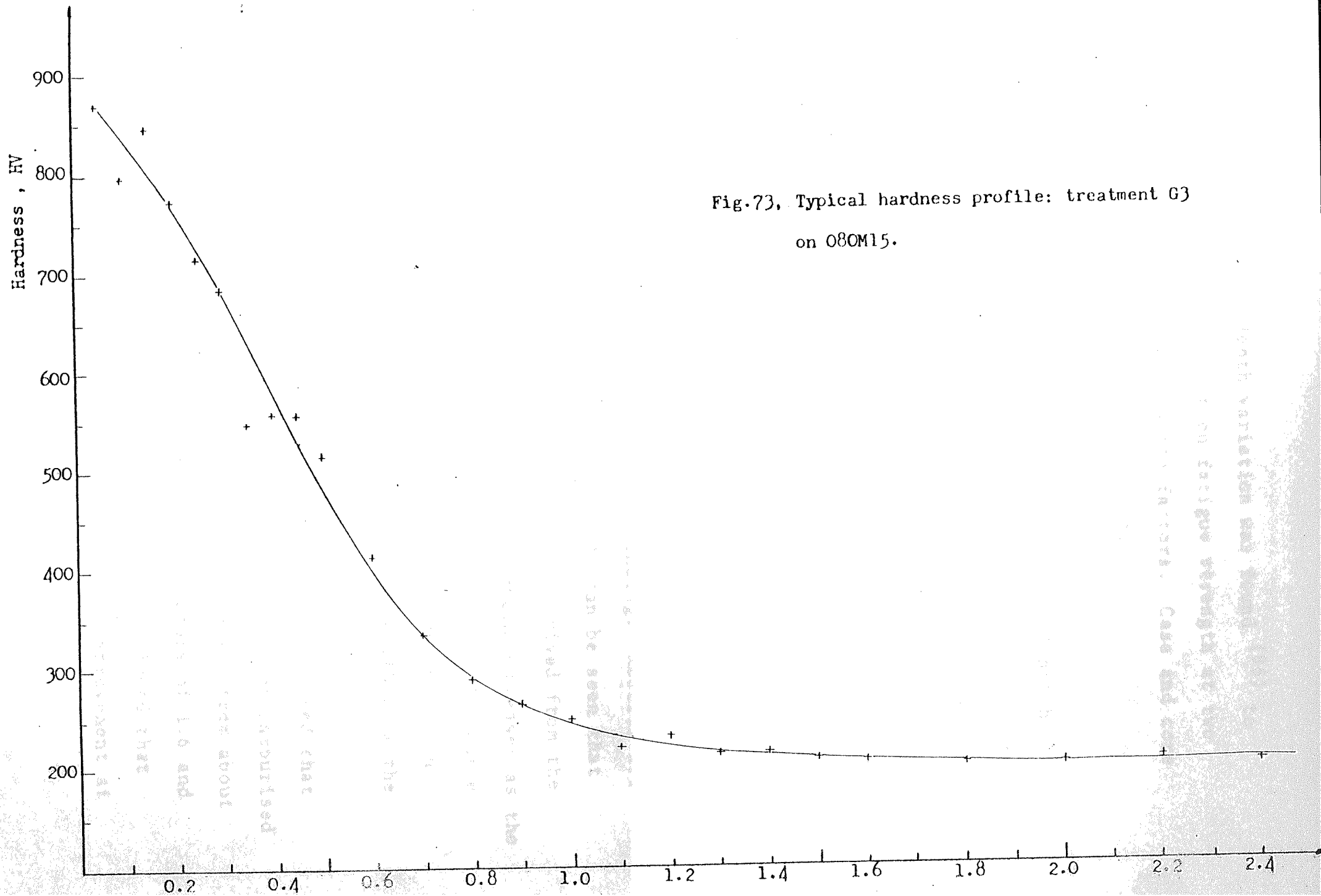

Fig.73, Typical hardness profile: treatment G3 on 080M15.

0.6 mm; such case depth variation was found [86] to exert little or no effect on fatigue strength at two values of stress concentration factors. Case and core microstructure are shown in Fig. 74.

Under completely elastic conditions and full notch sensitivity the fatigue strength at any stress concentration value may be derived from the plain fatigue strength.

In case hardened specimens, the notch effect can in part be relieved by compressive prestressing [75].

The fatigue strength of 080M15 carburised by G3 was examined under the influence of a range of stress concentration factors in unidirectional bending. Results are presented and plotted in Fig. 75. It can be seen that the fatigue strength is higher than if derived from the plain condition, and that fatigue strength decreases as the value of the stress concentration increases. The curve starts to level out at about 2.8 stress concentration factor. The deviation of the fatigue strength from the theoretically derived value, increases with stress concentration factor, as other results [86] showed that the improvement, of notched fatigue strength of carburised in comparison to normalised 080M15, increases from about 150% to 270% at stress concentration factors of 1.6 and 7.5 respectively. Therefore it may be concluded that carburising resulted in more significant improvement at higher stress concentration factors.

(a)

(b)

Fig.74, Typical microstructure of 080M15 carburised by G3, (a). Case. (b). Core. (x1000).

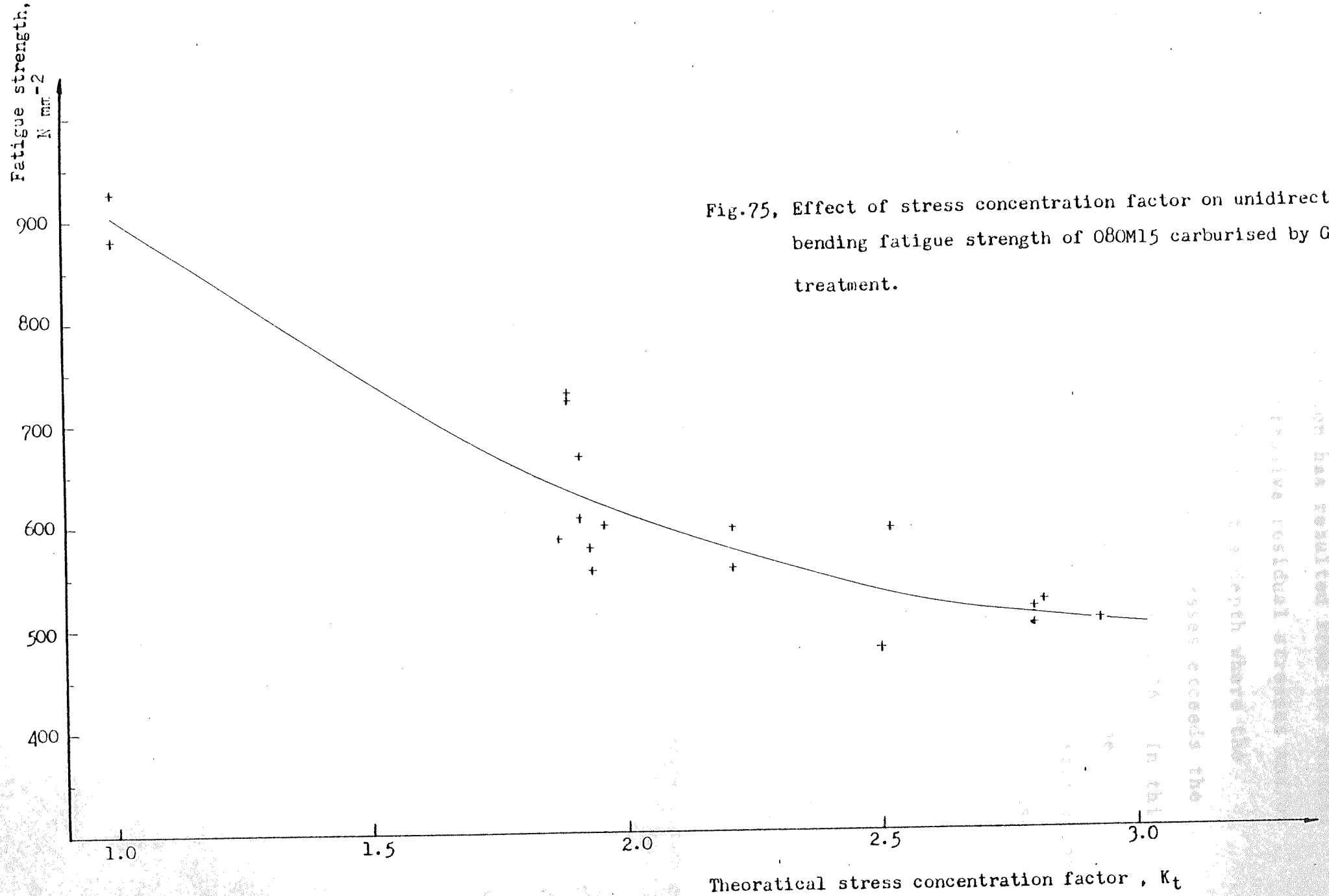

Fig.75, Effect of stress concentration factor on unidirectional bending fatigue strength of 080M15 carburised by G3 treatment.

Fatigue strength deviation has resulted from the reduced notch effect due to compressive residual stresses and/or local yielding sub-cutaneously at a depth where the summation of applied and residual stresses exceeds the yield value of the material there, see Fig. 76. In this event the locally tensile residual stresses become compressive and in effect, the residual stress distribution may be modified favourably to produce a general increase in the bending fatigue strength.

In order to validate the mentioned possibilities and for accurate assessment, the residual stress distribution is needed, as this was not the case here. It is apparent therefore that further work is required in this respect.

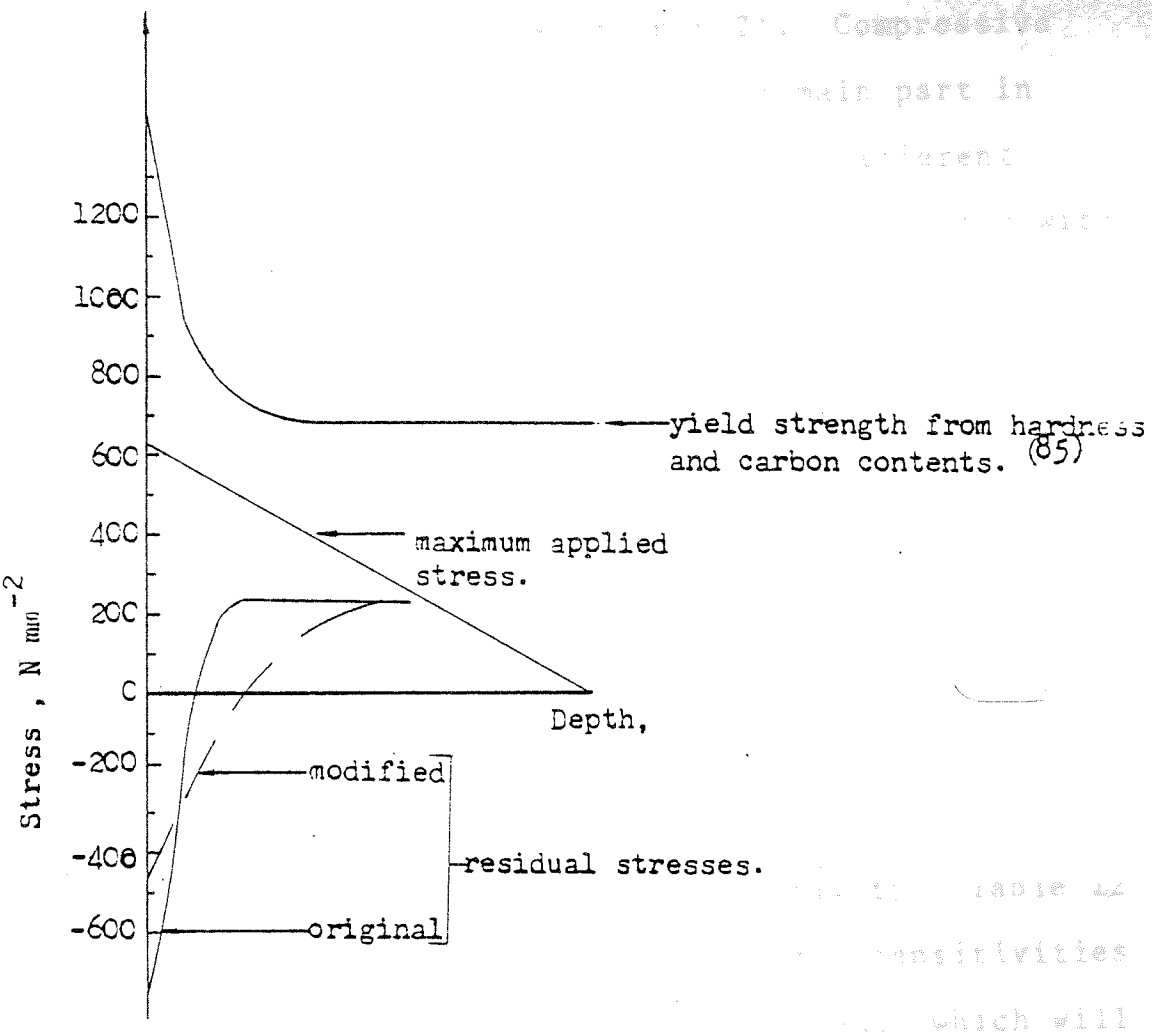

Fig.76, Schematic illustration of modified residual stress distribution due to subcutaneous yielding.

6.6 Plain and Notched Fatigue Strength

The reduced effect of the notch in carburised 835A15 has already been noticed (see section 6.2). Compressive residual stresses appeared to play the main part in improving the notched fatigue strength. Different carburising conditions were found to be associated with variation in the residual stresses. Therefore notch effect is examined here, under different carburising and hardening conditions, and the notched fatigue strength is evaluated.

In spite of the fact that plain fatigue strength was determined under three point bending, while the notched fatigue strength was determined under four point bending. It is still possible to compare them from the point of view of notch effect, i.e. notch sensitivity. Table 12 shows the experimentally determined notch sensitivities (Q) for the steels and the treatments involved, which will be discussed in succession.

1. Uncarburised hardened - H

   Hardening on its own is not expected to produce a significant level of residual stress - as they are tensile in through hardened - which is generally experienced in carburised and hardened pieces. In fact the previously discussed reduced notch sensitivity due to compressive residual stresses is not possible in the hardened condition H. Therefore it would be expected that the notch is more effective

TABLE 12

Effect of Carburising and/or Hardening on the Notch Sensitivity

Steel-treatment Code	Surface Carbon %	Residual Stress Nmm^{-2}	Fatigue Strength Reduction Factor	Stress Concentration Factor	Notch Sensitivity
635A14 - G1	0.78	-661	1.05	1.5	0.1
635A14 - V1	0.8	N.D.**	1.06	1.5	0.12
635A14 - G2	0.48	+103	0.97	1.5	0*
635A14 - G3	0.82	-507	1.10	1.5	0.20
635A14 - G5	1.2	-306	1.3	1.5	0.57
635A14 - H	0.17	-	1.24	1.5	0.47
080A15 - G3	0.7	-507	1.21	1.5	0.43
835A15 - G4	0.96	N.D.	1.65	2.8	0.36
835A15 - G6	0.87	N.D.	1.44	2.8	0.24
835A15 - G7	0.8	N.D.	1.53	2.8	0.30

* Similar behaviour was quoted by Forrest [74]

** Not determined

and notch sensitivity is increased. Actually the present results due to H showed a notch sensitivity of about 0.47, see Table 12, which among other values, indicate that uncarburised uniformly hardened material has higher notch sensitivity than when carburised.

2. Carburised and hardened

The present experimental determination has shown that the highest notch sensitivity was experienced in the group overcarburised as G5, where as has been discussed, the case microstructure contained large carbide particles in globular or intergranular form. Consequently they may be responsible to cause an internal embrittlement effect [75] and in turn raise the notch sensitivity to the value quoted in table 12, of 0.57, The high notch sensitivity can also be seen by considering the relatively low value of compressive residual stresses (306 Nmm^{-2}), as compared to other carburising conditions. On the other hand the lowest notch sensitivity was due to G1, bearing in mind the high compressive residual stresses estimated to be 661 Nmm^{-2}. It is only to be expected that it will exert the highest effect to reduce the notch sensitivity and therefore increase the notched fatigue strength. Carburising by V1 resulted in similar notch sensitivity as it produced comparable profiles to that of G1. In between those two extreme notch sensitivities, carburising by G3 has resulted in a

notch sensitivity of 0.2 , and considering the value of residual compressive stresses estimated to be 507 Nmm^{-2}, the slightly higher notch sensitivity has accompanied the little loss in compressive residual stresses, as can be seen from table 12.

Surface decarburisation (G2) was found to be associated with tensile residual stresses. Accordingly one would expect the notch sensitivity to raise, but instead it is decreased and the behaviour was not normal, considering the relatively high notch sensitivity due to H, where the effect of residual stresses is negligible.

This particular behaviour of decarburised G2 showing the higher notched fatigue strength than in the plain condition may be explained on the basis of the assumption that local yielding at the root of the notch, Fig. 77, has at least relaxed any tensile residual stresses, and perhaps caused the occurrence of compressive residual stresses there. This would effectively increase the bending fatigue strength and perhaps raise it over that in the plain condition, where the tensile residual stresses are expected to operate in lowering the bending fatigue strength which has already been discussed.

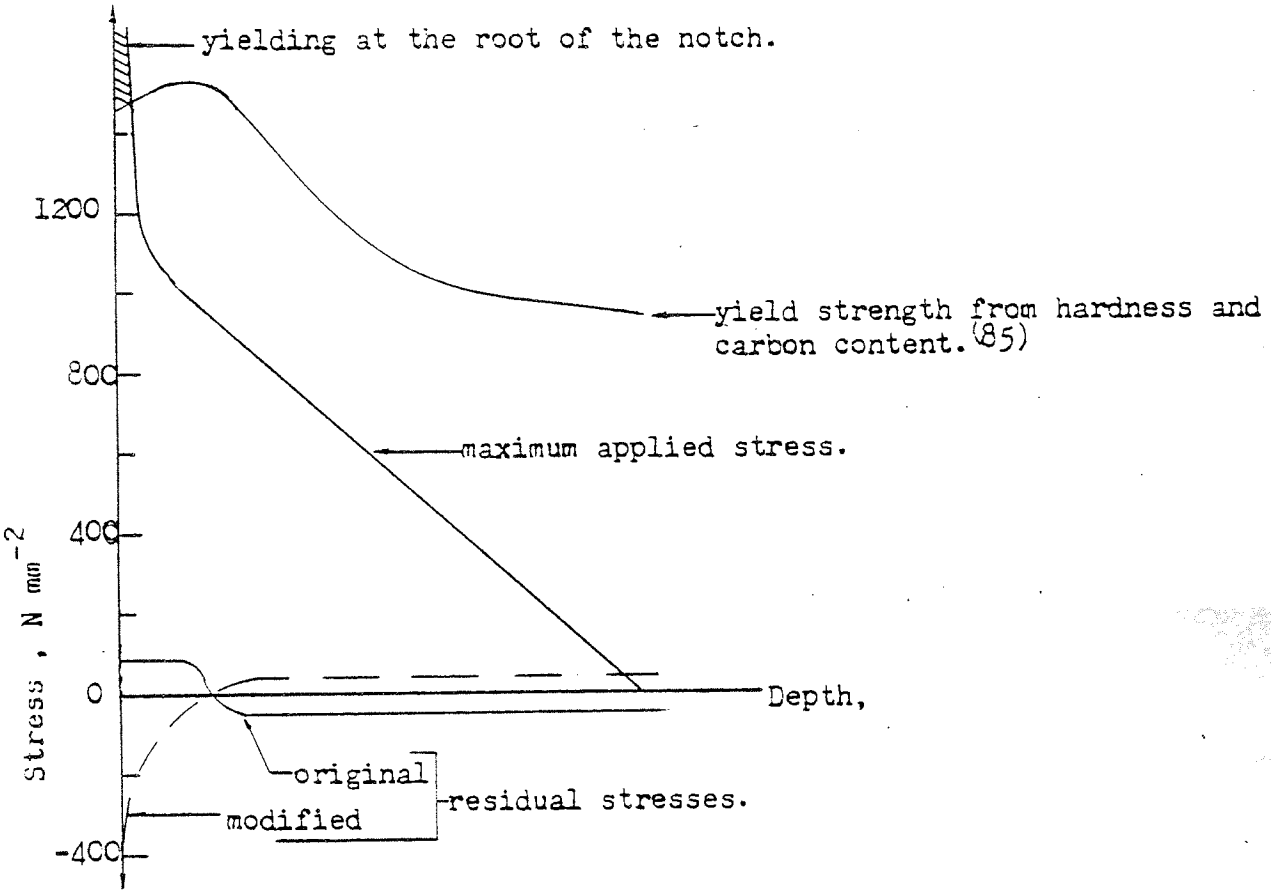

Fig.77 , Schematic illustration of residual stress distribution in decarburised (C2),as influenced by local yielding at the root of the notch.

Notch sensitivity of 0.24 - 0.36 was observed due to 835A15 carburised in G4, G6 and G7, associated carbon profiles were comparable to those found as a result of carburising 635A14 by G1 and G3.

6.7 Initiation of Fatigue Crack

The early difficulties in incorporating the potential drop equipment on plain specimens made it necessary to use notched specimens to enable detection of crack initiation and therefore to determine the stress to initiation.

Notched fatigue strength determined is based on the initiation of a fatigue crack at the root of the notch. Statistical analysis of variance showed no significant difference between the estimated fatigue strength based on initiation and failure, consequently stress to initiation is similar to that of failure at least under the present test conditions of unidirectional bending at a stress ratio of 0.3. It may be due to the brittle nature of the test pieces as they were not tempered. This has also resulted in some instant failures. The relatively high stress ratio (0.3) may have assisted in that brittle failure. In this respect Clark et al [87] in their study of fatigue crack growth in case hardened layers, showed that the mean stress has to be increased from stress ratio of 0.1 to 0.44, so that crack growth continues. In addition they showed higher propagation rate in the untempered condition.

Fracture surface examination showed no sign of sub-surface initiation of a fatigue crack. The introduction of the hardened layer and the beneficial residual stresses will both increase the material resistance to crack initiation and/or delay the development of the micro-crack into a macrocrack stage.

Once the crack is initiated or developed to produce a voltage increase of 2 to 3 μv it proceeds to propagate through the case. When the crack front reaches the core, its rate of propagation will be influenced by both case and core. This was the case with cylindrical test pieces where carburising was allowed to occur all round the test piece.

The crack front will undergo a change of shape due to the difference in the propagation rate in the case, core and at the interface between them. This can be seen in Fig. 78. The crack front shape characterises the propagation rate. In the same figure the crack front is leading on the edges of the piece which is indicative of the fast propagation rate in the high carbon brittle case.

Crack propagation direction

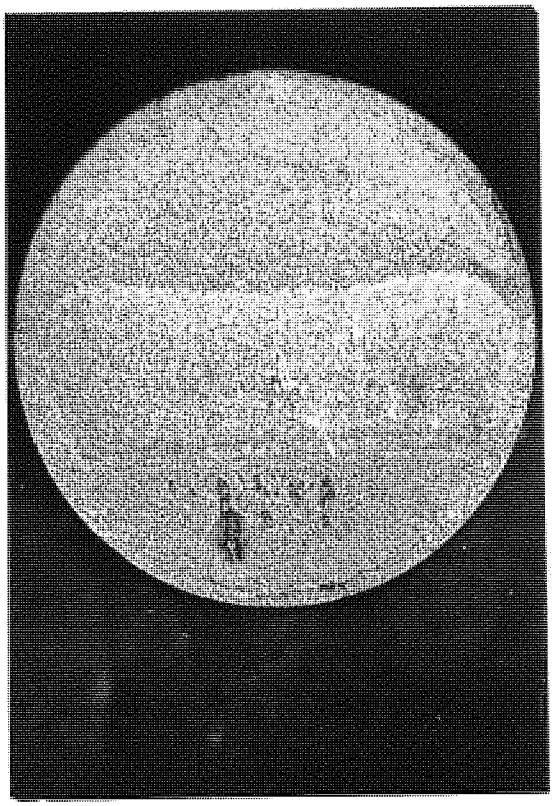

Fig.78, Crack front behavior influenced by different propagation rates.(x 4)

6.8 Fracture Topography

Fracture surface examination of carburised and hardened 635A14 has shown the transgranularity of fatigue crack initiation and the intergranularity of its propagation.

Crack initiation has always been associated with localised transgranular fracture mode. The initiation zone has not been easily recognised. It appeared flat due to the transgranular cracking process, and was located at the edge, where the maximum fibre stress has acted. There was no sign of sub-surface initiation. Although initiation sites may extent to include a limited area near the edge, there has been no indication to suggest that crack initiation did not occur at the surface where the maximum stress acted. Samples were randomly chosen from different groups notched and plain and the above findings were valid. The initiation zone on few fracture surfaces are shown in Fig. 79 a, b, c, d, and e. It can also be noticed, in most of the microphotographs, that surrounding the transgranular area of initiation is an intergranular type of fracture. This is indicative of the fact that the crack has propagated along the grain boundaries. In order to show the changes of fracture mode from brittle transgranular to an intergranular and eventually to a ductile, three micrographs are included in Fig. 80. They show the transgranular initiation at the immediate surface, intergranularity of propagation up to a depth of about 0.5 mm from the edge, then the fracture is mixed inter-transgranular, and finally the low carbon core fracture is ductile. The branching nature of the crack in the core,

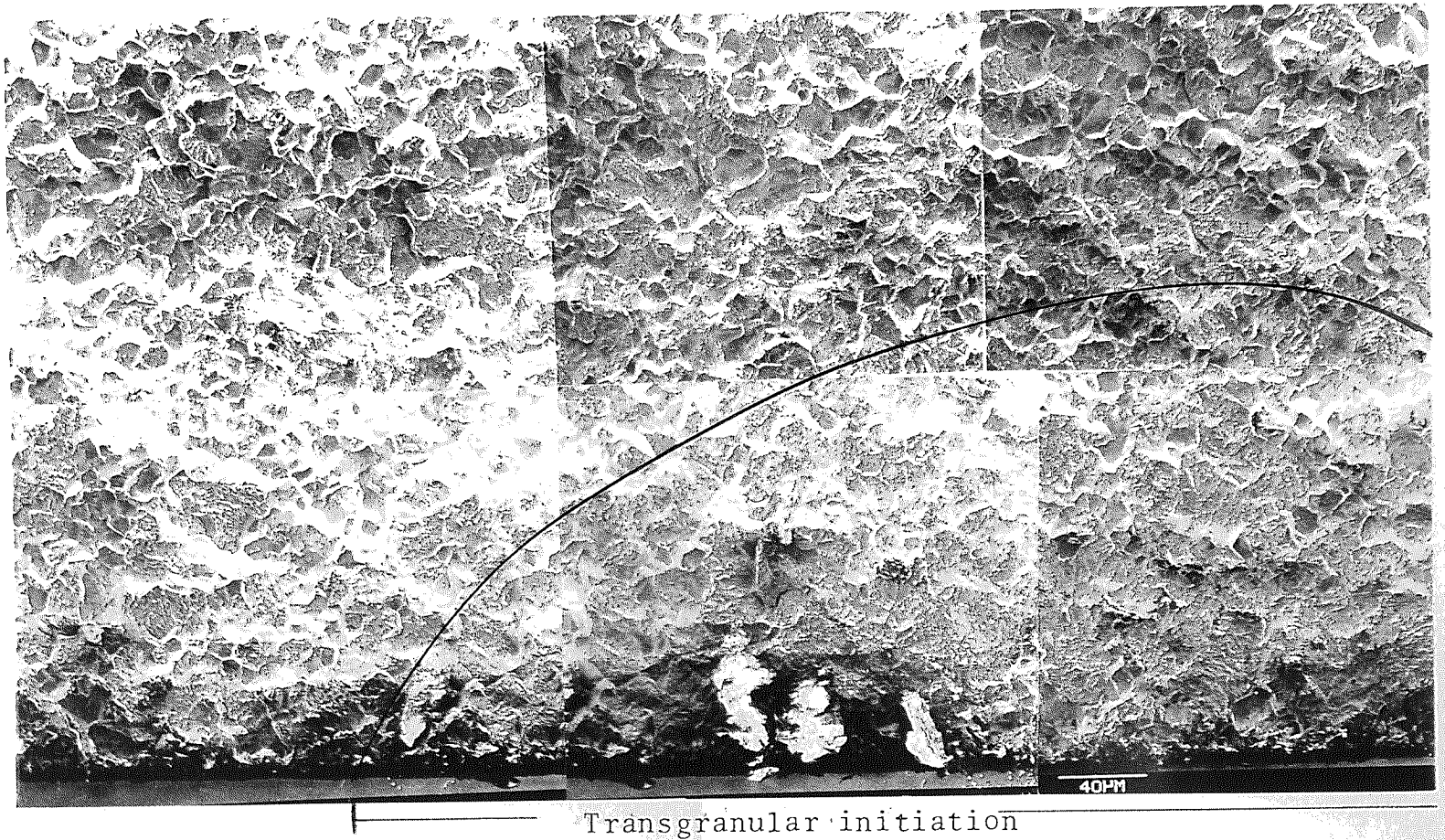

Fig.79-a. Crack initiation sone in 635A14, carburised by boost-diffuse (G1), and tested in three point bending.

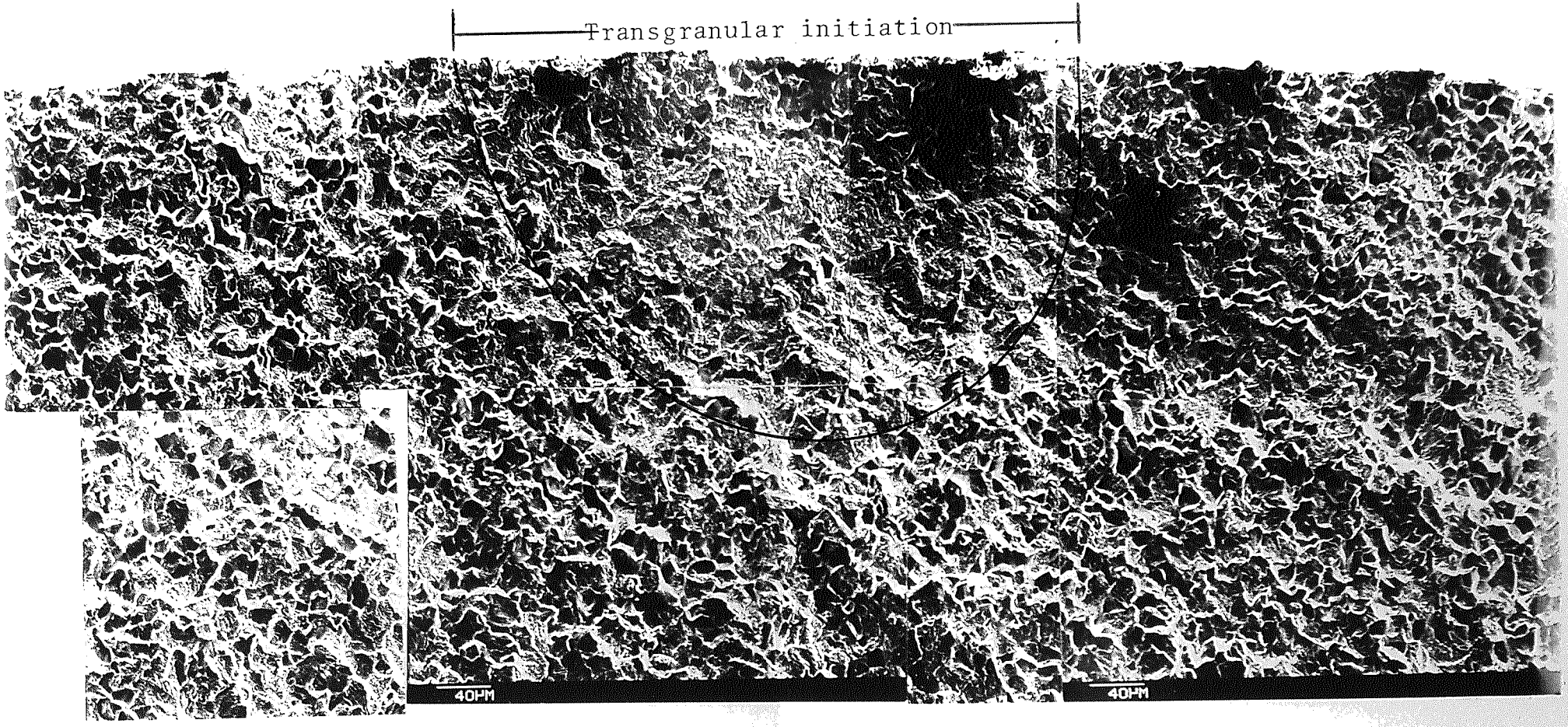

Fig.79-b. Crack initiation zone in 635A14, carburised by single stage (G3), and tested in four point bending

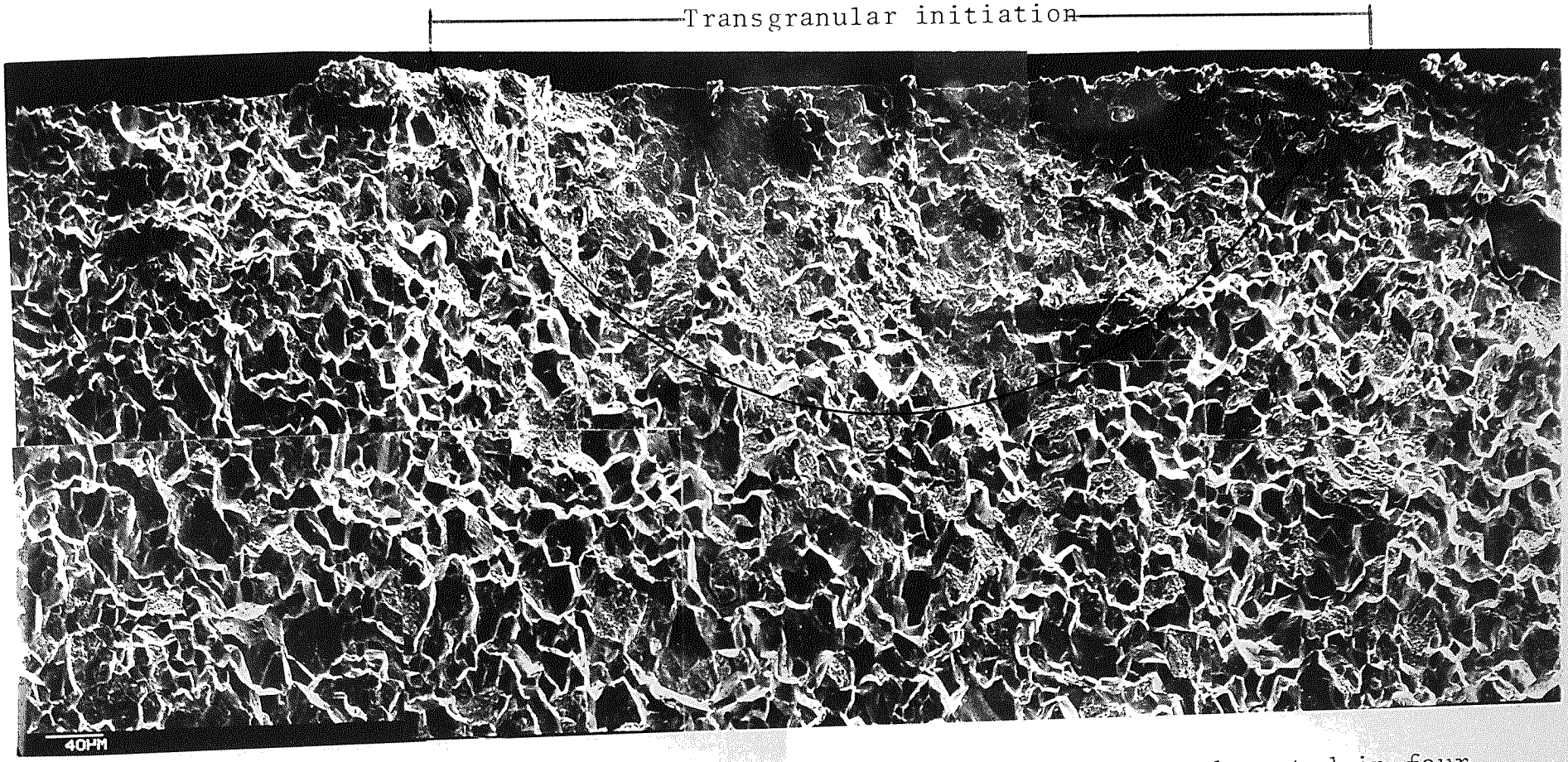

Fig.79-c. Crack initiation zone in 635A14, vacuum carburised by (V1), and tested in four point bending.

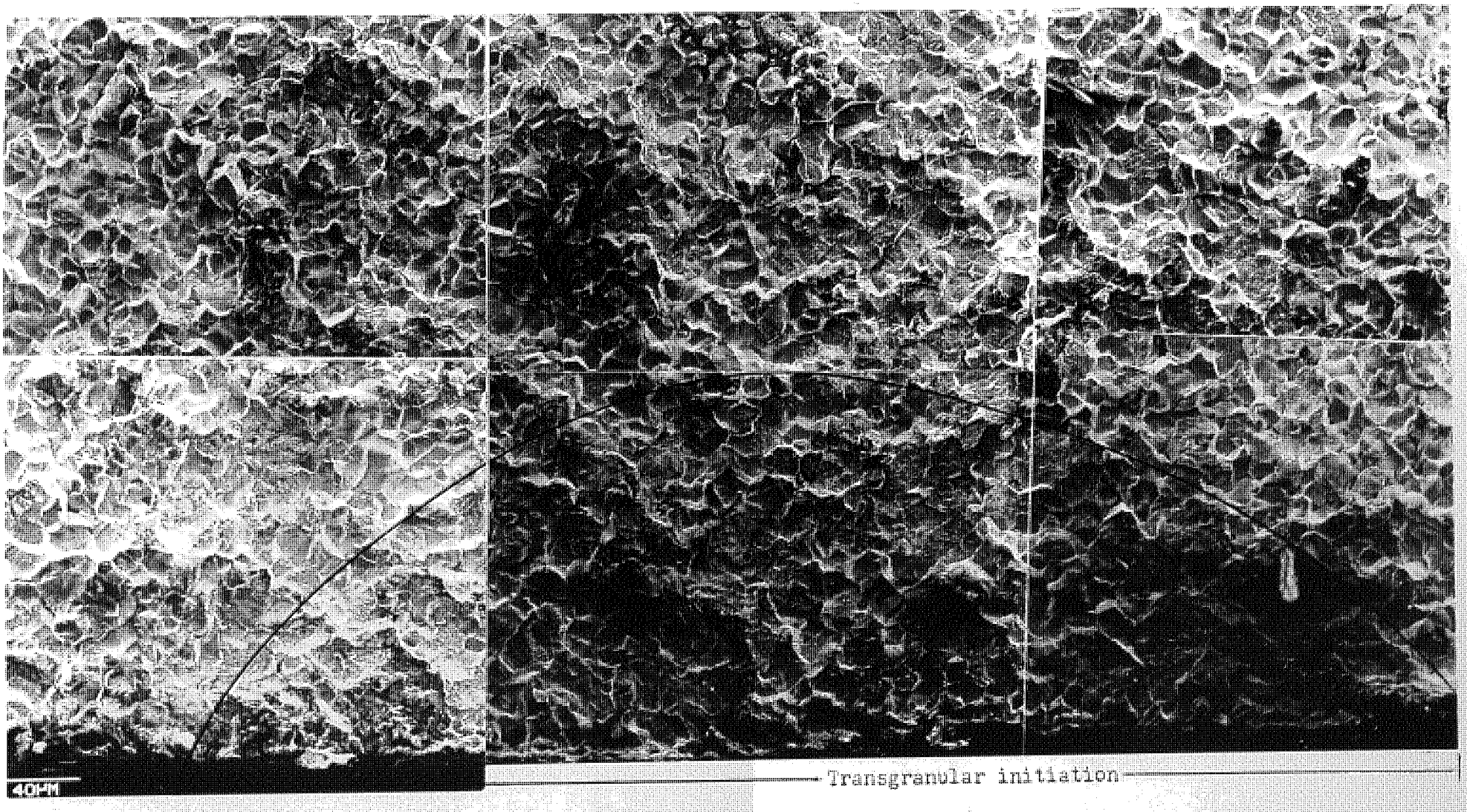

Fig.79-d, Crack initiation zone in 635A14,decarburised by boost-diffuse(02),and tested in three point bending.

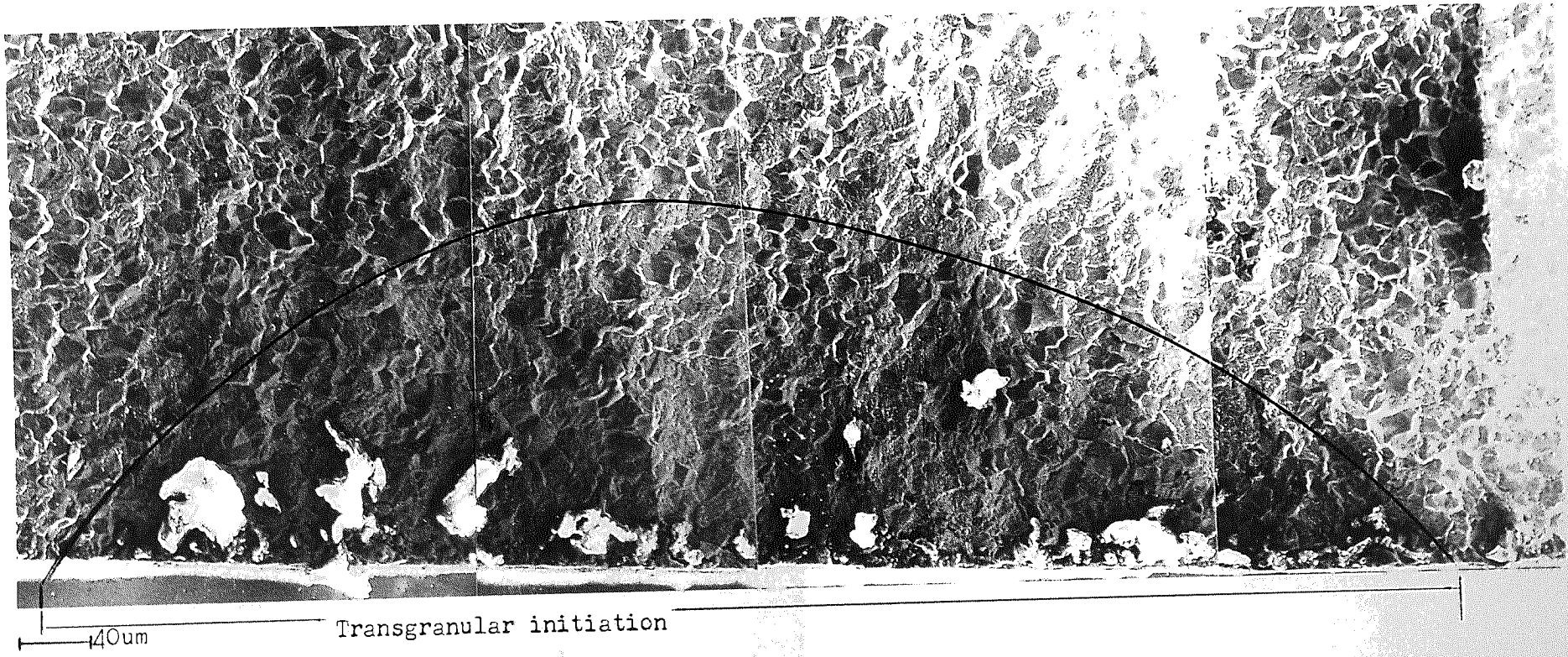

Fig.79-e, Crack initiation zone in 635A14,carburised by single stage(G4),and tested in three point bending.

Depth, mm		Mode of fracture
0.1	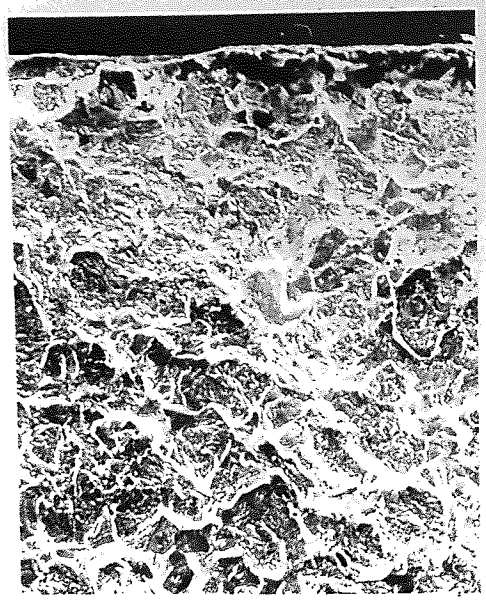	Transgranular initiation.
0.5	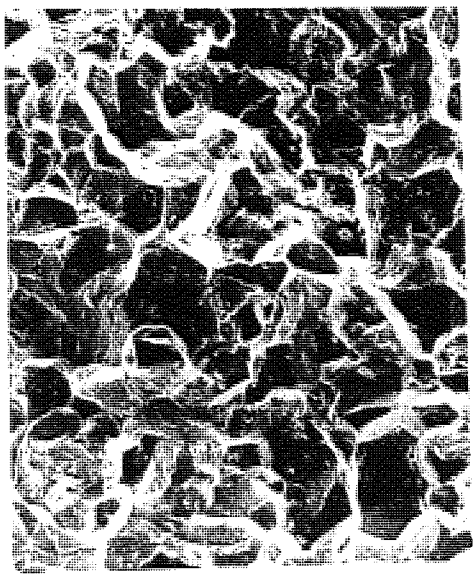	Intergranular.
0.8	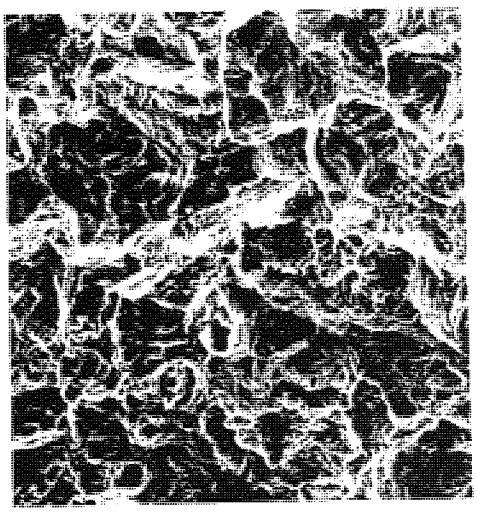	Ductile.

40um

Fig.80, Fracture mode variation with depth in carburised 635A14.

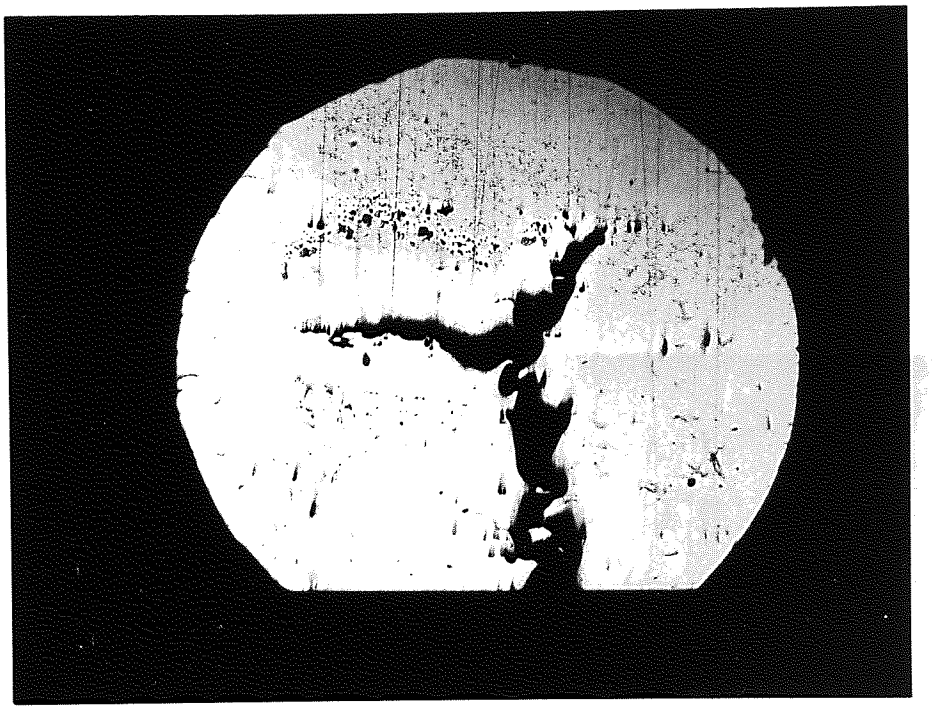

Fig.81, Crack branching in the core of 635A14 tested in 3-P.E. (x 50)

see Fig. 81, is also indicative to the ductility of the core. Fracture surface examination of a rotating bending sample has shown similar behaviour, see Fig. 82a. The transgranular initiation can also be seen in Fig. 82b, which also illustrates the intergranular nature of the case. Therefore it may be suggested that the fatigue fracture behaviour is not influenced by the type of loading, i.e. whether unidirectional or rotating bending.

Macrophotographs are shown in Fig. 83, to illustrate the behaviour of the crack front in the case, core and at the interface between them. While the crack front in unidirectional bending is defined by the direction of crack propagation, it is not the case in rotating bending, Fig. 84; the crack may spread circumferentially before propagating towards the core. In fact the initiation zone was found to spread along the circumference and cover a greater area, see Fig. 82a.

Fracture surface of tensile test pieces are shown in Fig. 85 for both the carburised and the hardened conditions. The latter illustrates the ductile cup and cone type of fracture, while the former demonstrates the flat brittle fracture.

Fatigue fracture surface was examined in conjunction with the microstructure. The intergranular case and the ductile core fractures are shown in Fig. 86 in the light of the corresponding microstructure.

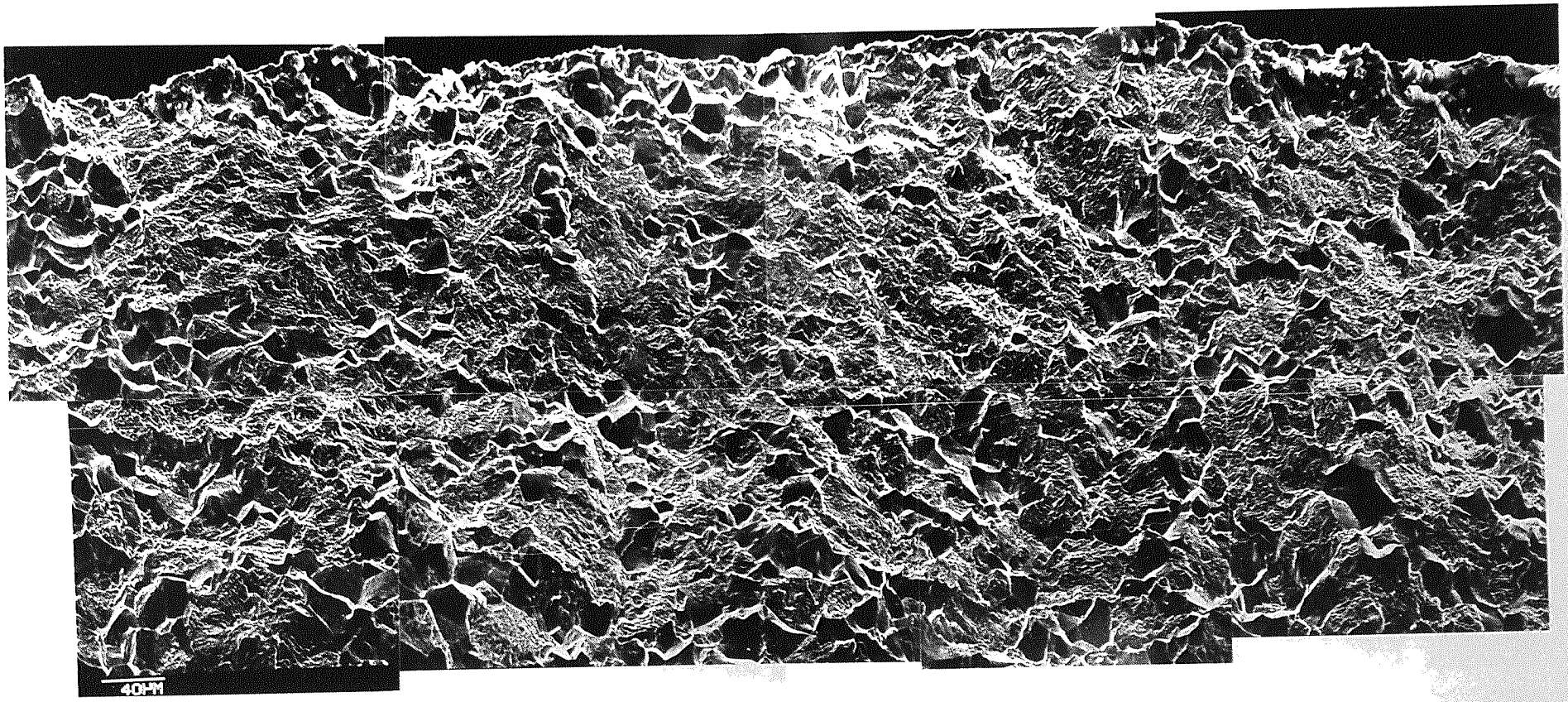

Fig.82-a. Crack initiation zone in 635A14, carburised by single stage (G3), and tested in rotating bending.

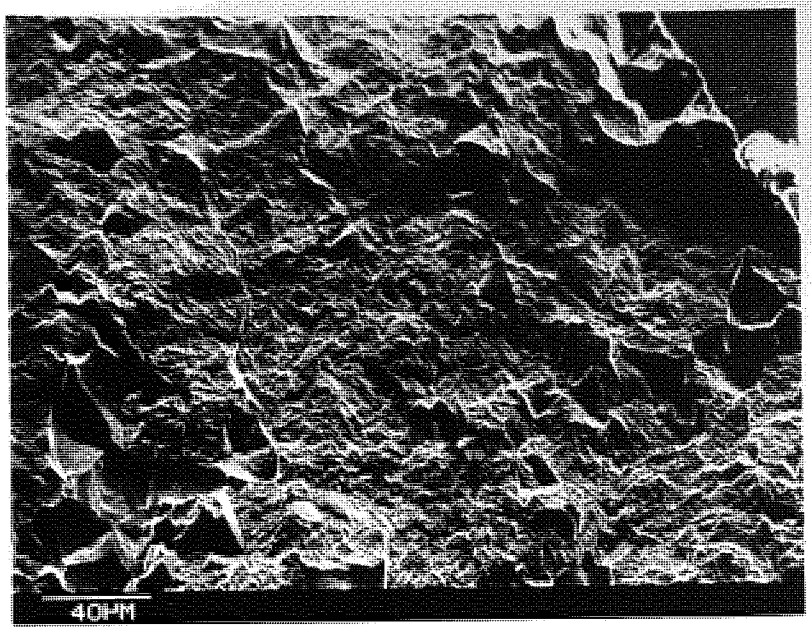

(i)

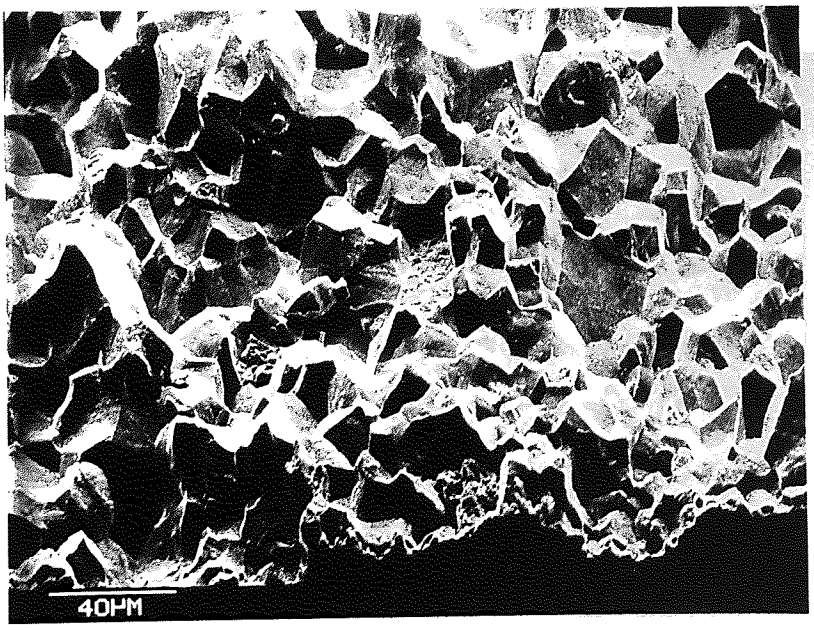

(ii)

Fig.82-b, Typical case fracture in carburised 635A14, tested in rotating bending.(i).Transgranular initiation; (ii).Intergranular propagation.

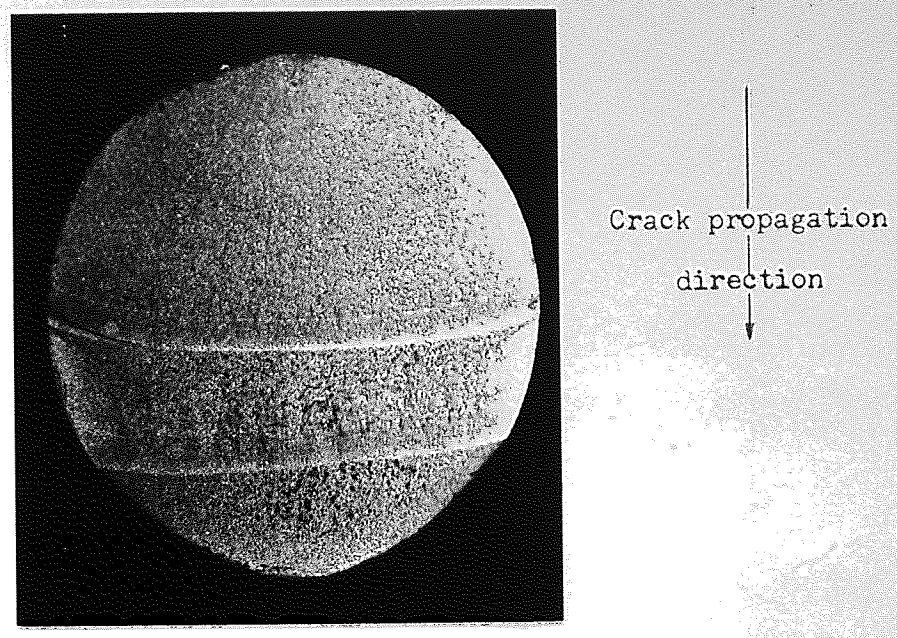

Fig.83-a, Crack front behaviour in 635A14 uncarburised-hardened, tested in three point bending.(x 4)

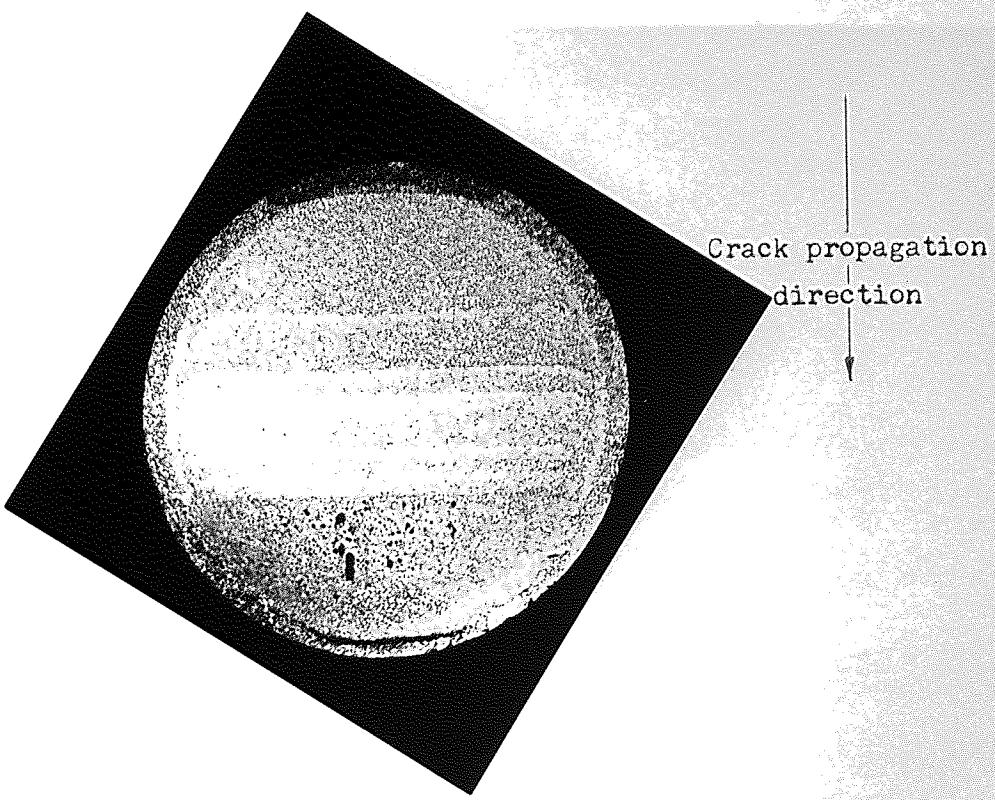

Fig.83-b, Crack front behaviour in 635A14 carburised, tested in three point bending. (x 4)

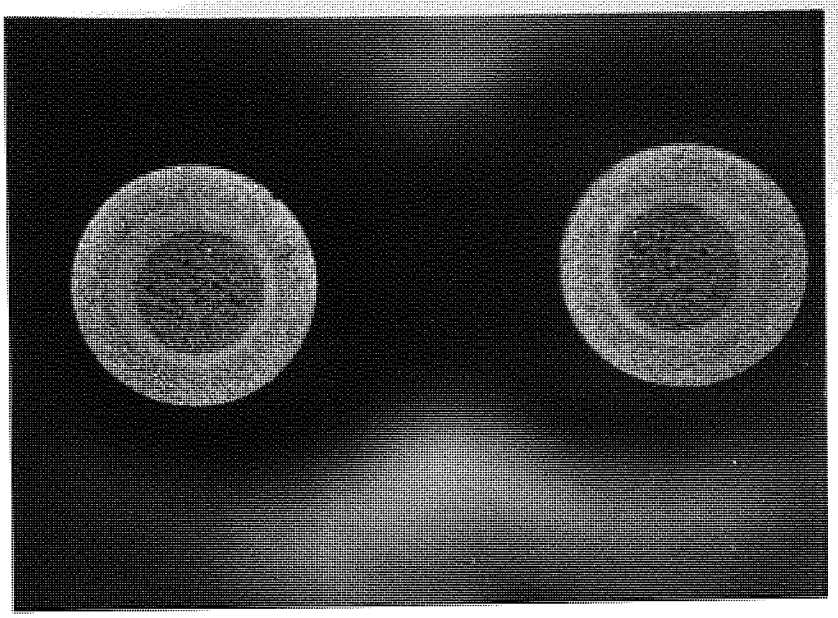

x 4

(a)

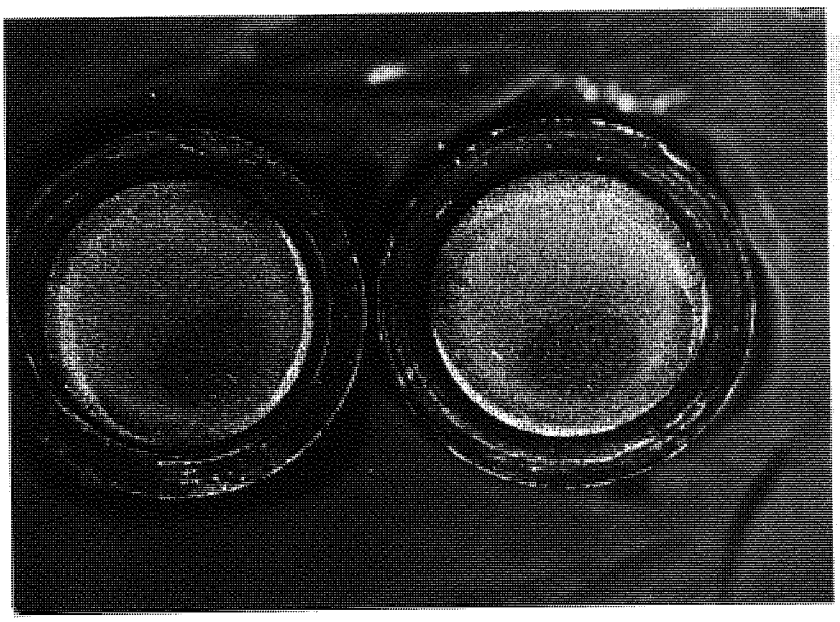

x 4.5

(b)

Fig.84, Fracture surfaces of carburised 835A15, tested in rotating bending.(a).Plain ;(b).Notched.

(a) (b)

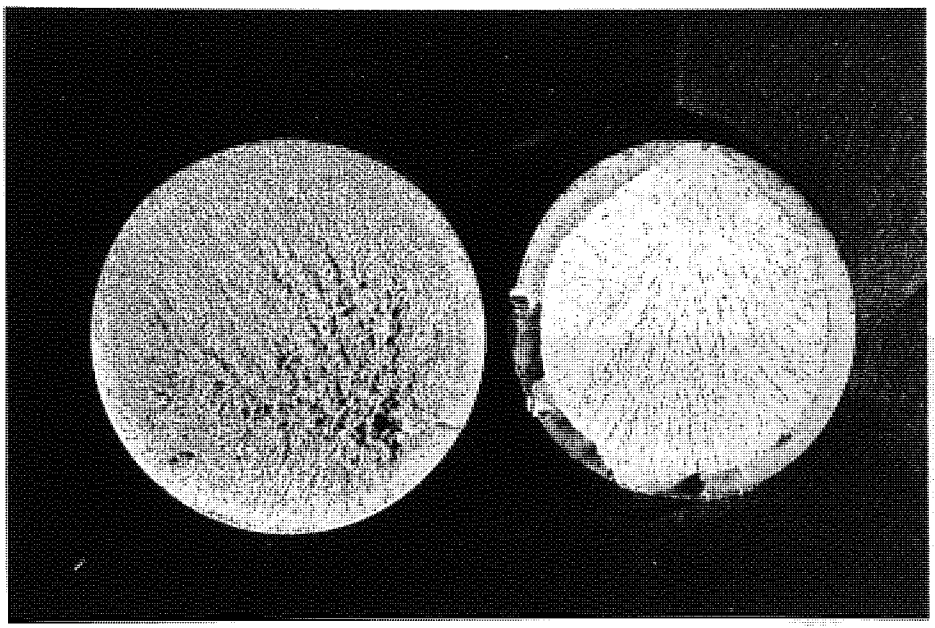

Fig.85, Fracture surfaces of tensile test piece of 635A14,
(a).carburised; (b).uncarburised-hardened.(x 4)

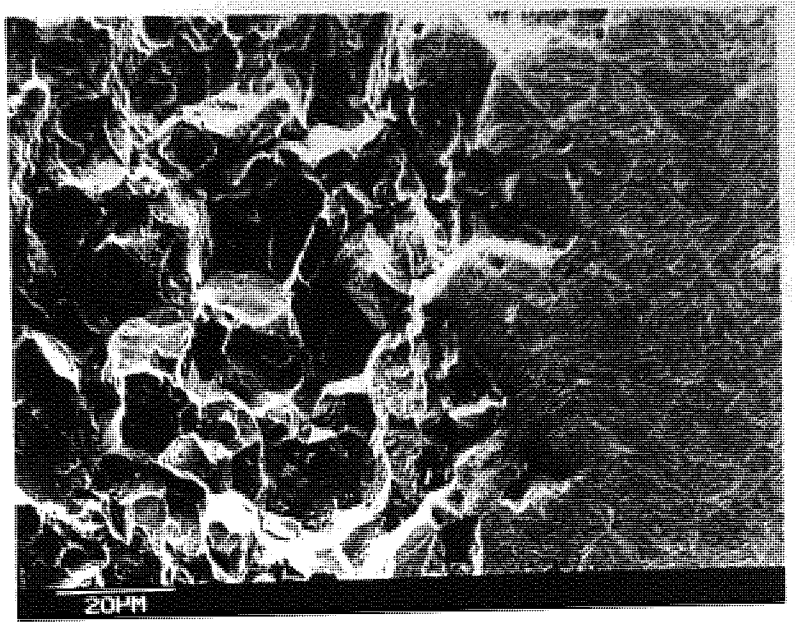

(a)

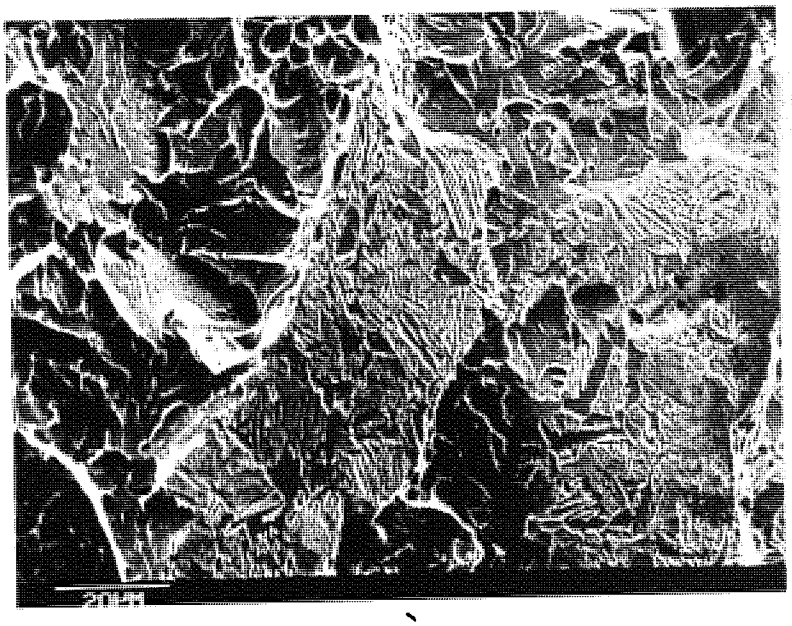

(b)

Fig.86, Fracture surface/microstructure of carburised 635A14,
(a).Case ; (b).Core. (scanning electron micrographs).

Fracture surface examination of carburised 080M15 revealed again regions of transgranular fracture at the root of the notch, as shown in Fig. 87a. It can be seen that the flat fatigue fracture extends along the notch root at varying depths, some intergranular fracture, Fig. 87b, appeared in the top left part of the micrograph. The transgranular fracture magnified is a typical appearance of the initiation zone at the root of the notch. On the other hand, Fig. 87b reveals notch root fracture at the side of the notch, where fracture is intergranular, this may suggest that crack has initiated somewhere within the thickness and extended from there towards the sides, in fact during fatigue testing it was not possible to see the crack, despite initiation being indicated by the potential drop equipment. Crack was seen when it was allowed to grow.

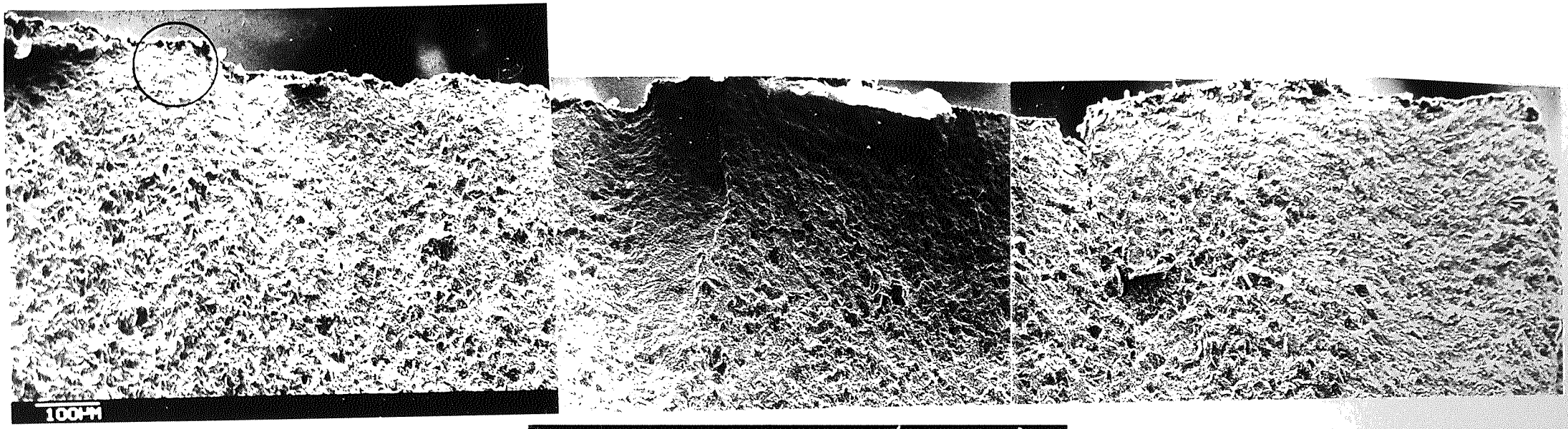

Circled zone

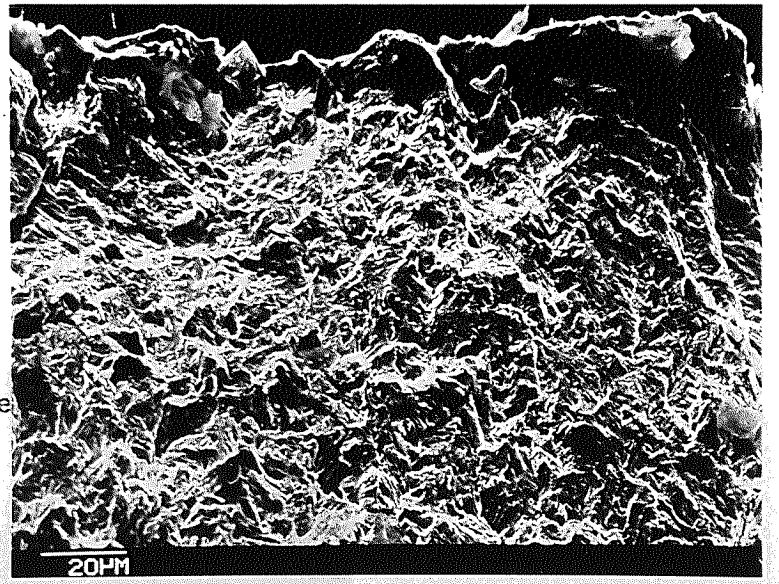

Fig.87-a, Transgranularity of initiation (notch root), in 080M15 carburised by single stage (G3), and tested in three point bending.

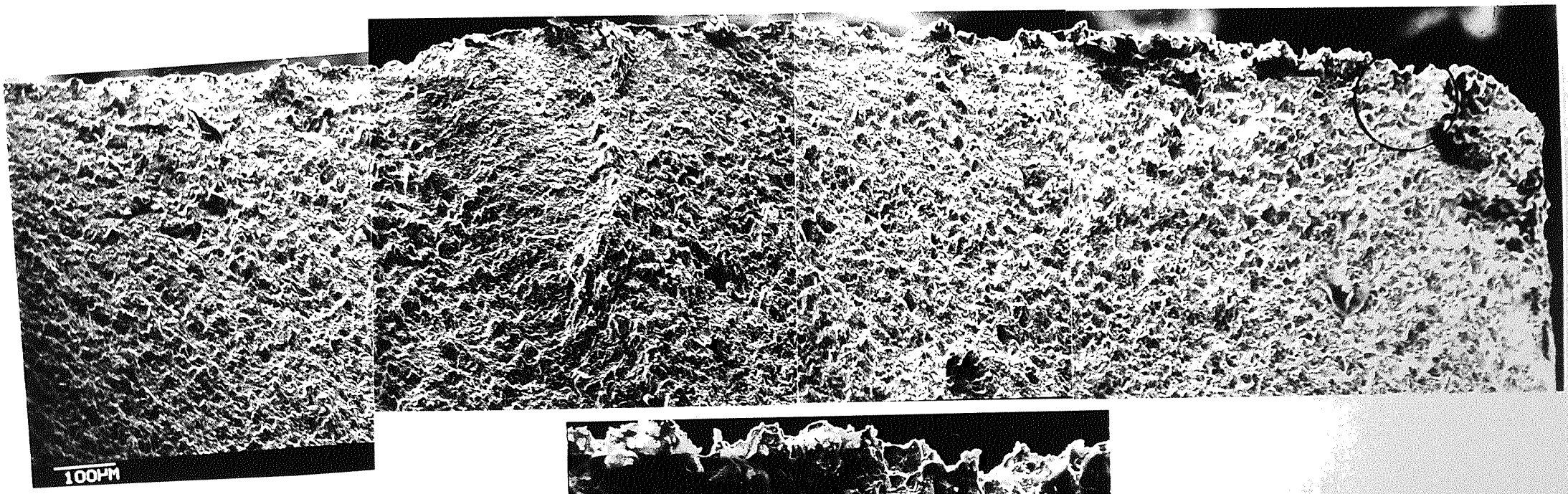

Circled zone

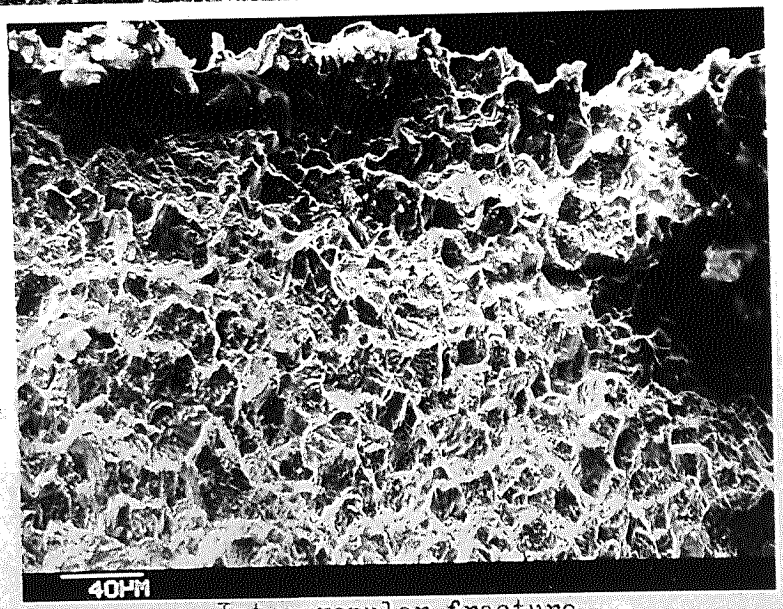

Intergranular fracture

Fig.87-b, Fracture surface at the root of the notch in 080M15, carburised by single stage(G3),and tested in three point bending.

7.0 Conclusions

1. Most of the fatigue testing was carried out in unidirectional bending and, at a stress ratio of 0.3, carburising in general was not found to improve the fatigue strength over that of the uncarburised hardened.

2. Carbon profiles from single stage and from boost-diffuse cycles with a surface carbon content of 0.8%, gave similar unidirectional bending fatigue strength of 635A14.

3. A carbon profile with 1.2% C at the surface, as a result of overcarburising, resulted in a significant loss in the unidirectional bending fatigue strength of 635A14. This was attributed to the presence of globular and/or intergranular carbide particles.

4. Single stage carburising resulted in a carbon profile with 0.94% C at the surface, which was associated with about 28% retained austenite. This was found to be detrimental to unidirectional bending fatigue strength of 635A14. However the same carburising procedure on 835A15 resulted in a 0.97% C at the surface, which was associated with about 35% retained austenite. This was not found to be detrimental to rotating bending fatigue strength.

5. A carbon profile with surface decarburisation, resulted in about 15% loss in the unidirectional bending fatigue strength of 635A14.

6. Carburising as expected, resulted in favourable compressive residual stresses, except when the surface was decarburised to about 0.5% C, while 0.74% C was maintained at about 0.35 mm, residual stresses were tensile. Unexpectedly the boost-diffuse carbon profile with plateau, showed the highest compressive residual stresses.

7. Vacuum carburising brought about a considerable gain in the unidirectional bending fatigue strength of 635A14, by preventing the occurrance of internal oxidation encountered in gas carburising. Over-carburising in vacuum was not detrimental to uni-directional bending fatigue strength of 635A14, despite the presence of uniformly distributed fine carbide particles, as a result of reheating for hardening. This however would contribute towards raising wear resistance and therefore improve the fatigue performance of carburised components designed to operate under combined contact and bending fatigue.

8. Increasing the mean stress resulted in decreased bending fatigue strength of 635A14, whether carburised or only hardened. At medium value of mean stress, namely at a

stress ratio of 0.3, the fatigue strength is comparable in both cases. However, carburisation showed its advantages at low mean stress and in particular zero mean stress, where the stress ratio is -1.0. On the other hand fatigue strength results at high mean stress, namely at a stress ratio of 0.7, indicated that carburisation showed little or no advantages over the uncarburised hardened condition. As a confirmation, tensile strength results indicated the harmful effect of carburisation.

9. Unidirectional bending fatigue strength of carburised 080M15 exhibited the expected decrease with increasing stress concentration factor. However the decrease becomes less pronounced when stress concentration factors of about 2.8 are reached, then fatigue strength remains nearly constant.

10. Notch sensitivity is reduced by carburising. The effect was found to be more pronounced in unidirectional than in rotating bending. The reduction is controlled by the magnitude of compressive residual stresses, as different carbon profiles result in different magnitudes of residual stresses, the higher they are the lower is the notch sensitivity.

11. The initiation of fatigue crack in carburised 635A14 or 080M15 was characterised by a trans-granular fracture. This was found to be independent to the type of loading, i.e. whether rotating or unidirectional bending. The trans-granular initiation spread over a limited zone adjacent to the surface, however there was no clear evidence of sub-surface initiation. The propagation was intergranular through the high-carbon brittle case.

8.0 Recommendation for Future Work

1. Certain carbon profiles were found to be preferable on the basis of pure bending fatigue, however carburised engineering components may perform under contact as well as bending fatigue. Therefore these carbon profiles should be investigated under contact fatigue so that direct assessment for practical applications can be made.

2. A boost-diffuse carbon profile with a plateau resulted in a slight loss of unidirectional bending fatigue strength in comparison to that of a single stage profile despite the higher compressive residual stresses of the former. This lack of correlation might be due to the local yielding depending upon the residual stress distribution. Consequently qualitative assessment and accurate comparison of such profiles in future demands the determination of residual stress distribution.

3. Notch sensitivity was found to be reduced by compressive residual stresses due to carburising. However the deviation of notched fatigue strength of carburised 080M15 from the elastic behaviour may also be as a result of favourably modified residual stresses caused by localised sub-surface yielding. In this respect further work is required to validate or dismiss the above hypothesis by determining residual stress distribution or by using higher strength steel, thus avoiding residual stress redistribution.

4. Retained austenite was found to exert different effect as its presence was detrimental in unidirectional bending, and did not influence rotating bending fatigue strength. This may be an indication of its different effect at different stress levels. In this respect and for accurate assessment of such differences, further work may be useful if done in plain bending at two or three levels of mean stress including zero mean stress (reverse bending).

5. Retained austenite is claimed to decrease the bending fatigue strength to an enhanced degree in the untempered condition [41]; however tempering reduces compressive residual stresses. Tempering was not practiced in order to maximise residual stresses and to allow for examining their full effect on the bending fatigue strength. Therefore further work is required to broaden our understanding and reveal the speculated effect of retained austenite on the fatigue strength in conjunction with tempering and residual stresses.

6. Grain coarsening due to high vacuum carburising temperature may have some effect on the fatigue properties, thus further work in this respect may be interesting.

APPENDIX 1

Dimensions and Corresponding Stress Concentration Factor of O80A15 Steel Specimens

Specimen Code	Thickness mm	Width mm	Notch Depth mm	Root Radius mm	Stress Concentration Factor
1A	6.0	14.9	0.9	1.35	1.96
1B	6.02	14.95	0.8	1.35	1.93
1C	6.0	14.97	0.7	1.35	1.91
1D	6.0	14.9	0.7	1.35	1.93
2A	5.97	14.6	0.9	0.75	2.52
2B	6.05	14.8	0.9	0.75	2.5
3A	6.0	11.0	0.7	0.75	2.21
3B	5.92	11.0	0.8	0.76	2.21
4A	5.91	10.96	1.1	1.5	1.89
4B	5.96	10.97	1.05	1.5	1.87
4C	5.98	10.87	1.1	1.5	1.89
4D	5.93	10.97	1.17	1.5	1.91
5A	5.94	13.2	0.74	0.45	2.8
5B	5.92	13.1	0.55	0.45	2.82
6A	5.96	11.4	0.93	0.55	2.8
6B	6.01	11.4	1.04	0.5	2.93

APPENDIX 2

FATIGUE STRENGTH CALCULATIONS

Random samples of calculations are chosen to illustrate the procedure followed in determining the tabulated results.

1. Failure stress in rotating bending was calculated using equation (4), see section 4.2.1

   e.g. G3RB5

   $S = 63$ mm $\quad d = 6.72$ mm $\quad P = 392$ N

   $$\sigma = \frac{32}{\pi} \frac{63 \times 392}{(6.72)^3}$$

   $$\sigma = 830 \text{ N mm}^{-2}$$

2. Failure stress in unidirectional bending (3-P.B.) was determined using equation (5), see section 4.2.2.

   e.g. G1 2

   $S = 50$ mm $\quad D = 16$ mm $\quad P = 16800$ N

   $$\sigma = \frac{16}{\pi} \frac{16800 \times 50}{(16)^3}$$

   $$\sigma = 1044 \text{ N mm}^{-2}$$

   While the stress to initiation was determined on 4 P.B. test pieces, using equation (7), e.g. G 18

   $a = 26$ mm $\quad d = 13$ mm $\quad P = 17200$ N

   $$\sigma = \frac{16}{\pi} \frac{17200 \times 26}{(13)^3}$$

   $$\sigma = 1036 \text{ N mm}^{-2}$$

The estimated bending fatigue strength was determined by taking the mean value between the stress value at which failure or initiation occurred and that of the preceeding survival run

e.g. G1 2

Estimated fatigue strength = $\frac{1044 + 1010}{2}$

= 1027 N mm^{-2}

The mean stress was calculated using equation (3)

i.e. $\sigma_m = \sigma_{max} \frac{1+R}{2}$

Depending upon the stress ratio, and the following example shows the determination of the mean stress and the stress amplitude as both represent one point on the Gerber diagram

e.g. G3 19 tested at a stress ratio of 0.07 the estimated fatigue strength was determined to be 1098 N mm^{-2}

$\therefore \sigma_{max} = 1098$

$\sigma_m = 1098 \frac{1+0.07}{2}$

$\sigma_m = 587$ N mm^{-2}

However the stress amplitude σ_a

$\sigma_a = \sigma_{max} - \sigma_m$

$= 1098 - 587$

$= 511$ N mm^{-2}

The stress to initiate a crack at the root of the notch, in test piece of carburised 080M15, was determined using equation (6), see section 4.2.2.

e.g. 1A

$s = 60$ mm, $b = 6.0$ mm $h = 14.0$ mm

h = width - notch depth

$P = 8000$ N

$\sigma = 1.5 \frac{PS}{bh^2}$

$= 1.5 \frac{8000 \cdot 60}{6.0(14)^2}$

$= 613$ N mm^{-2}

Tensile strength was calculated by

$$\sigma = \frac{P}{A_o}$$

$$P = 201 \times 10^3 \text{ N} \qquad d_o = 13.7 \text{ mm}$$

$$A_o = \frac{\pi d_o^2}{4} = \frac{\pi}{4}(13.7)^2 = 147.4 \text{ mm}^2$$

$$\sigma = \frac{201 \times 10^3}{147.4} = 1364 \text{ N mm}^{-2}$$

APPENDIX 3

Data and Calculation of Residual Stresses on Carburised 080M15

Thermo-chemical Treatment	Deflection (Δf) mm	Effective case depth (d) mm	Dimension, mm thickness (t)	Dimension, mm width (w)	Load at zero deflection (P) N
G1	-1.8	0.88	7.0	15.9	720
G2	+0.2	0.79	6.9	15.9	100
G3	-1.5	1.0	7.0	14.2	560
G5	-1.8	1.6	7.0	15.8	600

Residual stress calculation was carried out using

$$\sigma_s = \frac{\sigma t}{3d} \quad \text{(see section 4.2.6)}$$

$$\sigma = \frac{MY}{I}$$

$$= \frac{PS}{2} \cdot \frac{t/2}{wt^3} \cdot 12$$

$$= \frac{3PS}{2wt^2}$$

$$\therefore \quad \sigma_s = \frac{3}{2}\frac{PS}{wt^2} \cdot \frac{t}{3d}$$

$$= \frac{PS}{2wtd} \quad \text{(Span length S was always 180 mm)}$$

For example G1

$$\sigma_s = \frac{720(180)}{2(15.9)(7)(0.88)}$$

$$\sigma_s = 661 \text{ N/mm}^2$$

APPENDIX 4

Amount of Eccentricity Found in Rotating Bending Specimens due to Distortion by Carburising and Hardening Treatments

Specimen	Geometry	Location on Specimen		
		Fixed end * (a)	(b)	Loading end (c)
G4 1	Plain	0.01765	0.02033	0.01368
G4 2	Plain	0.01734	0.02156	0.02757
G4 3	Plain	0.01693	0.02049	0.01882
G4 4	Plain	0.01645	0.02098	0.0184
G4 5	Plain	0.01736	0.02029	0.03145
G4 6	Plain	0.0176	0.02185	0.03015
G4 1	Notched	0.01609	0.01965	0.0187
G4 2	Notched	0.01730	0.041930	0.0143
G4 3	Notched	0.01712	0.01940	0.00805
G4 4	Notched	0.01725	0.02062	0.02175
G4 5	Notched	0.01507	0.02085	0.02555
G4 6	Notched	0.0148	0.02110	0.03010
G6 1	Plain	2.3985	2.3985	2.4018
G6 2	Plain	0.0019	0.0115	0.0072
G6 3	Plain	0.0086	0.0002	0.007
G6 4	Plain	0.0034	0.0102	0.0102
G6 1	Notched	0.0042	0.004	0.000
G6 2	Notched	0.0062	0.0023	0.0005
G6 3	Notched	0.0000	0.0029	0.0003
G6 4	Notched	0.005	0.0029	0.0006

* Fixed end reading is a reference point and it is not the actual values which matter but it is the amount of difference from the fixed end which is important.

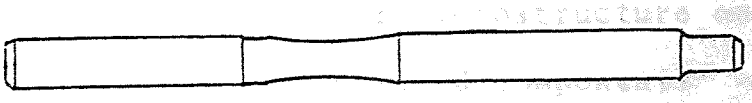

9.0 References

1. J.B. Bidwell, "Fatigue Durability of Carburised Steel", Introduction, ASM, pp. 1-10, 1957

2. ASM Committee on Failures of Gears "Failure of Grears", Facture analysis and prevention, ASM Metal Handbook, 10, p. 507, 1975

3. G. Parrish, "The influence of microstructure on the properties of case carburised components", - Internal oxidation -, Heat Treatment of Metals, 1, pp. 6-12, 1976

4. V.S. Sagaradze, "Effect of carbon content on the strength of carburised steel", Metal Science and Heat Treatment, No. 3, pp. 198-200, March, 1970.

5. C. Dawes and R.J. Cooksey, "Surface treatment of engineering components", Heat Treatment of Metals; Special Report 95, I.S.I., pp. 68-105

6. C. Dawes and D.F. Tranter, "Production gas carburising control", Heat Treatment of Metals, 4, pp. 121-130, 1974

7. H.C. Child, "Vacuum Carburising", Heat Treatment of Metals, 3, pp. 60-65, 1976

8. G. Parrish, "The influence of microstructure on the properties of case carburised components" - Decarburisation - , Heat Treatment of Metals, 2, pp. 49-53, 1976

9. K.E. Thelning, "Steel and its Heat Treatment", Butterworths, 1974

10. E.C. Rollason, "Metallurgy for Engineers", p. 185, Arnold, 1973

11. G. Parrish, "The influence of microstructure on the properties of case carburised components" - Retained Austenite -, Heat Treatment of Metals, 4, pp. 101-109, 1976

12. D.P. Koistinen, "The distribution of residual stresses in carburised cases and their origin", Trans, of ASM, 50, pp. 227-241, 1958

13. H.E. Frankel, J.A. Bennett and W.A. Pennington, "Fatigue properties of high strength steels", Trans. ASM, 52, pp. 257-276, 1960

14. D.E. Diesburg, "Influence of retained austenite and residual stress on the fracture toughness in carburised cases of Ex 32 and SAE 8620; Climax Molybdenum, Nov. 15, 1976

15. M.A. Balter and M.L. Turovskii, "Resistance of case-hardened steel to contact fatigue", Metal Science and Heat Treatment, 3, pp. 177-180, March, 1966

16. A Diament, R. El Haik, R. Lafont and R. Wyss, "Surface fatigue behaviour of the carbonitrided and case hardened layers in relation to the distribution of residual stresses and the modification of the crystal lattice occurring during fatigue", Paper presented at the 25th Colloque International, Caen, France, pp. 29-31, May, 1974; Translation BISI 12455

17. R.H. Richman and R.W. Landgraf, "Some effects of retained austenite on the fatigue resistance of carburised steel", Metallurgical Trans., 6A, pp. 955-964, May, 1975

18. R.G. Dawes, "The Theory and Practice of sub-zero Treatment of Metals", Heat Treatment of Metals, 1, pp. 29-32, 1974

19. J.G. Roberts and R.L. Mattson, "Fatigue Durability of Carburised Steel", ASM, p. 105, 1957

20. G. Parrish, "The influence of microstructure on the properties of case carburised components" - Carbides -, Heat Treatment of Metals, 3, pp. 73-79, 1976

21. I.S. Kozlovskii, A. Ya Novikova, A.T. Kalnin and V.F. Nikonov, "Increase in the strength of tractor gears by case hardening and nitrocementation", Metal Science and Heat Treatment, 5, pp. 388-390, May, 1966

22. E. Mitchell, R.J. Cooksey and C. Dawes, "Ican alloy carburising steels, low alloy steels", Iron and Steel Institute, 114, pp. 31-36, 1968

23. I. Ya Arkhipove, "Internal Oxidation of Steel 18 Kh 2N4VA", Metal Science and Heat Treatment, 15, 7, pp. 622-624, July, 1973

24. I. Ya Arkhipove, V.A. Batyrev and M.S. Polotskii, "Internal oxidation of the case on carburised alloy steels", Metal Science and Heat Treatment, 14, 6, pp. 508-512, 1972

25. G.H. Robinson, "Fatigue Durability of Carburised Steel"- the effect of intergranular oxidation on fatigue life -,ASM, pp. 33-46, 1957

26. S. Gunnerson, "Fracture anomalies in the surface region of gas carburised case-hardened steel", Metal Treatment and Drop Forging, 30, 213, pp. 219-229, June, 1963

27. A. Rose and H.P. Hougardy, "Transformation characteristics and hardenability of carburising steels", Symposium Transformation and Hardenability in steels; pp. 155-166, Feb. 27-28, 1967

28. L.J. Ebert, "The role of residual stresses in the mechanical performance of case carburised steels", Metallurgical Trans., 9A, pp. 1537-1551, 1978

29. W.S. Coleman and M. Simpson, "Fatigue Durability of Carburised Steels"- Residual stresses in carburised steels -, ASM, pp. 60-64, 1957

30. M.A. Balter and I.S. Dukarevich, "The relationship between the properties of steel subjected to thermochemical treatment and the fatigue limit", Metal Science and Heat Treatment, 13, 9, pp. 729-732, Sept., 1971

31. V.S. Sagaradze and C.V. Malygina, "Influence of decarburisation on the properties of case hardened steel", Metal Science and Heat Treatment, 7, pp. 560-563, July, 1966

32. K. Kuo, "Carbides in chromium, molybdenum and tungsten steels", Journal of the Iron and Steel Institute, 173, pp. 363-375, April, 1953

33. G. Parrish, "The influence of microstructure on the properties of case carburised components" - Post hardening treatments (thermal) -, Heat Treatment of Metals, 7, pp. 73-80, 1977

34. D. Kirk, P.R. Nelms and B. Arnold, "Residual stresses and fatigue life of case-carburised gears", Metallurgia, 74, 446, pp. 225-257, Dec., 1966

35. V.S. Sagaradze and C.V. Malygina, "Effect of structure on the fatigue limit of carburised steel 20Kh 2N4A", Metal Science and Heat Treatment, 1-2, pp. 27-31, Jan-Fed, 1969

36. J.M. Chaney, "The effect of decarburisation on the bending fatigue resistance of carburised EN 36", Metallirgucal Report H/R 24J, David Brown Gear Industries Ltd.

37. L.R. Jackson, H.J. Grover and R.C. McMaster, "Fatigue properties of aircraft materials and structures", OSRD No. 6600, March, 1946

38. K. Sachs, "Decarburisation definition and measurement", I.S.I., 133, pp. 13-27, 1977

39. G.H. Robinson, "Fatigue Durability of Carburised Steel" - The effect of surface decarburisation on fatigue life -, ASM, pp. 10-22, 1957

40. G.V. Kozyrev and G.V. Toporove, "Effect of retained austenite on the impact fatigue strength of steel", Metal Science and Heat Treatment, 15, 12, pp. 1064-1066, Dec., 1973

41. C. Razim, "Influence of residual austenite on the strength and properties of case-hardened test pieces during fatiguing", Härterei-Technische Mitteilungen, 23, pp. 1-8, April- 1968; Translation BISI 6448

42. H. Weigand and G. Tolsch, "The interaction of various factors on raising the alternating bending fatigue strength of case hardened test pieces", Härterei-Technische Mitteilungen, 22, pp. 213-220, Oct., 1967; Translation BISI 6081

43. F. R. Kern, "Selecting steels for carburised gears", Metal Progress, 102, 1, pp. 25-29, July, 1972

44. G. Krauss and A. Charles, "Martensite, Micro-cracks and fatigue in carburised 8620 steel", Proceedings of the Third International Conference on the strength of metals and alloys, Vol. 1, paper 90, pp. 441-445, Aug., 1973

45. J.G. Roberts and R.L. Matton, "Fatigue Durability of Carburised Steel"- Effect of refrigeration after hardening on fatigue properties -,ASM, pp. 95-97, 1957

46. I.S. Kozlovskii, "Steels for carburising and carbonitriding", Metal Science and Heat Treatment, 14, 4, pp. 287-289, Apr., 1972

47. E.L. Gyulikhandanov and V.G. Khoroshailov, "Carburising of heat resistant steels in a controlled endothermic atmosphere", Metal Science and Heat Treatment, 13, 8, pp. 650-654, Aug., 1971

48. G.H. Robinson, "Fatigue Durability of Carburised Steel"- Effect of network carbide on fatigue life -,ASM, pp. 22-32, 1957

49. V.S. Sagardaze, "Effect of heat treatment on the properties of high carbon alloyed steels", Metal Science and Heat Treatment, 12, pp. 720-724, Dec., 1964

50. A.L. Geller and L.G. Kozhushnik, "Contact fatigue limit of carburised 25Kh 2GNTA steel", Metal Science and Heat Treatment, 6, p. 474, June, 1968

51. C. Razim, "Effect of structure of case-hardened gears on susceptibility to pitting", Härterei-Technische Mitteilingen, 22, 4, pp. 317-325, 1967; Translation BISI 6328

52. I. Ya Arkhipove, M.S. Polotskii, A. Ya Novikova, S.A. Yurasov and V.F. Nikonov, "The increase in the strength of teeth carburised and carbon-itrided gears", Metal Science and Heat Treatment, 10, pp. 867-871, Oct., 1970

53. W. Beumelburg, "The effect of surface oxidation on the rotating bending fatigue strength and static bending strength of case-hardened steel specimens", Härterei-Technische Mitteilungen, 25, 3, pp. 191-194, Oct., 1970

54. D.E. Diesburg, "Alternates for fine European carburising steels", Climax Molybdenum of Michigan, Dec. 30, 1977

55. J.P. Sheehan and M.A.H. Howes, "The effect of case carbon content and heat treatment on the pitting fatigue of SAE 8620 steel", Society of Automotive Engineers, Paper 720268, p. 16, 1972

56. W.J. Doelker, "Vacuum Carburising", Metal Progress, pp. 50-56, May, 1977

57. G. Parrish, "Influence of microstructure on the properties of case carburised components" - Core Properties and Case Depth -, Heat Treatment of Metals, 2, pp. 45-54, 1977

58. R.B. Pathi, "Influence of carburised case depth on fatigue and impact strength of IS-20 MnCr carburising steel", 2nd International Conference on Mechanical Behaviour of Metals, pp. 834-837, 1976

59. K. Funatain, "Fatigue and impact strength of carburised chromium molybdenum steels", International Conference on Strength of Metals and Alloys, Supplement to Vol. 9, pp. 1025-1031, 1968

60. H. Tauscher, "Relationship between carburised case depth, stock thickness and fatigue strength in carburised steel", Symposium on Fatigue Damage of Machine Parts, Prague, 1960; Translation BISI 11340

61. R.G. Luther and T.R.G. Williams, "Influence of surface reinforcement on the fatigue strength of low carbon steel", Metallurgia and Metal Forming, pp. 72-77, March, 1974

62. B. Syren, H. Wohlefahrt and E. Macherauch, "The influence of residual stresses and surface topography on bending fatigue strength of machined CK45 in different heat treatment conditions", 2nd International Conference on Mechanical Behaviour of Metals, pp. 807-811, 1976

63. Ya S. Umaniskii, I.G. Grinchenku and A.E. Schennikova, "Variation of the fatigue limit with surface hardening of metals", Metal Science and Heat Treatment, 3-4, pp. 208-210, March-Apr., 1970

64. R.F. Thomson, "Fatigue Durability of Carburised Steel", - Summary -, ASM, pp. 106-115, 1957

65. N.E. Frost, K.J. Marsh and L.P. Pook, "Metal Fatigue", pp. 54, 65, 137-139, 154 and 349, Clarendon Press, Oxford, 1974

66. R.W. Gradiner, "Effect of overheating on fatigue strength and other mechanical properties of carburised and uncarburised VAR S82 steel", Metal Technology, pp. 536-547, Dec., 1977

67. T. Ericsson and M. Knuuttila, "Fatigue properties of carburised and carbonitrided C-Mn and C-Mn-B steels", 2nd Inter. Conference on the Mechanical Behaviour of Metals, pp. 822-828, 1976

68. N. Lazaridis, "Fractography of fatigue fractures of carburised steel", Material Science and Engineering, 30, pp. 23-31, 1977

69. R.A. De Paul, "High cycle and impact fatigue behaviour of some carburised gear steels", Metal Engineering Quarterly, 10, pp. 25-29, Nov., 1970

70. A.H. Cottrell, "The mechanical properties of matter", Fracture of Solids, pp. 243-274, London, 1964

71. T. Hayama and H. Yoshitake, "Effect of mean stress on fatigue strength of carburised steels", Bulletin of J.S.M.E., 14, 78, pp. 1272-1280, 1971

72. T. Funakawa and S. Tanaka, "Fatigue crack propagation behaviour of carburised steel", J. Soc. Mater. Sci., Jpn., 25, 270, pp. 283-289, March 1976

73. A. Vallance and V.L. Doughtie, "Design of machine members", McGraw Hill, pp. 326, 1951

74. P.G. Forrest, "Fatigue of Metals", Pergamon Press, p. 153, 1962

75. H. Weigand and G. Tolasch, "Fatigue behaviour of case hardened samples", Härterei-Technische Mitteillungen, 22, 4, pp. 330-338, Dec., 1967; Translation BISI 6329

76. W. Morris, O. Buck and H.L. Macrus, "Fatigue crack initiation and early propagation in Al-2219-T851", Metallurgical Trans., 7A, pp. 1161-1165, Aug., 1976

77. J. Lankford, "Initiation and early growth of fatigue cracks in high strength steel", Engineering Fracture Mechanics, 9, pp. 617-624, 1977

78. G.V. Kozyrev and G.V. Topurov, "Features of developing fatigue cracks in case-hardened specimens during impact loading", Translated from Zavokskaya Laboraturiva, 40, 12, pp. 1514-1516, Dec., 1974

79. L. Magnusson and T. Johanneson, "Fatigue of case hardened low alloy steel", Scandanavian Journal of Metallurgy, 6, pp. 40-41, 1977

80. ASTM, "A guide for fatigue testing and statistical analysis of fatigue data", Supplement to manual on fatigue testing, STP No. 91-A, pp. 13-14, 1963

81. T.S. Dolan, "Certain mechanical strength properties of Al alloy 25 S-T and X 765 T" NACA TN914, Oct., 1943

82. A.J. Bush, "Experimentally determined stress intensity factor for single edge crack round bars loaded in bending", Experimental Mechanics, 16, p. 249, 1976

83. K.D. Jones and G. Krauss, "Effect of high carbon specimens corners on microstructure and fatigue of partial pressure carburised steel", Heat Treatment, 79, ASM, pp. 46-51, May, 1979

84. R.E. Peterson, "Stress concentration factors" - charts and relations useful in making strength calculations for machine parts and structural elements -, Wiley, London, pp. 67-70, 1973

85. H. Muir, B. Averbach and M. Cohen, "The elastic limit and yield behaviour of hardened steels", Trans., ASM, 47, pp. 380-407, 1955

86. Private Communications, A. Nadkarni and J.T. Barnby

87. G. Clark and J.F. Knott, "Effect of notches and surface hardening on the early growth of fatigue cracks", Metal Society, Conference on Fatigue, pp. 37-42, March, 1977

88. Handbook supplement, "Residual stress measurement by X-ray diffraction" - Residual stresses: types and sources -, SAE J784a, Report of Iron and Steel Technical Committee approved Sept., 1980 and last revised by Fatigue Design and Evaluation Committee Aug., 1971, pp. 3-26, part A

10.0 ACKNOWLEDGEMENT

The author wishes to express his gratitude to Mr. H.C. Child for his invaluable supervision, patience, helpful discussions and useful advice throughout the project. Thanks are also due to Professor I.L. Dillamore, the Head of the Department of Metallurgy and Materials Engineering, and Professor J.T. Barnby for their advice.

The author is appreciative of the assistance rendered by the Research Centre at Lucas and G.K.N.

The author also wishes to thank the laboratory and administrative staff of the Department of Metallurgy and Materials Engineering and Mrs. H. Howell for her diligence in typing this thesis.